1-25-2019 2:00 PM

The role of H3K4 methyltransferases in Drosophila memory

Nicholas Raun
The University of Western Ontario

Supervisor
Kramer, Jamie M.
The University of Western Ontario

Graduate Program in Biology
A thesis submitted in partial fulfillment of the requirements for the degree in Master of Science

Abstract

Gene transcription required for long-term memory requires the modification of histones. However, there are still many uncertainties about the identity and spatial expression of genes regulated by histone modifications during memory related processes. In this project I examined the role of *Drosophila melanogaster* methyltransferases *Set1* and *trx* in courtship memory. Genetic knockdown of *Set1* and *trx* in the mushroom body (MB) revealed that *Set1* was necessary for short- and long-term memory, while *trx* was only required for long-term memory. Transcriptional profiling of MBs following *trx*-knockdown revealed expression changes in MB-enriched genes and genes involved in RNA processing. Among the MB-enriched genes altered in *trx*-knockdown, *Ldh* exhibited dramatically reduced expression relative to control flies. Preliminary tests showed that *Ldh*-knockdown resulted in reduced courtship memory. Therefore, *Ldh* is likely a downstream effector of *trx*-regulated memory function. The results of this study provide novel insight into histone methyltransferase function in memory.

Keywords

Drosophila melanogaster, epigenetics, memory, histone H3K4 methyltransferases, *Set1*, *trx*, *Mnn1*, courtship conditioning, RNA-sequencing, transcriptome analysis

Co-Authorship Statement

This project was conducted under the supervision of Dr. Jamie M. Kramer. The project was devised and funded by Dr. Kramer, and all experiments were planned and designed in cooperation with Dr. Kramer. Some *Drosophila* lines used in this project were created by Dr. Tara Edwards or Ariel Frame. All experiments were performed by the author. Courtship video analysis was aided by research assistants and laboratory volunteers: Crystal Keung, Mohammed Sarikahya, and Alycia Crooks. Bioinformatic pipelines were established by Kevin C.J. Nixon.

Acknowledgments

First and foremost, I must thank Dr. Jamie Kramer for the mentorship and encouragement he provided throughout my program. Without you none of this was possible. I hope my work will serve you as well as your inspiration and guidance have served me.

I would also like to thank every current and past member of the Kramer lab. This is especially directed toward the original Kramer Rangers: Kevin Nixon, Spencer Jones, Melissa Chubak, Max Stone, and Taylor Lyons. The help and companionship you provided me throughout this journey is immeasurable.

I also extend a grateful thank you to my committee members, Dr. Graham Thompson and Dr. Robert Cumming. Your keen intuition and thoughtful feedback have always been a great support.

Finally, to my grandfather Don Raun, and to my parents Grant and Tami Doblanko, I thank you for the love and support you gave throughout my education. I never would have made it this far without the care you took in my upbringing or the passion for learning and science you instilled in me.

Table of Contents

List of Tables

List of Figures

List of Appendices

List of Abbreviations

Act5C	actin-5C
AMPA	α-amino-3-hydroxy-5-methyl-4-isoxazolepropionic acid
ASC-2	Apoptosis-associated speck-like protein containing a CARD 2
ash2	absent, small, or homeotic discs 2
BDSC	Bloomington Drosophila Stock Centre
bioGRID	Biological General Repository for Interaction Datasets
bond	james bond
Ca^{2+}	$calcium^{2+}$
cAMP	cyclic AMP
CBP	CREB binding protein
cDNA	complementary DNA
CI	courtship index
COMPASS	complex of proteins associated with SET1
CpG	cytosine-phosphodiesterase bond-guanine
CR	conditioned response
CRE	cAMP responsive element
CREB	cAMP responsive element binding protein
CRTC1	CREB regulated transcription co-activator 1
CS	conditioned stimulus
cVA	cis-vaccenyl acetate
CyO	Curly of Oscar
DNA	deoxyribonucleic acid
Dpy-30L1	Dpy-30-like 1
DUP99B	Ductus ejaculatorius peptide 99B
$GAL80^{ts}$	temperature sensitive GAL80
GFP	green fluorescent protein
GO	gene ontology
GPCR	G-protein coupled receptor
GTP	guanosine triphosphate
H3K4me	histone H3 lysine 4 methylation
H3K4me1	histone H3 lysine 4 monomethylation
H3K4me3	histone H3 lysine 4 trimethylation
HDAC	histone deacetylase
Hox	homeobox
hpRNA	hairpin RNA
INTACT	isolation of nuclei tagged in a specific cell type
KD	knockdown
KMT2A	lysine methyltransferase 2A
KMT2B	lysine methyltransferase 2B
KMT2C	lysine methyltransferase 2C
KMT2D	lysine methyltransferase 2D
Ldh	Lactate dehydrogenase
LTM	long-term memory
MB	mushroom body

mCD8	mouse cluster of differentiation 8
MeCP2	methylation CpG binding protein 2
MFS3	major facilitator superfamily transporter 3
MI	memory index
Mnn1	Menin 1 or multiple endocrine neoplasia type 1
mRNA	messenger RNA
NMDA	N-Methyl-D-aspartic acid
NAD+	oxidized nicotinamide adenine dinucleotide
NADH	reduced nicotinamide adenine dinucleotide
PcG	polycomb group
PDE	phosphodiesterase
PKA	protein kinase A
PMF	premated female
PTM	post-translational modification
Rbbp5	retinoblastoma binding protein 5
RISC	RNA-induced silencing complex
RNA	ribonucleic acid
RNAi	RNA interference
rRNA	ribosomal RNA
Set1	suppresser(variegation)3-9, enhancer-of-zeste and trithorax 1
siRNA	small interfering RNA
SP	sex peptide
STM	short-term memory
trr	trithorax-related
trx	trithorax
TrxG	trithorax group
UAS	upstream activating sequence
unc84	uncoordinated 84
UR	unconditioned response
US	unconditioned stimulus
VDRC	Vienna *Drosophila* Resource Centre
wds	will die slowly
WRAD	wds, Rbbp5, ash2, Dpy-30L1 complex

Chapter 1

1 Introduction

Learning and memory are the processes of collecting, storing, and retrieving information from the environment to adapt behaviour. The vast complexity of these processes makes them some of the most interesting and challenging topics in biology. Indeed, appreciation of memory as an area of study reaches as far back as antiquity, however, the actual study of memory as a molecular process truly began in earnest over the last century (Brunelli et al., 1976; Castellucci et al., 1970; Dudai et al., 1976; Quinn et al., 1974). To date, there is still much to elucidate about how memory is regulated and epigenetics has emerged as a promising new field for uncovering novel molecular mechanisms in memory biology.

1.1 Learning and memory

Acquisition of new information begins with learning, through non-associative or associative processes (Lau et al., 2013). Non-associative forms of learning, like habituation and sensitization, are based on decreased or increased responsiveness to a specific repeated stimulus (Castellucci et al., 1970). Conversely, associative learning is based on establishing an association of one external stimulus with another to produce a particular behavioural response (Carew et al., 1981; Quinn et al., 1974). In associative learning there is a temporal pairing of an unconditioned stimulus (US), which produces an involuntary biological response (an unconditioned response [UR]), to a neutral stimulus (Domjan, 2005), which does not originally trigger any particular response. Through repeated presentations of both the neutral stimulus and US, the neutral stimulus becomes a conditioned stimulus (CS) and can elicit a behavioural response independently of the US; known as a conditioned response (CR). The CR to a particular CS is often almost biologically identical to the UR of the originally paired US. In associative fear learning, for example, an aversive shock (US) causes freezing in rodents (UR). Repeated pairing of the shock to a neutral tone or light (CS) eventually causes the rodent to freeze in response to the tone or light alone (CR).

Meaningful expression of learned behavioural changes require an organism to store what was learned during training and recall it, and it is this process of storage and recall that we refer to as memory. A short-term memory (STM) may be formed after brief training periods and acts as a transient trace of learning. However, with sufficient and repeated training a persistent long-term memory (LTM) may form (Quinn et al., 1974). These processes are critically important for adaptation to the environment and the mechanisms of associative memory are extremely well conserved across animal species (Milner et al., 1998). Specifically, associative memory is one of the best studied modalities of memory and the early pathways of associative short-term and long-term memory are fairly well defined due to research in multiple model organisms.

1.2 Cellular and molecular mechanisms of associative memory

Studies into the cellular and molecular underpinnings of associative memory began with pioneering work in the sea slug *Aplysia californica* and the fly *Drosophila melanogaster* (Brunelli et al., 1976; Dudai et al., 1976). At the cellular level pairing of US and CS requires coordinated activity of neuronal circuits (Hawkins, 1984). For this to occur two circuits must propagate sensory information about environmental stimuli, the US and CS, to a convergent target neuron whereupon US and CS signals modulate the target neurons outputs, culminating in behaviour changes that link the CS to the CR. In the case of *Aplysia*, sensory neurons in the mantle shelf and foot converge onto target motor neurons that are directly in charge of gill or siphon withdrawal in response to an electrical shock (Hawkins, 1984). In *Drosophila*, the convergence of US and CS leads to more complex behavioural changes, like avoidance of certain odours once paired with an aversive shock (Aso et al., 2014; Quinn et al., 1974).

At the molecular level, coupling of US to CS can occur through production of cyclic adenosine monophosphate (cAMP), a second messenger that regulates signaling pathways particularly important for the production of both STM and LTM (Figure 1). Initial studies in *Aplysia* identified cAMP as an important molecule for memory induction and additional studies in *Drosophila* demonstrated that memory depends on the continuous production and turnover of cAMP (Dudai et al., 1976; Livingstone et al., 1984). A typical means

through which the US can act upon cAMP pathways is by stimulating G-protein coupled receptors (GPCR). GPCRs are cell surface receptors that release intracellular molecules in response to extracellular stimuli. In memory, ligand binding to GPCR releases a GTP bound α subunit (Gα), which then activates adenyl cyclases (Figure 1), the enzymes responsible for cAMP production (Connolly et al., 1996; Levin et al., 1992; Livingstone et al., 1984; Schwaerzel et al., 2003). Adenyl cyclases are also responsive to the CS through Ca2+ dependent signalling. Activation of several receptor channels by CS signals, such as NMDA-and AMPA-type receptors, leads to an influx of Ca2+ into the neuron (Davis, 2011). At high levels, intracellular Ca2+ binds calmodulin, leading to activation of adenyl cyclases and increased cAMP synthesis (Figure 1). The entire process of cAMP synthesis is antagonized by the activity of cAMP phosphodiesterases (PDE), which degrade cAMP into linear adenosine monophosphate (AMP) (Dudai et al., 1976), ensuring proper maintenance of cAMP homeostasis (Figure 1).

Sufficient stimulation of adenyl cyclase, through coincidental stimulation of US and CS, will eventually overcome PDE activity and lead to levels of intracellular cAMP that are capable of enacting cellular changes. Protein kinase A (PKA) is a tetramer composed of 2 catalytic and 2 regulatory subunits and is responsive to the cytoplasmic concentration of cAMP. The regulatory PKA subunits bind and inhibit the catalytic subunits, but high concentrations of cAMP promote the release of the regulatory subunits from the catalytic subunits, thereby activating the kinase activity of PKA which facilitates cellular changes required for memory formation (Drain et al., 1991). In STM, for example, short bursts of PKA activity can act to increase the sensitivity of ion channels to temporarily change synaptic strength (Figure 1) (Drain et al., 1994; Goodwin et al., 1997). For LTM to occur bursts of PKA activity must be longer than what is required for STM, as extended PKA activity is a critical factor for LTM formation (Müller, 2000). Repeated PKA stimulation over a period of time is necessary to create robust LTM over that of decaying STM from single or massed training sessions (Tully et al., 1994). This is because the long-activated catalytic PKA is translocated into the nucleus where it can phosphorylate additional targets required for LTM (Figure 1). One particularly important target of PKA phosphorylation is the cAMP responsive element binding protein (CREB), a transcription factor that is key for LTM (Bourtchuladze et al., 1994).

A defining molecular characteristic of LTM is that it requires gene transcription and protein synthesis. The transcription factor CREB is an indispensable factor for cAMP mediated induction of gene transcription in associative memory (Bourtchuladze et al., 1994; Yin and Tully, 1996). Indeed, blocking transcription or translation prevents LTM from forming altogether (Agranoff et al., 1966; Montarolo et al., 1986). To initiate transcription, CREB binds to cAMP responsive elements (CRE) and recruits a variety of coactivators including CREB-binding protein (CBP) (Figure 1), an epigenetic regulator for histone acetylation (Hirano et al., 2016). The discovery that CREB works in tandem with epigenetic regulators like CBP, highlights the importance of epigenetics in memory, although the transcriptional responses that are initiated and maintained to support LTM via this process are poorly understood.

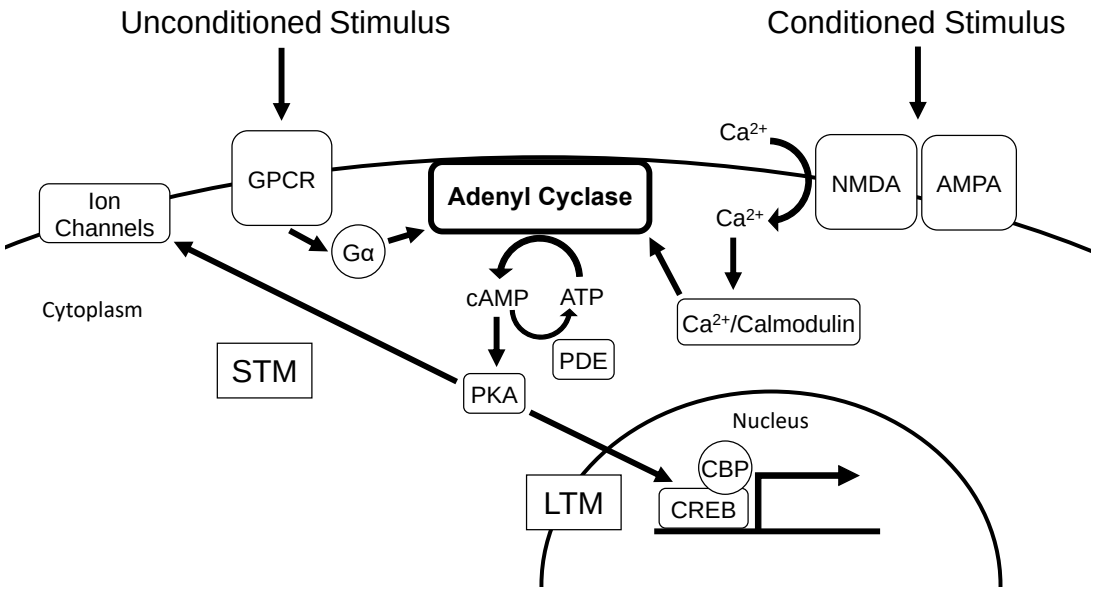

Figure 1: Molecular mechanisms of associative memory.

A simplified diagram showing the molecular pathway of associative memory formation. Specific focus is placed on the role of the cAMP signaling pathway. Associative memory forms when signals initiated by the conditioned stimulus (CS) and the unconditioned stimulus (US) converge at the molecular level onto adenyl cyclases. This occurs when CS activates adenyl cyclases via NMDA- and AMPA-type receptors concurrently with US activation of adenyl cyclases via G-protein coupled receptors (GPCR). Simultaneous stimulation by CS and US is required to increase levels of intracellular cAMP high enough to activate protein kinase A (PKA). Without concurrent stimulation, phosphodiesterase (PDE) prevents accumulation of cAMP and PKA is never activated. Active PKA phosphorylates ion channels to help form STM and phosphorylates cAMP responsive element binding protein (CREB) in the nucleus to induce transcription required for LTM formation in association with co-factors like CREB-binding protein (CBP). Figure adapted from Waddell & Quinn 2001.

1.3 Epigenetics in memory

Epigenetics is the study of gene expression changes that are independent of the underlying DNA sequence (Dupont et al., 2009). The mechanisms of epigenetic regulation include a number of biochemical modifications that can alter the accessibility of DNA to the transcriptional machinery. In cells, genomic DNA exists in a compact and organized structure known as chromatin, and the degree of chromatin compaction naturally limits the accessibility of DNA to transcriptional machinery. At the simplest level, chromatin is repeated stretches of DNA wrapped around histone octamers, together referred to as nucleosomes (Quina et al., 2006). Chromatin exists in one of two states, either heterochromatin, a state characterized as highly compact and transcriptionally inactive, or euchromatin, an open state amenable to transcription and therefore gene activation. Switching between these antagonistic states of chromatin depends on epigenetic modifications made around cis-regulatory elements and gene promoters. Epigenetic regulators alter chromatin state by either acting directly on DNA, via cytosine methylation, or through a variety of post-translational modifications (PTM) to different histone subunits. Each of the histone subunits, H2A, H2B, H3, and H4, have an exposed amino-terminal tail that is available for PTMs, such as post-translational acetylation, phosphorylation, or methylation (Bannister and Kouzarides, 2011). The specific amino-acid and form of modification for each histone depends on the class of enzyme catalyzing the reaction. For example, histone methyltransferases and demethylases catalyze the addition and removal of methyl groups to histones respectively. The outcome of gene expression ultimately depends on the sum effect of repressive and active epigenetic modifications to the local chromatin state.

Originally, epigenetics was studied in the context of cell differentiation and tissue specification (Ingham and Whittle, 1980; Kohyama et al., 2008; Nüsslein-Volhard and Wieschaus, 1980; Rai et al., 2006). Early drosophilists made major contributions to defining the role of epigenetics in development following the discovery that *Hox* genes determine cellular identity along the anteroposterior axis of segmented animals (Schuettengruber et al., 2017). In these studies the first epigenetic regulators discovered were genes later classified into the Polycomb group (PcG) and Trithorax group (TrxG),

both of which encode proteins with histone methyltransferase activity. PcG genes were shown to cause *Hox* gene silencing by promoting closed heterochromatin through, for example, the repressive methylation of histone H3 lysine 27 (Geisler and Paro, 2015). Conversely, TrxG genes antagonize PcG genes by the promotion of open euchromatin through activating histone marks like histone H3 lysine 36 and lysine 4 methylation. A necessary function for epigenetic changes in development is that they must persist long after the initial transcription regulators disappear, specifically, they must persist through the rapid cell cycle phases during early development. Epigenetic regulators, like the ones for the *Hox* genes, maintain genic activation or silencing through mitotic replication by perpetually reproducing the chromatin states across cellular generations (Schuettengruber et al., 2011). Together, the PcG and TrxG genes cooperate to ensure *Hox* genes are properly expressed in different tissues through development.

In long-term memory the convergent signals between US and CS culminate in altered gene expression and protein synthesis, and resulting changes in neuronal connectivity and responsiveness. But how are these changes maintained? The normal turnover of proteins presents a problem for memory biologists; if normal proteins only persist on the timescale of hours, how can a LTM persist indefinitely? Since epigenetic modifications stably contribute to developmental patterning across cellular generations researchers hypothesized that epigenetic modifications may also play a role in stabilizing molecular changes in memory. Early studies identified a number of epigenetic regulators that were necessary for LTM like the CREB associated CBP (Korzus et al., 2004). A seminal study in the burgeoning field now dubbed “neuroepigenetics” also found that histone H3 acetylation was greatly enriched in rodents following certain memory paradigms (Levenson et al., 2004; Swank and Sweatt, 2001). Over the following decade additional modifications like DNA-methylation, histone H3 phosphorylation (Chwang et al., 2006; Miller and Sweatt, 2007), and H3 lysine 4 trimethylation (H3K4me3) were also implicated in memory (Gupta et al., 2010). Of these, H3K4me3 is one of the most recently discovered and least understood histone modification in memory, and the study presented here will attempt to further investigate its function.

During a learning task there are significant increases in levels of hippocampal H3K4me3 (Gupta et al., 2010). Interestingly, this increase coincided with an increase of DNA-methylation around the promoter of *Zif268*, a gene important for memory consolidation. Typically, DNA-methylation around the promoter region would repress expression of the downstream gene. However, in the case of *Zif268*, increased DNA-methylation at its promoter resulted in increased expression. A model for this phenomenon has been proposed whereby H3K4me3 blocks methylation CpG binding protein 2 (MeCP2) from binding to its canonical silencing sites, instead allowing MeCP2 to recruit CREB and initiate *Zif268* transcription (Gupta et al., 2010). Thus, H3K4me3 appears to be an important PTM in memory, irrespective of whether it is stably maintained, based on the observation that it can be dynamically regulated during LTM formation.

Subsequent studies showed a necessity of the various H3K4 methyltransferases in associative memory (Figure 2). From the relatively small number of H3K4 methyltransferases in rodents, including *Set1a*, *Set1b*, and lysine methyltransferase 2 isoforms a, b, c and d (*Kmt2a*, *Kmt2b*, *Kmt2c* and *Kmt2d*) and the orthologues in *Drosophila*, including *Set1*, *trithorax* (*trx*), and *trithorax-related* (*trr*), only a small number have been studied in memory. In rodents, conditional knockout of *Kmt2a* and *Kmt2b* has been shown to interfere with STM and LTM (Kerimoglu et al., 2013, 2017). Knockouts for *Kmt2a* and *Kmt2b* coincided with gene expression changes to synaptic plasticity and metabolic genes respectively. Interestingly, the *Drosophila* orthologue to *Kmt2a* and *Kmt2b*, *trx*, was shown to be dispensable for 4-day LTM maintenance (Hirano et al., 2016), indicating that the critical time for the activity of these histone methyltransferases is closer to the induction of LTM. As of yet, no studies have shown whether *trx* is required for memory formation. However, it was shown that 1 day after spaced-training the promoter of *trx* itself was bound by CREB, CREB regulated transcription co-activator 1 (CRTC1), Histone H3 lysine 9 acetylation, and poised RNA polymerase II; all indicators of active transcription. Despite increased transcription factor binding, no significant changes were found in levels of *trx* mRNA (Hirano et al., 2016), potentially due to post-transcriptional regulation of *trx*, indicating an extra level of care taken by the cell to regulate this gene. Finally, a recent study in *Drosophila* has revealed a role for *trr* in regulation of STM and metabolic processes (Koemans et al., 2017a). This leaves a number of enzymes still

untested in *Drosophila* and mammalian LTM formation (Figure 2). Establishing the functions of the remaining enzymes will be necessary to fully understand how regulation of histone H3K4 methylation (H3K4me) is involved in memory formation.

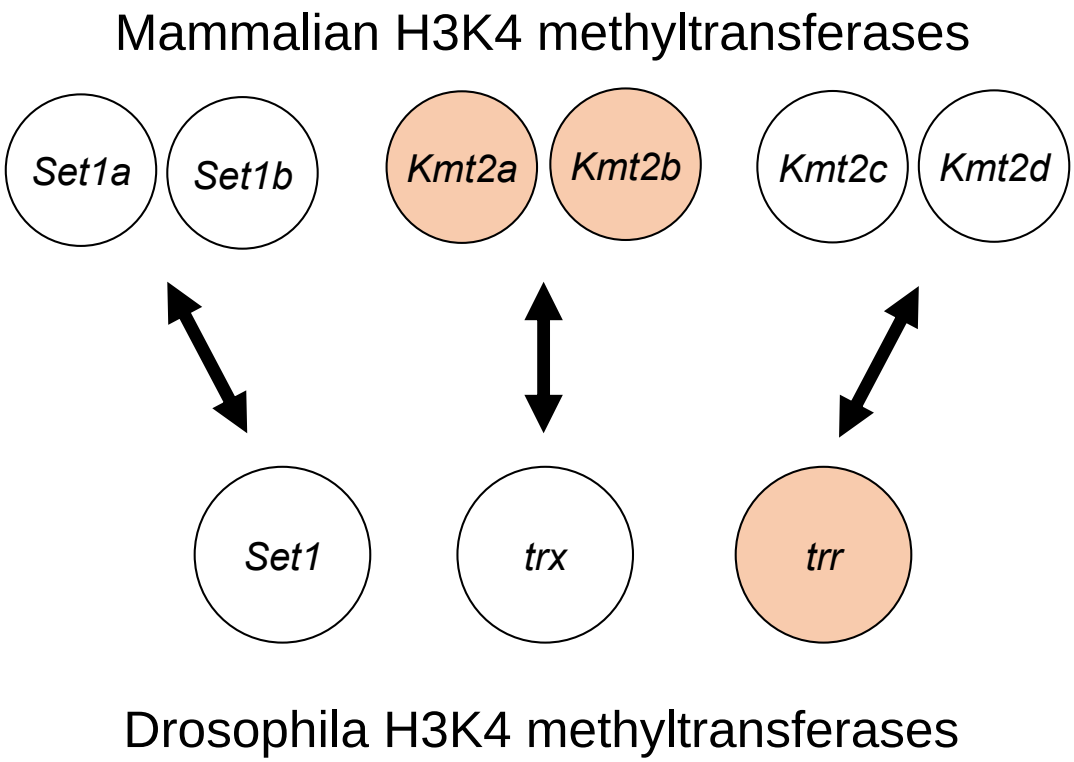

Figure 2: Conservation of Drosophila and mammalian H3K4 methyltransferases.

The highly conserved H3K4 methyltransferases in *Drosophila* and mammals share a one-to-two evolutionary relationship, indicated by two-way arrows. Methyltransferases that have been previously linked to learning and memory formation are indicated in orange. For this study *Set1* and *trx* in *Drosophila* were investigated.

1.4 Epigenetics in neuronal cell identity

Memory depends on the proper functioning and connection of neurons. In associative memory neurons propagate signals triggered by US and CS, and the activated neural networks eventually integrates US/CS signals to form lasting behavioural changes. Therefore, proper neurodevelopmental processes are critical for ensuring memory can form. In addition to their role in developmental patterning, epigenetic regulators are also required for terminal neuron differentiation (Huang et al., 2015), and for maintaining neuronal identity (O'Meara et al., 2010).

The transition from proliferative neuroblast to post-mitotic neuron is caused by transcription factors responding to development signals that subsequently drive differentiative gene programs (Achim et al., 2014; Hobert, 2011). The genetic removal of differentiative transcription factors from post-mitotic neurons results in the loss of specialized neuronal features, including neurotransmitter and neurotransmitter-receptor identities, while leaving generalized features, such as the vesicle processing machinery, intact (Deneris and Hobert, 2014). In some cases, these gene regulatory programs are also necessary for neuronal survival by balancing the expression of pro- and anti-apoptotic factors (Ninkovic et al., 2010; Tsarovina et al., 2010). These findings have led to the prevailing hypothesis that the gene regulatory programs initiated during neuronal differentiation must be maintained for normal neuronal functions. In neurons the stability of these differentiative programs is important because of their longevity and intrinsic plasticity. Essentially, neuronal cellular programs must be highly durable, lasting decades in the case of mammalian neurons, and flexible enough to enact the changes required by an ever adapting brain. This is especially important in processes like memory, where compromised neuronal plasticity can disrupt the complex neuronal networks required for memory (Holtmaat and Caroni, 2016). Additional research has shown that epigenetic modifiers also contributed to differentiation and patterning of memory brain regions like the mammalian hippocampus, and therefore their disruption may cause memory dysfunction like what is observed in intellectual disability (You et al., 2015).

Epigenetic regulators work in tandem with differentiative transcription factors to engage terminal neuron differentiation along with terminal identity maintenance. Kmt2a,

which also promotes trimethylation of H3 histones in zebrafish, helps initiate neuron differentiation in embryonic neural progenitor cells (Huang et al., 2015). Additionally, post-embryonic differentiation of subventricular zone neuronal stem cells in rodents also requires KMT2A function for proper differentiation (Lim et al., 2009). With regards to identity maintenance, *Caenorhabditis elegans* researchers have found that asymmetrical left/right neuron identity maintenance requires histone acetylation by the MYST complex (O'Meara et al., 2010).

Our understanding of the underlying mechanisms that initiate and maintain neuronal gene expression programs during neurodevelopment and in memory is far from complete. Primarily this is because there are a plethora of neuronal cell types that all have the potential to react to various external signals in different ways (Nelson et al., 2006). Until recently, most research in neuronal gene expression responses has been placed on differentiative transcription factors, yet it is becoming more apparent that the role of epigenetic regulators in neuronal identity establishment and maintenance should be further studied. How epigenetic regulators contribute to terminal neuron identity initiation and maintenance will no doubt be interesting to see, especially if the findings converge on work done with LTM gene regulation. In this study, the role of H3K4 methyltransferases will be investigated in both neuronal identity and LTM gene regulation to further characterize this class of epigenetic regulators.

1.5 Activity of H3K4 methyltransferases

Methylation of histone H3 lysine 4 is mediated by the SET1 methyltransferase family of proteins, first discovered as the *Set1* gene in *Saccharomyces cerevisiae* (Santos-Rosa et al., 2002). The SET1 family can catalyze different forms of histone methylation *in vivo*, including mono-, di-, and tri-methylation. Each of these modifications are catalyzed by different enzymes from the SET1 family at different loci across the genome, facilitating gene activation. In higher organisms, *Drosophila* and rodents for example, there is a divergence from the *Set1* gene into conserved subclasses of SET1 proteins, including *Set1a, Set1b, Kmt2a, Kmt2b, Kmt2c,* and *Kmt2d* in rodents, and *Set1*, *trx*, and *trr*, in *Drosophila* (Figure 2) (Zhang et al., 2015). Set1 in *Drosophila*, along with its mammalian orthologues, are responsible largely for the bulk H3K4 methylation across the genome

(Hallson et al., 2012; Mohan et al., 2011; Wu et al., 2008). Conversely, *Drosophila* and mammalian-related *trx* and *trr* proteins appear to have a much more specific and targeted effect on gene regulation (Hallson et al., 2012; Mohan et al., 2011; Schuettengruber et al., 2011). The differential targeting of these enzymes seemingly results in unique roles for these enzymes across different cellular processes.

SET1 proteins activate gene expression in different ways depending on the modifications they produce at a given loci. Monomethylation of H3K4 (H3K4me1), is highly enriched around enhancers (Heintzman et al., 2009), and the 3' end of active genes (Hallson et al., 2012), antagonizing the binding of gene silencing complexes like the PcG genes and allowing the binding of transcription factors. Trimethylation of H3K4 (H3K4me3), however, is almost exclusively enriched around the transcription start sites (TSS) of actively transcribed or poised genes (Guenther et al., 2005; Santos-Rosa et al., 2002). While the exact mechanism by which H3K4me3 promotes gene activation is unknown, it is well supported that this mark is required for normal gene transcription. Indeed, mutations within either Set1 or H3K4 in yeast have reduced gene expression *in vivo* (Santos-Rosa et al., 2002). Additionally, only genes with endogenously high levels of H3K4me3 within their TSS can be artificially induced with the introduction of HDAC inhibitors (Wang et al., 2009). Because of this H3K4me3 is often used to define active promoters.

The methyltransferase activity of SET1 proteins, specifically of KMT2A (Avdic et al., 2011; Odho et al., 2010), is primarily stimulated by complex associating proteins. These functionally active complexes, usually dubbed as a complex of proteins associated with SET1 (COMPASS), share common subunits; such as the *Drosophila* orthologues Wds, Rbbp5, Ash2, and Dpy-30L1 (WRAD) (Ali and Tyagi, 2017; Ernst and Vakoc, 2012). The specificity of the SET1 family methyltransferases are thought to be conferred by uniquely binding co-activators. For example, MENIN-1 (MNN1) only binds to complexes forming around KMT2A and KMT2B to allow for specific binding at *Hox* loci or to estrogen receptor genes (Dreijerink et al., 2006; Hughes et al., 2004; Milne et al., 2005). Likewise, the ASC-2 protein associates with KMT2C and KMT2D complexes to confer its own target specificity (Lee et al., 2006). It is reasonable to suspect then that differences in activity of

SET1 family proteins in memory may be due in part to associations with their specific co-activators. However, many of these enzymes have not yet been investigated. In this study, previously untested H3K4 methyltransferases in *Drosophila* memory formation, namely *Set* and *trx*, will be further characterized.

1.6 Drosophila as a model organism for studying memory

The proud roots of *Drosophila melanogaster* as a model organism began with the serendipitous discovery of a white eyed fly (as opposed to the natural red eye) by T.H. Morgan in 1910 (Morgan, 1910). Since then, there has been an explosion of genetic tools available for fly researchers making *Drosophila* a major model in animal genetic research. The capacity of *Drosophila* to learn and form lasting memories was discovered by the S. Benzer laboratory (Quinn et al., 1974). Backed by over a century of genetic research, the use of *Drosophila* as a model to better understand the genetics of memory was an easy choice. Over the decades, *Drosophila* has been used to discover many key molecular mechanisms in memory, including early characterization of CREB (Yin et al., 1994). The key brain region in all of these studies and the region that endows *Drosophila* with the capacity to form associative memories is the mushroom body. To further understand memory in *Drosophila*, some working knowledge of this brain region is required.

The mushroom body (MB) is the olfactory learning and memory centre of the fly (Han et al., 1992; Heisenberg et al., 1985). The MB is composed of a symmetrical pair of neuropils in the brain that integrates olfactory sensory information and translates it into learned behavioural responses (Aso et al., 2014). Intrinsic MB neurons, the Kenyon cells, are the site of convergence for signals from the US and CS (Aso et al., 2014). Kenyon cells are classified into 3 functionally distinct neuronal subtypes; the α/β, α'/β', and γ neurons. The different lobes of the MB are responsible for processing different phases of memory, with the α/β and α'/β' lobe primarily processing LTM (Cervantes-Sandoval et al., 2013; Pascual and Préat, 2001), and the γ lobe primarily processing STM (Zars et al., 2000a). Both these brain regions, while functionally independent, produce memory using cAMP dependent signalling pathways (Blum et al., 2009). Two to 4 hours after memory acquisition, information is transferred between STM specific neurons to LTM specific neurons in a process called consolidation (Cervantes-Sandoval et al., 2013). Memory

consolidation is critical to strengthen the nascent memory trace into a stable memory. Early stages of this information transfer are dependent on the dorsal paired medial neurons and the α'/β' neurons sending information to the α/β lobe (Krashes et al., 2007). After consolidation, memory recall becomes entirely dependent on the α/β lobe (McGuire et al., 2001). The different functions found between MB neurons could be supported in part by different transcriptional profiles in different MB neuron subtypes (Shih et al., 2018). Recently, transcriptional profiling of the MB revealed enriched expression of many genes implicated in memory related functions when compared to overall expression in the whole head; this included functions like GPCR mediated adenyl cyclases activity, cAMP dependent protein kinases activity, and increased synaptic vesicle processing (Jones et al., 2018).

Therefore, genetic manipulation of MB gene expression offers a powerful tool to elucidate the molecular mechanisms required for memory formation and retrieval. Following these genetic manipulations it is necessary to assess the effect on memory function in a quantifiable way. Researchers have established a number of assays to probe the memory of *Drosophila*, including courtship conditioning (Siegel and Hall, 1979), aversive shock conditioning (Tully and Quinn, 1985), spatial learning paradigms (Zars et al., 2000b), and visual pattern memory paradigms (Liu et al., 2006), to name a few. Here, courtship conditioning was used to effectively investigate the consequences of H3K4 methyltransferases disruption on associative memory.

1.7 Courtship conditioning as a measure of memory in *Drosophila*

Courtship conditioning is an ethological form of memory assessment, as it is an ecological behaviour not largely dependent on contrived laboratory manipulations, making it a staple in the study of *Drosophila* memory (Kamyshev et al., 1999; Siegel and Hall, 1979). Moreover, formation of memory during courtship conditioning is dependent on the MB (McBride et al., 1999), making genetic alterations within this brain region relatable back to the principle molecular mechanisms of associative memory.

Normal courting in male flies includes a set of easily recognizable behaviours (Koemans et al., 2017b; Siegel and Hall, 1979) directed toward a potential female mate. In addition, female receptivity to copulation also plays a key role in male courting behaviour. For example, if the target of the male's courting is a previously mated female (PMF), the female will reject the male fly and copulation will not occur. The reduced receptiveness of a PMF to new courting attempts is due to the delivery of the sex molecules Ductus ejaculatorius peptide 99B (DUP99B) and sex peptide (SP) by the male's ejaculate during initial copulation (Ottiger et al., 2000), which alter the females behaviour. Additionally, cis-vaccenyl acetate (cVA) is also deposited during copulation and acts in combination with female specific pheromones to repulse other males (Ejima et al., 2007). With functional learning and memory, male flies will robustly supress their latent courting behaviour after physical rejection and detection of cVA (Ejima et al., 2007; Kamyshev et al., 1999; Siegel and Hall, 1979). It is hypothesized that for associative courtship memory, detection of cVA acts as the principal CS while physical rejection acts as the US, enhancing male repulsion to cVA (Ejima et al., 2007; Keleman et al., 2012). Males that have successfully learned courtship rejection maintain suppressed courting for hours or days depending on the strength of their training and the persistence of neuronal circuit activation (McBride et al., 1999; Zhao et al., 2018).

In the laboratory, researchers compare the time a male fly spends courting after rejection to that of a socially naïve fly to quantify the capacity of the rejected fly to learn and form memories. Courtship activity can be used to study both STM and LTM by altering the duration of training and the latency to testing. With dysfunctional memory, a male fly will be unable to durably supress courting behaviour and will continue to court new pairing partners even after continuous rejection. A recent study showed that following 8 hours of courtship training, the MB of male learners begins to upregulate genes of many biological processes involved in LTM formation (Jones et al., 2018). Therefore, whether or not *Drosophila* H3K4 methyltransferases *Set1* and *trx* are involved in forming courtship memory along with the associated increases in gene transcription is the prime focus of this study.

1.8 Research hypothesis and rationale

How animals collect, store, and recall memories is critically important for adaptation to a changing environment. The pairing of two environmental stimuli to create new behavioural outputs is known as an associative memory and long-term retention of these memories depends on gene transcription and synthesis of new proteins. Histone H3K4 methyltransferases are required for gene transcription in memory yet there is still uncertainty about when these enzymes function and what genes they are regulating. The biggest gap to our understanding is what occurs during the critical first 24 hours after training when H3K4me3 peaks then returns to baseline – as of yet no study has investigated this timeframe at a genomic level. This project will further expand on the role of H3K4 histone methyltransferases in memory, identifying potential target genes contributing to dysfunctional memory processes and probing the transcriptional changes in relevant brain regions during memory acquisition.

In this study I leveraged the diverse genetic tools in *Drosophila* to characterize both functionally and transcriptionally the role of *Drosophila* H3K4 methyltransferases in associative memory. In light of the high level of conservation between *Drosophila* and mammalian H3K4 methyltransferases, and the conserved molecular mechanisms associated with LTM, the results of this investigation should be broadly applicable to understanding memory biology. Previously, our lab showed that *trr* was required for STM function, but the two other *Drosophila* H3K4 methyltransferases, *trx* and *Set1*, are still unstudied in memory formation. Here I first focused on *Set1*, as no prior work has been done to characterize its function, or the function of its mammalian orthologues, in memory. Previous work has shown that orthologues of *trx* are necessary for memory formation in rodents, but the role of *trx* in *Drosophila* LTM formation has not been evaluated. Lastly, the MB was chosen for transcriptional profiling following methyltransferase knockdown because it is especially important for *Drosophila* associative memory. The guiding hypothesis of this study was that *Set1* and/or *trx* promote LTM formation through the regulation of LTM-essential genes within MB neurons. The objectives of this study were as follows:

1. Use genetic knockdown in the MB to establish a role for *Drosophila Set1* and *trx* in memory function.

2. Identify transcriptional changes in the MB contributing to memory defects observed in objective 1.

This study is the first to investigate the roles of the *Drosophila Set1* and *trx* in associative LTM formation, and does so in a brain region especially relevant to memory function. I also identified potential mechanisms for *trx* regulated memory formation which can serve as a basis for further study into the physiology of memory.

Chapter 2

2 Methods

2.1 Fly stocks and genetics

Flies were reared on a standard medium (cornmeal-sucrose-yeast-agar) at 25°C and 70% humidity with a 12-h light/dark cycle. All fly stocks were obtained from the Bloomington Drosophila Stock Center (BDSC) (Perkins et al., 2015), or the Vienna *Drosophila* Resource Center (VDRC) (Dietzl et al., 2007). The genetic line used for testing the necessity of *Ldh* in memory was originally acquired from the VDRC, then outcrossed 5 times to a white eyed Canton-S genetic background by A. Frame for genome wide homogeneity. Female flies used for courtship conditioning were generated by J.M. Kramer with a Canton-S and Oregon-R mixed genetic background. *UAS-unc84-GFP* flies were donated by G.L. Henry (Henry et al., 2012). A list of all fly stocks used and a brief description is provided in Appendix A.

Knockdown (KD) of the various genes studied was achieved with RNA interference (RNAi) by the expression of short or long hairpin RNA (hpRNA) under the control of the transgenic UAS/GAL4 binary system. hpRNAs work in conjunction with endogenous proteins to form the RNA-induced silencing complex (RISC) to degrade target mRNAs. To do so hpRNAs must first be processed into small interfering RNAs (siRNA) of about 21 base pairs by Dicer-2. Short hpRNAs require minimal processing before they associate with RISC, however long hpRNA (hairpins greater than 300 base pairs) require more time before they are functional. In situations where long hpRNA were used *UAS-Dicer-2* was co-expressed to increase efficiency of the KD (Dietzl et al., 2007). For the purpose of restricting KD and/or expression of UNC84-GFP to the MB we used the transgenic driver *R14H06-GAL4,* which expresses GAL4 under the control of a MB specific enhancer fragment from the *rutabaga* gene (Jenett et al., 2012). For lethality assays we induced KD ubiquitously through the UAS-GAL4 system with an *Act5C-GAL4* driver, which utilizes the *Act5C* promoter.

Experimental and control genotypes indicated in Table 1 were made by crossing either RNAi fly lines or their genetic progenitors to a GAL4 driver fly line. RNAi lines are

produced through different methods with different genetic origins so it was important to ensure the proper control was used to reduce genetic background effects in an experiment. Groups of RNAi lines that share a genetic origin form libraries like the GD, KK, and TRiP libraries, indicated in Table 1 and Appendix A (Dietzl et al., 2007; Perkins et al., 2015). The GD and KK libraries originate from the VDRC and were generated by different methods. Likewise, the TRiP library originates from the BDSC and was generated by its own method. It is important to note that in all cases half of the genetic background in experimental and control genotypes was shared from the driver line, limiting the effect of genetic background again. In cases where *UAS-Dicer-2* was used to increase RNAi efficiency, comparisons were made to flies expressing *UAS-Dicer-2* alone to control for the effect of increased Dicer-2 expression. *UAS-mCherry* produced a non-targeting short hpRNA to control for the effects of non-specific short hpRNA expression and was utilized for transgenic lines sharing the same genetic origin.

Table 1: List of control and sample knockdown genotypes used for different experiments in this study.

UAS-RNAi represents generic RNAi stocks for various genotypes. Full genotypes of each RNAi-stock used and the corresponding controls are listed in Appendix A.

Lethality assay controls	**Control Genotype**	**Knockdown Genotype**
mCherry	$\frac{y^1, sc^*, v^1}{Y}; \frac{Act5C-GAL4}{+}; \frac{UAS-mCherry^{RNAi}}{+}$	$\frac{y^1 v^1}{Y}; \frac{Act5C-GAL4}{+}; \frac{UAS-RNAi}{+}$
		$\frac{y^1 v^1}{Y}; \frac{UAS-RNAi}{Act5C-GAL4}; \frac{+}{+}$
GD	$\frac{w^{1118}}{Y}; \frac{Act5C-GAL4}{+}; \frac{+}{+}$	$\frac{w^{1118}}{Y}; \frac{Act5C-GAL4}{UAS-RNAi}; \frac{+}{+}$
		$\frac{w^{1118}}{Y}; \frac{Act5C-GAL4}{+}; \frac{UAS-RNAi}{+}$
KK	$\frac{y^1, w^{1118}}{Y}; \frac{attP, y^+, w^{3\prime}}{Act5C-GAL4}; \frac{+}{+}$	$\frac{y^1, w^{1118}}{Y}; \frac{UAS-RNAi}{Act5C-GAL4}; \frac{+}{+}$
attp2	$\frac{y^1, v^1}{Y}; \frac{+}{Act5C-GAL4}; \frac{attP2}{+}$	$\frac{y^1, v^1}{Y}; \frac{+}{Act5C-GAL4}; \frac{UAS-RNAi}{+}$
Courtship controls	**Control Genotype**	**Knockdown Genotype**
mCherry	$\frac{y^1 v^1}{Y}; \frac{+}{+}; \frac{UAS-mCherry^{RNAi}}{R14H06-GAL4}$	$\frac{y^1 v^1}{Y}; \frac{+}{+}; \frac{UAS-RNAi}{R14H06-GAL4}$
		$\frac{y^1 v^1}{Y}; \frac{UAS-RNAi}{+}; \frac{+}{R14H06-GAL4}$
GD	$\frac{w^{1118}}{Y}; \frac{+}{UAS-Dicer2}; \frac{+}{R14H06-GAL4}$	$\frac{w^{1118}}{Y}; \frac{UAS-RNAi}{UAS-Dicer2}; \frac{+}{R14H06-GAL4}$

		$\frac{w^{1118}}{Y};\frac{UAS-Dicer2}{+};\frac{UAS-RNAi}{R14H06-GAL4}$
KK	$\frac{y^1,w^{1118}}{Y};\frac{attP,attP,y^+,w^{3\prime}}{UAS-Dicer2};\frac{+}{R14H06-GAL4}$	$\frac{y^1,w^{1118}}{Y};\frac{attP,UAS-RNAi}{UAS-Dicer2};\frac{+}{R14H06-GAL4}$
attp2	$\frac{y^1,v^1}{Y};\frac{+}{UAS-Dicer2};\frac{attP2}{R14H06-GAL4}$	$\frac{y^1,v^1}{Y};\frac{+}{UAS-Dicer2};\frac{UAS-RNAi}{R14H06-GAL4}$
Canton-S	$\frac{w^{1118}}{Y};\frac{+}{UAS-Dicer2};\frac{+}{R14H06-GAL4}$	$\frac{w^{1118}}{Y};\frac{+}{UAS-Dicer2};\frac{UAS-RNAi}{R14H06-GAL4}$
Temperature sensitive courtship controls	**Control Genotype**	**Knockdown Genotype**
GD(2)	$\frac{w^{1118}}{Y};\frac{tubP-GAL80^{ts}}{+};\frac{UAS-Dicer2}{R14H06-GAL4}$	$\frac{w^{1118}}{Y};\frac{tubP-GAL80^{ts}}{UAS-RNAi};\frac{UAS-Dicer2}{R14H06-GAL4}$
GD(3)	$\frac{w^{1118}}{Y};\frac{tubP-GAL80^{ts}}{UAS-Dicer2};\frac{+}{R14H06-GAL4}$	$\frac{w^{1118}}{Y};\frac{tubP-GAL80^{ts}}{UAS-Dicer2};\frac{UAS-RNAi}{R14H06-GAL4}$
RNA-sequencing controls	**Control Genotype**	**Knockdown Genotype**
GD	$\frac{w^{1118}}{Y};\frac{UAS-unc84-GFP}{+};\frac{UAS-Dicer2}{R14H06-GAL4}$	$\frac{w^{1118}}{Y};\frac{UAS-unc84-GFP}{UAS-RNAi};\frac{UAS-Dicer2}{R14H06-GAL4}$

2.2 Validation of RNAi knockdown by lethality assay

As a simple phenotypic test for assessing RNAi efficiency we measured the survival of flies during ubiquitous KD of target genes with the *Act5C-GAL4* driver (Table 2), as ubiquitous knockdown was expected to match the lethality observed during null mutations in *Set1*, *trx*, and *Mnn1*. Crosses were made between homozygous RNAi lines and the driver line *Act5C-GAL4/CyO* (Table 1). With this crossing scheme half of the progeny would receive Act5C-GAL4 and UAS-RNAi transgenes, and the other half would receive *CyO* and therefore be unable to induce the UAS transgenes. To track the inheritance of *Act5C-GAL4* versus *CyO,* the *CyO* chromosome has a visible dominant marker mutation giving flies the appearance of curly wings as opposed to the normal straight wings. Percent survival was then calculated by comparing the number of adult progeny with straight wings to the number with curly wings ($\% \, survival = \frac{N_{straightwingprogeny}}{N_{curlywingprogeny}}$). Significant changes in survival were determined with an unpaired t-test.

2.3 Memory tests with courtship conditioning assay

Flies were trained and tested for short-term memory (STM) or long-term memory (LTM) deficiency using the courtship conditioning assay as previously described (Koemans et al., 2017b; Siegel and Hall, 1979). Crosses were made as indicated in Table 1. In courtship conditioning a male fly is paired with a previously mated female (PMF) fly that rejects his courting attempts. Males that can remember this rejection reduce their future courting attempts on a different PMF fly, conversely, memory deficient flies do not. Males were isolated after eclosion and aged for 4 days in a 96 well plate containing 500 µL of media. For STM, 4-day old males were trained by pairing with a PMF for 1 hour and then placed back in isolation for 1 hour before introduction to a new PMF for testing. For testing, flies were placed in a 1 cm diameter mating chamber with transparent walls and courtship behaviour was recorded with a digital camera. LTM involved a 7 to 8 hour training session on 4-day old males, and a 20-24 hour latency to testing. A courtship index (CI) was determined for each male-female pair, calculated as the time the male spent courting over a 10 minute period. Tracked courting behaviours included orientation of male towards female, male pursuit of female, male wing “tapping”, male “licking” of female, and

attempted copulation (Koemans et al., 2017b). A memory index (MI) was calculated based on the formula: $MI=(CI_{naïve} - CI_{trained})/ CI_{naïve}$, to detect differences in courtship memory between KD flies and their respective controls. CIs were compared between naïve and trained flies using the Mann-Whitney test on GraphPad Prism version 7.03. A statistically significant reduction between naïve and trained flies' CIs indicates flies retained a memory of the training event and reduced their courting behaviour. For statistical comparison of MIs, a randomization test was performed with a custom bootstrapping R script (Koemans et al., 2017b). A statistically significant reduction in MI between control genotypes and KD genotypes indicates that some level of memory retention was lost due to the KD. In this manner, two evaluations of memory disfunction are statistically tested.

2.4 Brain dissections and microscopy

Adult and larval fly brains of crosses including *UAS-mCD8::GFP, R14H06-GAL4,* and *GAL80^{ts}* were dissected in PBS and fixed with 4% paraformaldehyde for 45 minutes at room temperature before mounting in Vectashield (Vector Laboratories). *UAS-mCD8::GFP* is a transgene that produces a cell surface glycoprotein fused to GFP for visualization. Brains were imaged using a Nikon SMZ800N fluorescent microscope. Images were processed using Nikon NIS Elements (version 5.02).

2.5 RNA-sequencing sample preparation

In this study the transcriptional effects of *trx*-KD in MB nuclei were captured by RNA-sequencing in naïve or courtship conditioned flies. Flies used for sequencing were snap frozen and stored at -80°C for future processing. To separate fly heads from the carcass, frozen flies were vortexed and passed through a series of sieves. Mushroom body nuclei were then extracted from the heads using the INTACT method, as previously described (Henry et al., 2012; Jones et al., 2018). The INTACT method required expression of the *UAS-unc84-GFP* transgene, which encodes for UNC84-GFP that selectively localizes to the nuclear membrane. The GFP tag on UNC84 allows for immunoprecipitation of nuclei from cell homogenates. Sample RNA extraction and library preparation were done as previously described using the PicoPure RNA isolation Kit (Invitrogen: KIT0204) and the Nugen Ovation Drosophila RNA-Seq System 1-16 Kit

(Nugen: NU035032) (Jones et al., 2018). During library preparation cDNA was sheared to 200-300 base pairs using a Covaris S2 sonicator. To assess library quality and size each sample was run on an Agilent 2100 Bioanalyzer with a High Sensitivity DNA kit. Libraries were then sequenced at the London Regional Genomics Centre on an Illumina NextSeq500 using the Illumina high output v2 75 cycle kit to a read length of 75 base pairs with single-end reads. Conditions for sequencing included flies that were trained with courtship conditioning as described above, and then re-isolated for only 1 hour before being collected along with age matched naïve flies. 50 male flies were collected per replicate. A subset of males were allowed to rest the full 20-24 hours after training to test that the memory deficiency was persistent.

2.6 RNA-sequencing data analysis

RNA-sequencing data was processed as previously described (Jones et al., 2018). Raw sequence reads were trimmed to a minimum base quality of 30 using Prinseq (version 0.20.4), equivalent to an error probability of 1 in 1000 base calls (Schmieder and Edwards, 2011). Trimmed reads were aligned using STAR (version 2.5.3a) to the *Drosophila melanogaster* genome (Ensembl release 88, dm6) (Aken et al., 2016; Dobin et al., 2013). Reads that aligned to one loci with >4 mismatches, and genes that mapped to *Drosophila* rRNA genes were removed.

Gene counts were obtained by HTSeq-count (version 0.7.1) using the default union setting (Anders et al., 2015). Y-chromosome and mitochondrial genes, along with genes with <50 counts in all conditions or genes with counts in fewer than 1/3 of samples in all conditions, were removed before differential expression analysis using DESeq2 (version 1.18.1) (Love et al., 2014). For a gene to be considered differentially expressed in our study it had to pass a cut-off of $q<0.05$, using the Benjamini & Hochberg procedure for p-value correction, and a fold change of >1.3 up or down.

2.7 Hypergeometric statistics, gene ontology, and network analysis

Overlap between datasets was determined in R (version 3.4.4), and Venn diagrams visualized using BioVenn (Hulsen et al. 2008; R Core Team 2016). Statistics of overlaps

in differentially expressed gene lists and comparisons to previously curated gene lists were calculated using a hypergeometric test in R. Gene ontology (GO) analysis was performed using PANTHER (version 13.1) (Ashburner et al., 2000; Mi et al., 2017) on the *trx*-KD differentially expressed genes. For biological process GO analysis all terms with $p<0.05$ (Fisher's Exact test with Bonferroni correction) were included. Network analysis was performed and visualized using the GeneMANIA app in Cytoscape (version 3.7) (Montojo et al., 2010; Shannon et al., 2003). The network was generated using annotations for physical interactions bioGRID small scale studies and predicted interactions.

Chapter 3

3 Results

3.1 *Act5C-GAL4* mediated knockdown of *Set1*, *trx*, and *Mnn1* dramatically reduces survival

Null mutations in *trx* and *Set1* have been shown to cause embryonic lethality (Breen, 1999; Hallson et al., 2012). In *Mnn1* null mutants, lethality occurs when there is an added external stressor (Papaconstantinou et al., 2005). Therefore, it was expected that ubiquitous KD of *Set1* and *trx*, and *Mnn1* with added temperature stress (reared at 29°C), would result in a similar phenotype as the null mutants. In this study, we used *Act5C-GAL4* to induce ubiquitous KD and screened for lethality to determine the efficiency of each *UAS-RNAi* line (Table 2). Lethality assays were done with a minimum of two RNAi lines that target different regions of the mRNA, and ideally were sourced from different transgenic libraries (*trx* and *Mnn1*). *Act5C-GAL4* mediated KD caused significant reduction in survival for males of 2 RNAi lines for *Set1*, *trx*, and *Mnn1* (Table 2), which were selected for further characterization. $Set1^{RNAi3}$ was the only RNAi line that did not cause lethality and was therefore not used for further analysis.

3.2 Genetic approach for repressing H3K4 methyltransferase expression and assessment of memory

In this study we aimed to characterize the roles of *Set1*, *trx*, and the *trx* associated *Mnn1*, in memory. As a first step, flies with genetic KD of *Set1*, *trx*, and *Mnn1* were screened for memory related phenotypes. We achieved this using MB specific GAL4 driven RNAi expression and the well-established courtship conditioning assay (Koemans et al., 2017b; Siegel and Hall, 1979). In courtship conditioning, male flies can be trained to reduce their latent courting behaviour after sufficient rejection from a non-receptive female. If genetic knockdown of target genes impeded memory we would expect the male flies to persist with courting after sexual rejection, and/or fail to remember the training as well as genetically matched controls. By training flies for 1 hour and then testing them after another hour of rest we were able to screen for phenotypes in STM, and by lengthening the

training to 7-8 hours and subsequently testing after 20-24 hours of rest, LTM was also screened. With this approach, unique patterns of memory dysfunction in *Set1*-, *trx*-, and *Mnn1*-KD flies were identified.

Table 2: Evaluation of RNAi efficiency using a lethality assay.

% survival was determined for each genotype indicated in Table 1. Significant changes in survival between flies with *Act-Gal4* and *Cyo* and *UAS-RNAi* were determined with an unpaired t-test. Flies were reared at 25°C unless otherwise noted.

Condition	**Control name/ Stock number**	**Survival (% ± SE)**	**n**	**p-value**
Controls	GD	166.7 ± 3.0	72	0.1196
	GD (29°C)	130.0 ± 54.4	23	0.6911
	KK (29°C)	114.3 ± 36.4	30	0.8285
	attP2	154.5 ± 36.5	84	0.1963
	mCherry	81.4 ± 15.3	107	0.2117
Set1-KD	33704	0	48	<0.0001
	38368	0	44	<0.0001
	40931	121.1 ± 45.8	84	0.3582
trx-KD	37715	0	35	0.0069
	31092	0	35	0.0208
Mnn1-KD	17701(29°C)	14.7 ± 12.4	39	0.0057
	110376 (29°C)	0	35	0.0042

3.2.1 *Set1* is required for STM and LTM in the MB

First we evaluated the role of the bulk H3K4 histone methyltransferase, *Set1*, in memory. For STM we measured the levels of courting after 1 hour of training with 1 control, $mCherry^{RNAi}$, and 2 RNAi lines, $Set1^{RNAi1}$ and $Set1^{RNAi2}$ (Figure 3 A, left panel). Courting of naïve and trained flies was significantly reduced in the $mCherry^{RNAi}$ control ($p<0.0001$), while there was no significant reduction in $Set1^{RNAi1}$ ($p=0.2155$) or $Set1^{RNAi2}$ ($p=0.0664$). We obtained similar results during the LTM test (Figure 3 A, right panel), which was measured after 7-8 hours of training and 20-24 hours of rest. For LTM (Figure 3 A, right panel) the $mCherry^{RNAi}$ control flies showed a significant reduction in courting in response to sexual rejection ($p<0.0001$), with no significant reduction for $Set1^{RNAi1}$ ($p=0.1033$) or $Set1^{RNAi2}$ ($p=0.3662$). Accordingly, $Set1^{RNAi1}$ (STM $p=0.0024$; LTM $p<0.0001$) and $Set1^{RNAi2}$ (STM $p<0.0001$; LTM $p=0.0034$) showed a significantly reduced memory index (MI) when compared to the control (Figure 3 B). These data show that *Set1* expression is required in the MB for both STM and LTM.

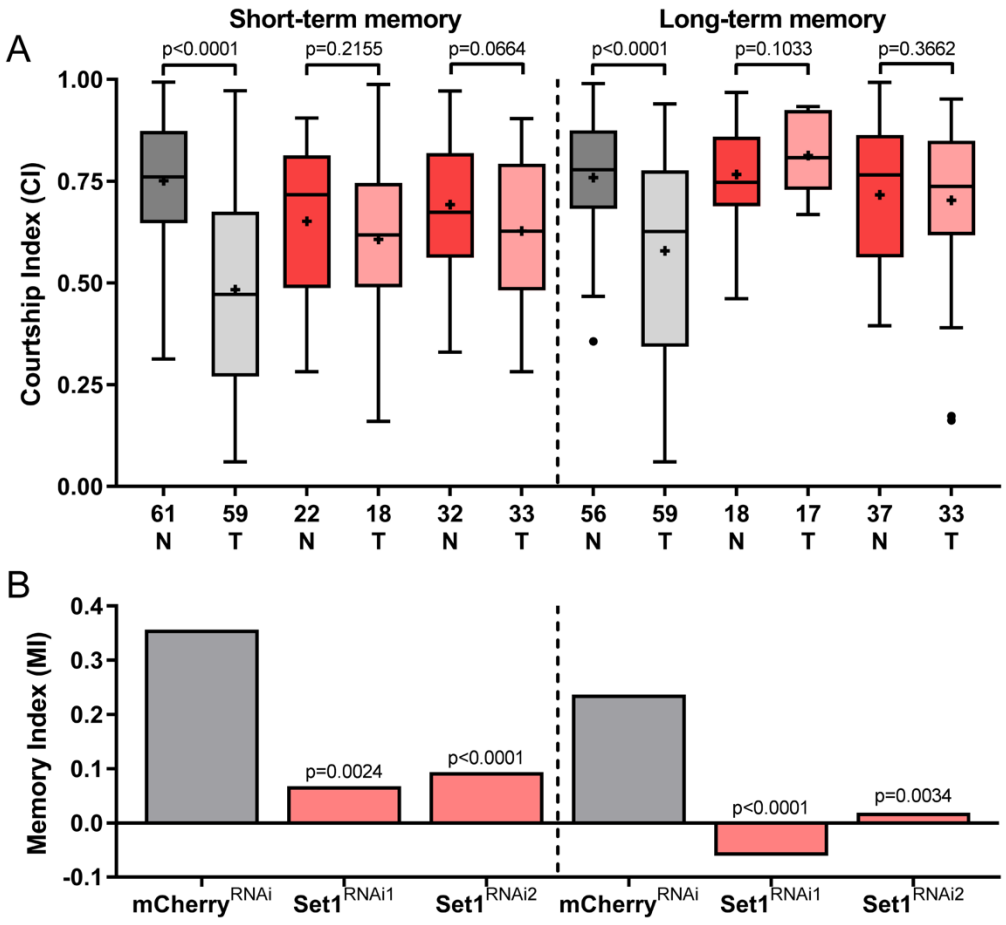

Figure 3: Mushroom body specific knockdown of *Set1* causes defects in memory.

(A) Boxplots show the distribution of Courtship Indices (CI) for naïve (N) and trained (T) flies of a single control (grey) and 2 *Set1* RNAi lines (red) for short-term and long-term memory assays. Statistical comparisons were made between naïve and trained flies within genotypes, showing loss of memory for *Set1*-KDs (Mann-Whitney Test). + indicates the mean. n is indicated along x-axis. (B) Comparison between knockdown and control memory indices (MI) shows a significant reduction in MI for both RNAi lines in STM and LTM tests (randomization test, 10,000 bootstrap replicates).

3.2.2 *trx* and *Mnn1* are required in the MB for LTM, but not STM

Interestingly, the pattern of memory dysfunction found with knockdown of *Set1* (Figure 3) was not seen following KD of the more specific H3K4 histone methyltransferase, *trx*. For the STM assay (Figure 4 A, left panel), courting was significantly reduced in the two control lines, GD ($p<0.0001$) and attP2 ($p<0.0001$), and the genetically paired RNAi lines, trx^{RNAi1} ($p<0.0001$) and trx^{RNAi2} ($p<0.0001$), during the test phase. Comparison of MIs showed that there was no loss of STM for trx^{RNAi1} ($p= 0.2992$) or trx^{RNAi2} ($p= 0.2726$) (Figure 4 B, left panel). However, when LTM was tested a significant reduction in courting was observed in the control flies (Figure 4 B, right panel), GD ($p<0.0001$) and attP2 ($p<0.0001$), whereas no reduction in courting behaviour was observed for knockdowns, trx^{RNAi1} ($p = 0.0617$) and trx^{RNAi2} ($p=0.3169$). Comparing LTM MIs (Figure 4 B, right panel), revealed that trx^{RNAi1} and trx^{RNAi2} were significantly reduced ($p=0.0015$ and $p=0.0192$) when compared to controls.

Because Mnn1 functionally interacts with trx in a catalytically active complex (Hughes et al., 2004; Milne et al., 2005), we next tested *Mnn1*-KD for memory phenotypes. In the STM assay (Figure 5 A, left panel), the GD ($p<0.0001$) and KK ($p=0.0004$) controls had a significant reduction in their time spent courting which was also observed in the respective knockdowns, $Mnn1^{RNAi1}$ ($p<0.0001$) and $Mnn1^{RNAi2}$ ($p=0.0003$). Comparisons of MIs (Figure 5 B, left panel) showed that there was a significant reduction in STM for $Mnn1^{RNAi1}$ ($p<0.0001$) but not in $Mnn1^{RNAi2}$ ($p= 0.5648$). In the LTM assay the GD ($p<0.0001$) and KK ($p<0.0001$) control lines showed a significant reduction in time spent courting (Figure 5 A, right panel), but this was not seen in the respective *Mnn1* knockdowns, $Mnn1^{RNAi1}$ ($p=0.3480$) or $Mnn1^{RNAi2}$ ($p=0.4426$). Comparing the memory of $Mnn1^{RNAi1}$ and $Mnn1^{RNAi2}$ lines to controls showed a significant reduction in MIs ($p<0.0001$; $p<0.0001$) (Figure 5 B, right panel).

Together, these data show that *trx* and its associated complex member *Mnn1*, are necessary for LTM in the MB, but are largely dispensable for STM.

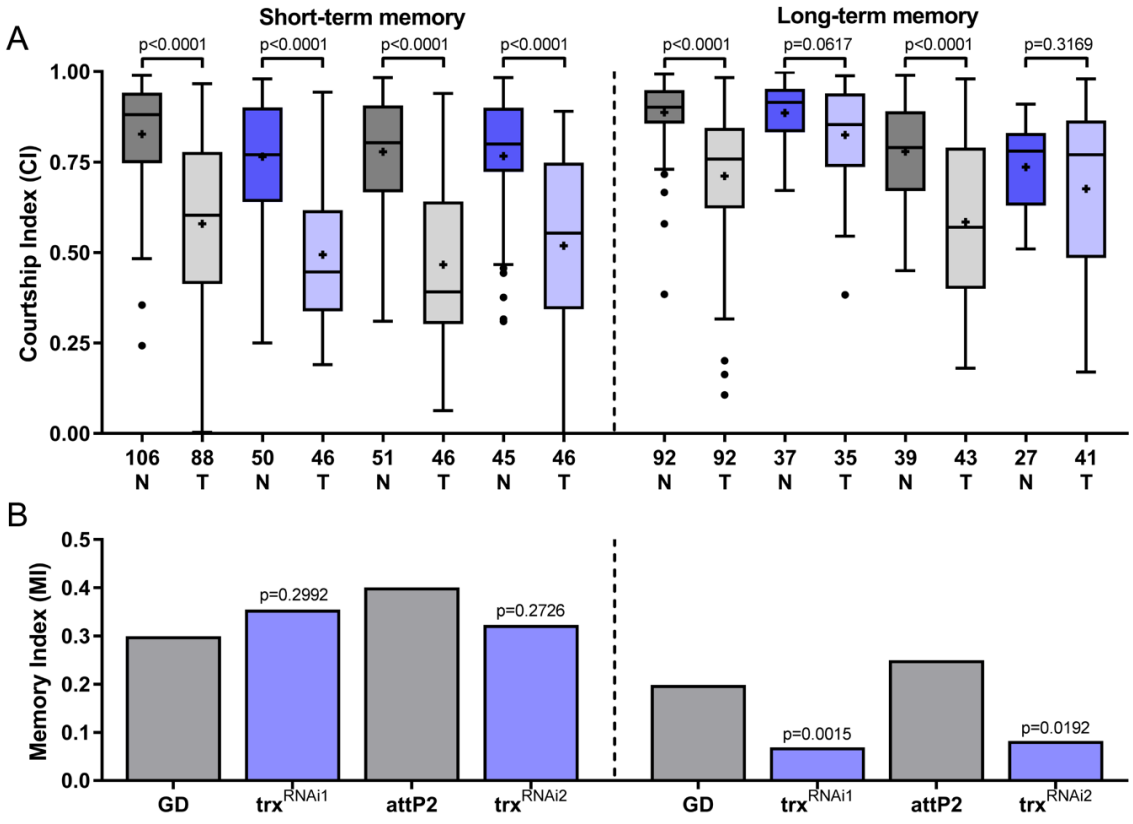

Figure 4: Mushroom body specific knockdown of *trx* causes defects in only long-term memory.

(A) Boxplots show the distribution of Courtship Indices (CI) for naïve (N) and trained (T) flies of 2 control groups (grey) and their respective *trx* RNAi lines (blue) for short-term and long-term memory assays. Statistical comparisons made between naïve and trained flies within genotypes shows loss of LTM during *trx*-KD (Mann-Whitney Test). + indicates the mean. n is indicated along x-axis. (B) Comparison between knockdown and control MIs shows a significant reduction in MI for both RNAi lines in the LTM test (randomization test, 10,000 bootstrap replicates).

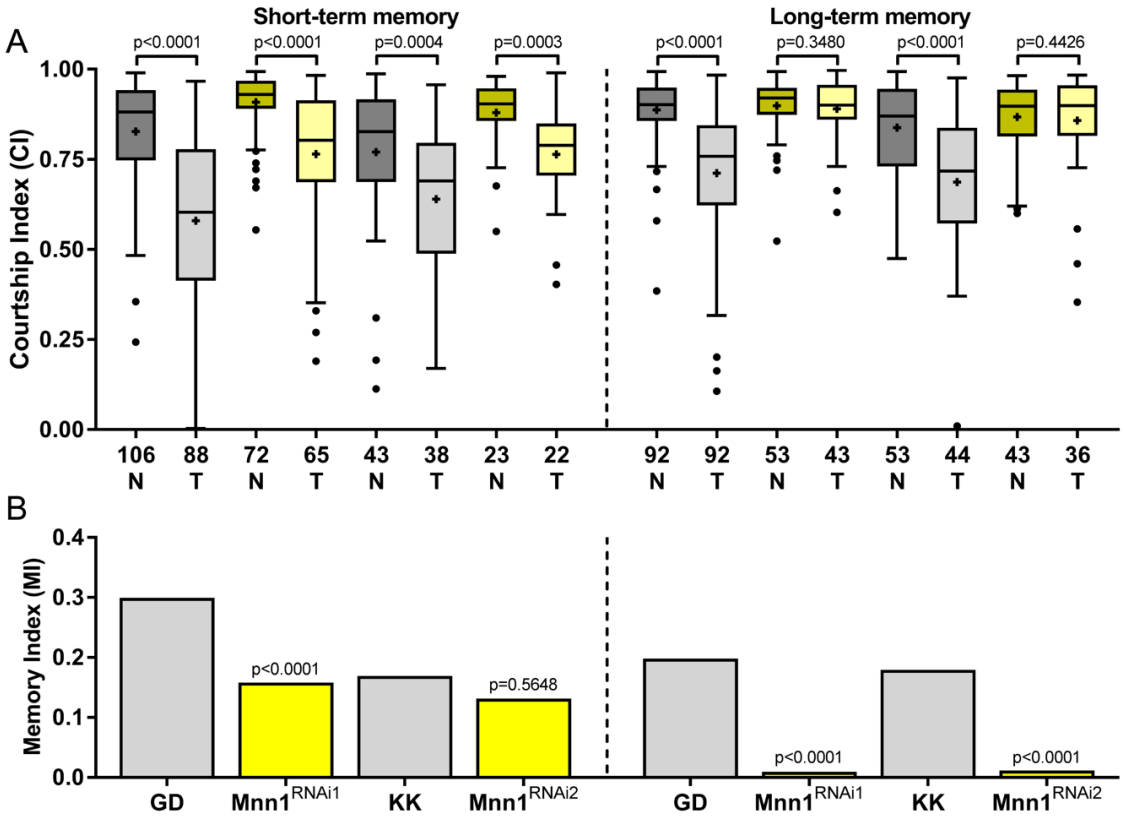

Figure 5: Mushroom body specific knockdown of *Mnn1* causes defects in memory.

(A) Boxplots show the distribution of Courtship Indices (CI) for naïve (N) and trained (T) flies of 2 control groups (grey) and their respective *Mnn1* RNAi lines (yellow) for short-term and long-term memory assays. Statistical comparisons made between naïve and trained flies within genotypes shows loss of LTM during *Mnn1*-KD (Mann-Whitney Test). + indicates the mean. n is indicated along x-axis. (B) Comparison between knockdown and control MIs shows a significant reduction in MI for $Mnn1^{RNAi1}$ line in the STM test, and for both RNAi lines in the LTM test (randomization test, 10,000 bootstrap replicates).

3.2.3 MB localized *trx* and *Mnn1* expression is required for memory only during the adult stage

Considering that *trx* and *Mnn1* may be required for normal neuronal development of the MB, or for adult processes like neuron identity maintenance and training responsive transcriptional regulation, it was of interest to know the temporal requirement of *trx* and *Mnn1* in memory. To narrow down the time requirements of *trx* and *Mnn1* expression for functional adult courtship memory various GAL4-UAS lines were generated.

The results from Figure 4 and 5 demonstrated the effects of *trx*- and *Mnn1-KD* using the *R14H06-GAL4* driver, which drives expression of GAL4 in post-mitotic MB neurons (Jenett et al., 2012). The post-mitotic MB neurons essential for memory originate during embryonic and larval development (Lee and Luo, 1999), therefore the effects of RNAi mediated KD are experienced in the MB during key developmental times. To determine if *trx* and *Mnn1* are required during development or the adult-phase we performed genetic knockdown of *trx* and *Mnn1* in the MB using the *R14H06-GAL4* driver in combination with a temperature sensitive GAL80 ($GAL80^{ts}$) to restrict KD to specific timepoints. GAL80 normally sequesters GAL4, preventing *UAS-GAL4* gene activation (Guarente et al., 1982), while mutant $GAL80^{ts}$ can be denatured at 29°C to allow for temperature specific GAL4 gene activation, or renatured at 18°C to restrict GAL4 gene activation, thus allowing precise GAL4 activation in flies reared at 29°C (Figure 6). The GAL4/GAL80ts system was used to induce temperature-specific expression of *trx*- and *Mnn1*-RNAi only during development (29°C to 18°C) or the adult stage (18°C to 29°C) (Figure 7 A).

Following LTM testing during the 29°C-18°C temperature cycle (Figure 7 A, left panel) it was observed that the CI for the control lines GD(2) ($p<0.0001$) and GD(3) ($p=0.0397$) had a significantly reduced CI after training (Figure 7 B, left panel) (number indicates preserved chromosome from the parental GD stock after generating crosses for experimentation [Table 1]). The 29°C-18°C developmental knockdowns for *trx* and *Mnn1*, trx^{RNAi1} ($p=0.0167$) and $Mnn1^{RNAi1}$ ($p=0.0213$), also had significant reductions in their courting after training. Comparisons of MIs for trx^{RNAi1} ($p=0.8672$) and $Mnn1^{RNAi1}$ ($p=0.7494$) showed no differences in the MIs of their respective controls (Figure 7 C, left

panel). The adult-specific temperature cycle, 18°C-29°C (Figure 7 A, right panel), showed that controls, GD(2) ($p<0.0001$) and GD(3) ($p<0.0001$), remembered their training by demonstrating reduced courting in trained flies (Figure 7 B, right panel). In contrast, adult-specific KD of trx^{RNAi1} ($p=0.3054$) and $Mnn1^{RNAi1}$ ($p=0.1338$) maintained high courtship activity during the test phase. Likewise, the MIs of trx^{RNAi1} ($p=0.021$) and $Mnn1^{RNAi1}$ ($p=0.0048$) were significantly reduced when compared to their controls (Figure 7 C, right panel).

These data show a pattern of memory dysfunction that indicates that both *trx* and *Mnn1* are required during adult stages of the fly for normal LTM function, but are dispensable during MB development.

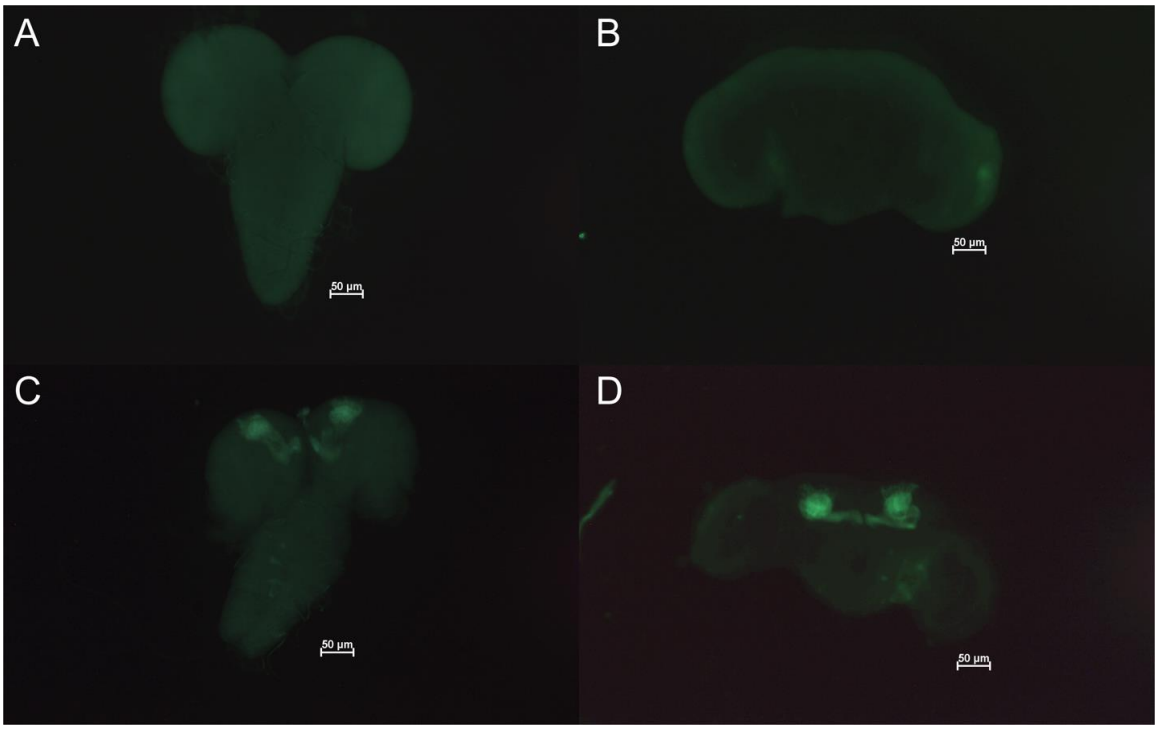

Figure 6: *GAL80^{ts}* allows for temperature dependent *UAS-GAL4* gene expression in the mushroom body.

GAL80^{ts} was validated as a means to limit *UAS-GAL4* gene activation by observing *UAS-mCD8::GFP* expression with fluorescence microscopy. No GFP expression was observed in the MBs of male flies raised at 18°C during the larval (A) or adult stage (B). GFP expression was observed in in the MBs of male flies raised at 29°C during the larval (C) and adult stage (D). Bars indicate the scale.

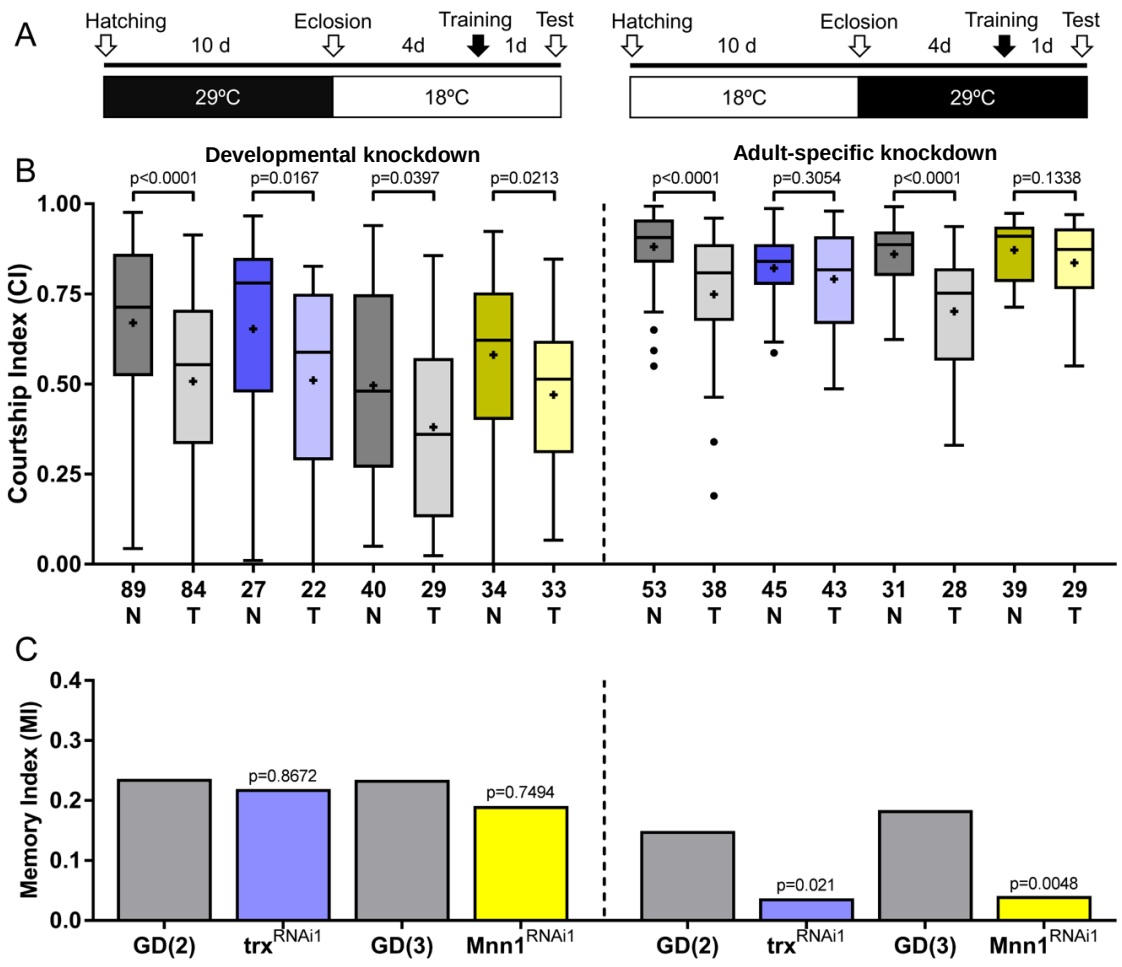

Figure 7: Long-term memory defects in *trx* and *Mnn1* are limited to adult-specific knockdowns.

(A) Timelines for courtship conditioning and temperature induced knockdown during development (left panel) and in adults (right panel) (B) Boxplots show the distribution of Courtship Indices (CI) for naïve (N) and trained (T) flies during a LTM assay following temperature rearing indicated in (A). 2 control groups (grey) and either a *trx* (blue) or *Mnn1* (yellow) RNAi line are shown. Statistical comparisons made between naïve and trained flies within genotypes shows loss LTM during adult-specific knockdown (Mann-Whitney Test). + indicates the mean. n is indicated along x-axis. (C) Comparison between knockdown and control MIs shows a significant reduction in MI for both *trx* and *Mnn1* during an adult-specific knockdown only (randomization test, 10,000 bootstrap replicates).

3.3 RNA-sequencing of *trx*-KD MB nuclei

Two guiding hypotheses instructed the manner in which transcriptional changes from *trx*-KD were related back to memory. The first was that post-mitotic MB neuronal identity and function could be dependent on gene expression programs regulated in part by *trx*. The second is that gene expression changes in response to courtship conditioning may also be regulated in part by *trx*. Therefore, in order to identify *trx*-dependent transcription in the MB, RNA-sequencing was done on naïve flies and flies that experienced courtship conditioning.

To identify transcriptional changes in *trx*-KD flies, we isolated MB nuclei from fly heads using the INTACT method, followed by RNA isolation and library preparation for RNA-sequencing (Henry et al., 2012; Jones et al., 2018). Libraries were made from crosses of *trx*-KD flies and their genetic background controls (Table 1), before (naïve) or after courtship conditioning (trained). Naïve control (n=3) and *trx*-KD (n=3), along with one-hour post-training control (n=4) and *trx*-KD (n=4). Libraries were then sequenced and trimmed reads were aligned to the *Drosophila* genome (Table 3). An average of 31,698,150 reads were generated across all samples, with 79.91% uniquely aligning with ≤4 mismatches. Good quality non rRNA genic counts were generated for use in differential expression analysis (Table 4). Additional gene removal included Y-chromosome and mitochondrial mapped genes, along with genes that had <50 counts in all conditions or genes with counts in fewer than 1/3 of samples in all conditions. To ensure nuclei pulldown was enriched for MBs, expression levels of a number of well characterized MB-enriched and MB-depleted genes were compared to the expression levels of whole head input samples (Figure 8) (Jones et al., 2018).

After filtering, 8161 genes were used for differential expression analysis. Differentially expressed genes were identified from a number of different comparisons: 1) trained control vs naïve control (CTvCN); 2) trained *trx*-KD vs naïve *trx*-KD (KTvKN); 3) naïve *trx*-KD vs naïve control (KNvCN); 4) trained *trx*-KD vs trained control (KTvCT) (Figure 9; for a full list of differentially expressed genes see Appendix B-E). Genes were considered differentially expressed if they had an adjusted p-value of <0.05 and a fold

difference of 1.3 up or down. GO term analysis was performed on upregulated and downregulated genes for each experimental comparison (Appendix F-M). These gene lists were then used for additional downstream analysis to identify candidate *trx* target genes involved in basal MB function or memory related processes.

Table 3: Read distribution of RNA-sequencing data.

Distribution of reads from RNA-sequencing for replicates in naïve *trx*-KD flies (KN) and *trx*-KD flies 1 hour after training (KT), and the naïve control flies (CN) and control flies 1 hour after training (CT). Total reads are the raw reads generated for each sequenced sample. Trimmed reads passed filtering with a quality score greater than 30. rRNA reads mapped to rRNA genes. Unmapped reads did not align to the *Drosophila* genome. Multi-mapped reads aligned to more than 1 loci in the *Drosophila* genome. Uniquely mapped reads aligned to a single loci, and mapping to a single loci with >4 mismatches is also indicated. Good reads are non-rRNA reads that were used to generate count tables for genic features (Table 4).

Sample Name	Total reads	Trimmed	rRNA	Non-rRNA	Unmapped	Multi-Mapped	Uniquely Mapped	>4 Mismatch	Good Reads
KT1	32,940,626	32,831,353	119,782	32,711,571	3,164,202	1,933,099	27,614,270	212,203	27,402,067
KT2	22,546,663	22,459,977	44,817	22,415,160	2,279,661	1,307,831	18,827,668	144,606	18,683,062
KT3	37,986,850	37,655,634	21,643	37,633,991	5,698,503	4,100,803	27,834,685	266,309	27,568,376
KT4	24,013,780	23,896,821	22,288	23,874,533	2,721,866	2,796,059	18,356,608	157,531	18,199,077
KN1	63,493,676	63,235,630	99,398	63,136,232	7,980,327	3,686,783	51,469,122	428,850	51,040,272
KN2	34,276,814	34,139,606	84,796	34,054,810	4,187,106	2,005,845	27,861,859	234,679	27,627,180
KN3	33,756,760	33,569,533	122,961	33,446,572	4,297,048	1,946,699	27,202,825	224,338	26,978,487
CT1	22,014,500	21,943,586	117,803	21,825,783	2,095,500	1,359,924	18,370,359	142,055	18,228,304
CT2	30,323,737	30,205,528	153,269	30,052,259	3,411,191	2,090,946	24,550,122	206,218	24,343,904
CT3	32,522,009	32,414,050	162,630	32,251,420	3,168,106	1,806,108	27,277,206	221,192	27,056,014
CT4	30,878,184	30,804,449	114,700	30,689,749	4,274,547	2,104,862	24,310,340	191,886	24,118,454
CN1	25,034,157	24,934,137	112,901	24,821,236	3,255,010	1,513,508	20,052,718	165,624	19,887,094
CN2	19,490,513	19,392,667	67,141	19,325,526	2,287,401	1,125,142	15,912,983	125,465	15,787,518
CN3	34,495,833	34,331,261	118,381	34,212,880	4,380,617	1,868,134	27,964,129	230,848	27,733,281

Table 4: Count distribution and efficiency of RNA-sequencing results.

Distribution of count data from sample reads indicated in Table 3. Genic counts mapped to introns and exons and were used for downstream analysis. Excluded from downstream analysis are mapped reads that could not be characterized (no feature) and reads that could be assigned to multiple features (ambiguous). Overall efficiency indicates the number of genic counts produced from total reads (Table 3).

Sample Name	Genic	No Feature	Ambiguous	Overall Efficiency
KT1	24,832,446	378,237	2,191,384	75.39
KT2	16,983,547	262,024	1,437,491	75.33
KT3	24,820,063	596,166	2,152,147	65.34
KT4	16,475,007	312,888	1,411,182	68.61
KN1	46,197,991	836,013	4,006,268	72.76
KN2	24,970,745	453,814	2,202,621	72.85
KN3	24,374,410	455,543	2,148,534	72.21
CT1	16,516,701	260,498	1,451,105	75.03
CT2	22,042,313	397,413	1,904,178	72.69
CT3	24,494,815	409,863	2,151,336	75.32
CT4	21,890,908	338,143	1,889,403	70.89
CN1	17,953,843	292,551	1,640,700	71.72
CN2	14,233,556	236,188	1,317,774	73.03
CN3	25,012,185	445,104	2,275,992	72.51

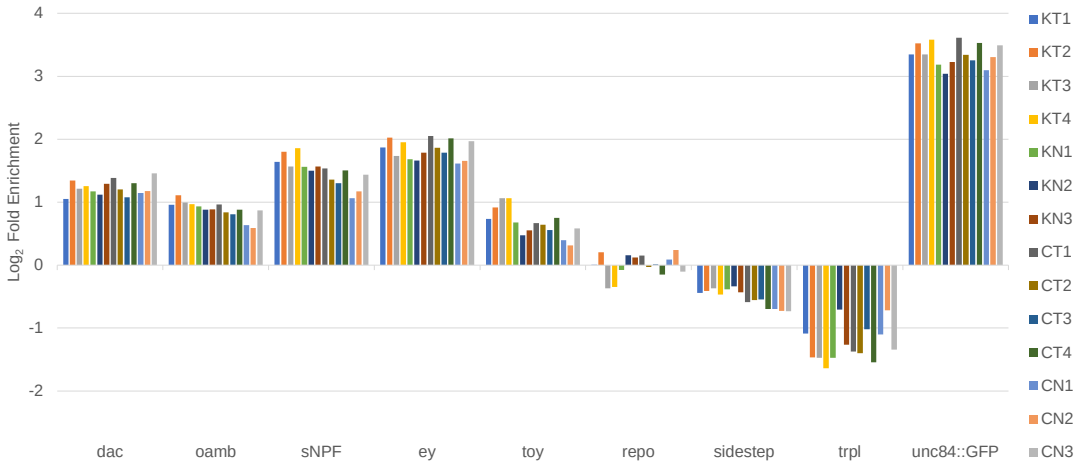

Figure 8: RNA isolated for RNA-sequencing are MB enriched.

Normalized counts from KT, KN, CT, and CN conditions were compared to counts for RNA isolated from whole head inputs from a previous sequencing study to show relative expression (Jones et al., 2018). Bar graphs show the relative expression of transgenic *unc84-GFP* as well MB-enrich genes (dac, oamb, sNPF, ey, toy), and MB-depleted genes (repo, sidestep, trpl) in INTACT isolated nuclei vs nuclei from the whole head. These profiles indicate a MB-enriched profile for our sequencing results (Jones et al., 2018).

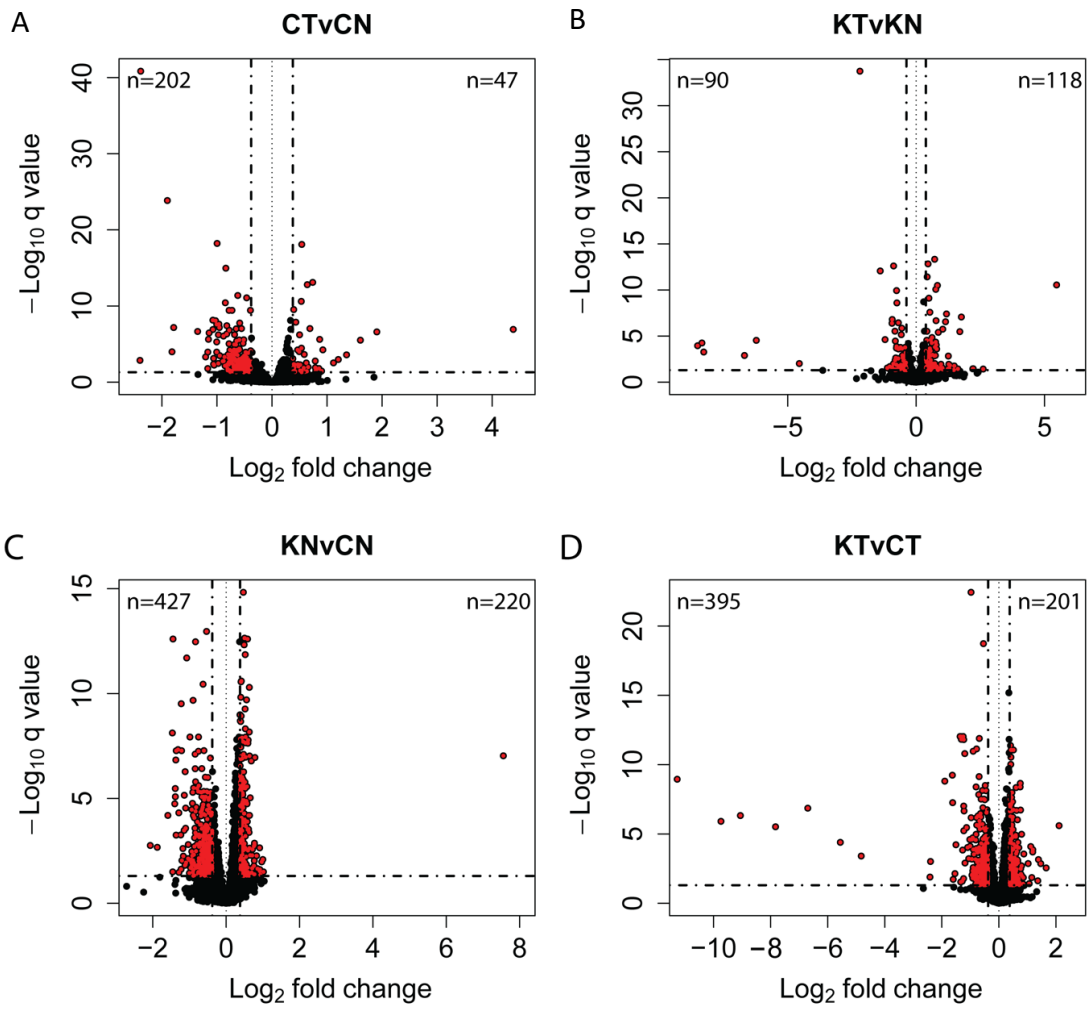

Figure 9: Visualization of differentially expressed genes in *trx*-KD and control flies with and without training.

Volcano plots of differential expression analysis for each experimental comparison used in this study. 8191 genes used for differential expression analysis are plotted, and differentially expressed genes are highlighted in red (Benjamini–Hochberg corrected $q<0.05$, fold change >1.3 up or down). Experimental conditions are, (A) trained control vs naïve control (CTvCN); (B) trained *trx*-KD vs naïve *trx*-KD (KTvKN); (C) naïve *trx*-KD vs naïve control (KNvCN); (D) trained *trx*-KD vs trained control (KTvCT).

3.3.1 *trx*-dependent regulation of candidate mushroom body identity genes

Previously, epigenetic regulators have been shown to be important for the establishment and maintenance of post-mitotic neuron identity (Hobert, 2011; Huang et al., 2015; Lim et al., 2009; O'Meara et al., 2010; You et al., 2015). Related gene regulatory programs required for neuronal differentiation and identity maintenance have also been shown to be required for specialized neuron functions (Deneris and Hobert, 2014). Therefore, in this study it was reasoned that *trx* may be required to establish and maintain the normal expression of genes involved in determining MB neuron identity, and likewise for the expression of certain specialized functions of the MB in memory.

To identify genes that were related to MB identity, INTACT and RNA-sequencing were performed on MB nuclei (Henry et al., 2012; Jones et al., 2018). Since neuronal identity requires stable gene expression, dysfunctional transcription following *trx*-KD should be continuous regardless of the flies experience. Therefore, experimental conditions KNvCN and KTvCT (Figure 9 C and D) were used to determine the effects of *trx*-KD relative to controls before and after training. Indeed, a significant portion of genes were found to overlap following *trx*-KD ($p=3.12 \bullet 10^{-72}$; n=129), regardless of the flies experience with courtship conditioning (Figure 10 A). Next, GO analysis was performed on these 129 overlapping genes and revealed no functional enrichment for biological functions. A comparison was then made between the 129 stably downregulated *trx* target genes and previously identified MB-enriched genes (Appendix N). The MB-enriched gene list used for comparison consists of genes that were previously shown to have expressions levels at >2 fold enrichment in the MB as compared to expression levels in the whole head (Jones et al., 2018). It was reasoned that these genes were so highly expressed in the MB because they were critical for normal MB function, and therefore potentially critical for MB neuron identity. Within the 129 *trx*-regulated genes 10 MB-enriched genes ($p=1.57 \bullet 10^{-5}$) were identified which represents a 5.36 fold enrichment over what would be expected by chance (Figure 10 B). The 10 overlapping genes from Figure 10 B represent candidate *trx*-regulated MB-identity genes, these genes are listed and briefly described in Table 5.

Of the 10 candidate MB identity genes, *lactate dehydrogenase* (*Ldh*) was chosen for further investigation of memory related phenotypes using the courtship conditioning assay. Ldh is an enzyme that causes the reversible metabolism of lactate into pyruvate. Ldh is of particular interest to this study because it has previously been shown that astrocyte derived lactate is necessary for rodent LTM formation (Suzuki et al., 2011), along with the observation that increased pyruvate metabolism occurs in *Drosophila* MBs following learning (Plaçais et al., 2017). Preliminary LTM analysis of *Ldh*-KD flies revealed that courting is not significantly reduced from naïve to trained flies following knockdown ($p=0.0741$), while controls exhibited reduced courting following training ($p<0.0001$) (Figure 10 C).

These data show that *trx* is required to maintain expression of 10 genes found to be highly enriched in the MB (Figure 10 B and Table 5). Furthermore, these 10 genes are candidates for *trx*-mediated maintenance of MB identity. Preliminary analysis of the candidate gene *Ldh* revealed that *Ldh*-KD interferes with normal memory during courtship conditioning and may be a possible downstream effector of *trx*-regulated memory processes.

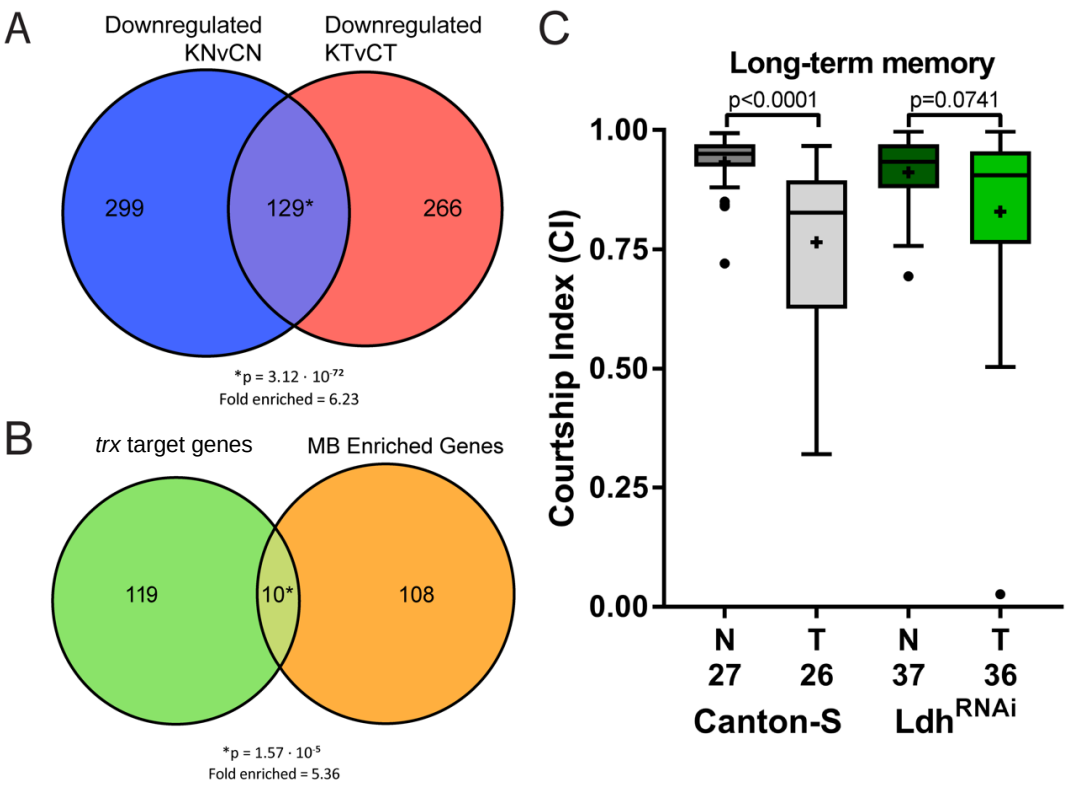

Figure 10: Effects of *trx*-KD on mushroom body gene expression.

(A) Venn diagram showing the overlap between downregulated genes in KNvCN and KTvCT, overlap represents genes downregulated independent of courtship conditioning task engagement. The overlap of 129 genes is larger than expected by random chance, based on a hypergeometric test ($p= 3.12 \cdot 10^{-72}$, 6.23 fold enrichment). (B) Venn diagram showing a significant enrichment for MB-enriched genes among *trx* target genes in the MB (hypergeometric test: $p=1.57 \cdot 10^{-5}$, fold change = 5.36. (C) Boxplots show the distribution of Courtship Indices (CI) for naïve (N) and trained (T) flies of the Canton-S control line and the Ldh^{RNAi} line in a long-term courtship memory assay. Statistical comparisons made between naïve and trained flies within genotypes shows memory dysfunction following *Ldh*-KD (Mann-Whitney Test). + indicates the mean. n is indicated along x-axis.

Table 5: List of candidate *trx* regulated mushroom body identity genes.

FlyBase ID	Gene name	Description
FBgn0001258	Ldh	Dehydrogenase for interconversion of lactate and pyruvate
FBgn0001218	Hsc70-3	Heat shock chaperone, assists in protein folding
FBgn0259219	CG42319	n/a
FBgn0260942	bond	Acyltransferase for fatty acid synthesis
FBgn0027836	Dgp-1	GTP-binding protein for translation initiation and elongation
FBgn0039411	dysf	Transcription factor for RNA polymerase II
FBgn0027586	CG5867	n/a
FBgn0031114	cactin	RNA splicing
FBgn0031264	CG11835	Putative nascent protein binding for protein localization
FBgn0031307	MFS3	Transmembrane transporter of amino acids and anions

3.3.2 *trx*-dependent regulation of genes in response to courtship conditioning

Since epigenetic regulators are broadly implicated in regulating memory responsive gene expression, it is possible that *trx* may also regulate genes in response to courtship conditioning. In support of this hypothesis are previous studies that showed enrichment of H3K4me3 in rodents following training (Gupta et al., 2010), along with CREB transcriptional assemblies around the TSS of *trx* 1 hour following aversive shock conditioning in *Drosophila* (Hirano et al., 2016). The 1 hour time point has also been shown to be a critical timepoint for LTM dependent gene transcription in *Drosophila* (Jones et al., 2018), and in such a way *Kmt2a* or *trx* may be required then to regulate gene transcription via H3K4 methylation.

RNA-sequencing analysis was performed on nuclei extracted from *trx*-KD MB using the INTACT method on naïve flies and flies 1 hour after training (Henry et al., 2012; Jones et al., 2018). The consistency of memory phenotypes between control and *trx*-KD flies was first validated with courtship conditioning because the combination of transgenic constructs for simultaneous *trx*-KD and nuclear tagging for nuclear immunoprecipitation could cause different titrations of GAL4. Using a small subset of flies from crosses made for RNA-sequencing (at least 5 per replicate, per condition), long-term courtship memory was tested in *trx*-KD flies co-expressing *UAS-unc84-GFP*. When the MI was measured there was a significant reduction in the memory of the *trx*-KD flies compared to their controls ($p = 0.0138$) (Figure 11 A). Thus, co-expression of *UAS-unc84-GFP* in *trx*-KD flies did not interfere with the memory deficit previously detected in *trx*-KD alone.

The first option for courtship conditioning dependent gene regulation by *trx* is that *trx* may be involved in inducing gene expression during LTM formation. To determine memory induced genes, upregulated genes in the CTvCN experimental comparison were investigated (Figure 9 A). Upregulated genes in this group represent genes that were induced in controls in response to training and include the known memory gene *jeb* (Gouzi et al., 2011), putative markers of neuron activation *Hr38* and *sr* (Chen et al., 2016; Fujita et al., 2013; Lutz and Robinson, 2013), and neuropeptides *spab* and *proc*. Some additional neuron activity induced genes were also identified including *CG4577*, *CG14186*,

CG17778, *Cdc7*, and again *jeb* (Chen et al., 2016). If *trx* was primarily involved in inducing memory genes after training, then the overlap of upregulated genes in the KTvKN compared to upregulated CTvCN would be no greater than chance alone, suggesting a failure to induce gene expression in the *trx*-KD. However, a significant overlap was detected between these two groups (Figure 11 B), including 27 genes, at an extremely high enrichment (hypergeometric test: $p= 6.86 \bullet 10^{-39}$, fold enrichment = 39.73). Overlapping genes included *jeb*, *Hr38*, *sr*, *CG14186*, and *Cdc7*. This shows that many memory induced genes are not effected in trx knockdown flies. Of the 20 genes that were only upregulated in controls following courtship conditioning a few candidates were identified, including neuropeptides *proc* and *spab*, and known activity induced genes *CG4577* and *CG17778*. These data indicate that if *trx* may play a role in regulating a subset of memory-induced genes. Interestingly, additional neuronal activity induced genes (*Glec* and *CG13055*) were seen to be induced after memory formation in *trx*-KD flies, but not in controls.

To identify genes additional genes that might be affected by *trx*-KD in response to training, genes in the KTvCT experimental comparisons were examined (Figure 9 D; Appendix E). Again, downregulated genes were primarily focused on for investigation because they likely represent direct targets of *trx* because of the established role *trx* and H3K4me has in gene activation. GO term analysis identified biological functions that were related to post transcriptional processing of RNA. Examples of terms in this GO analysis include “ribosome biogenesis”, “ncRNA metabolic process”, and “RNA modification” (Figure 12 A; Appendix M). Indeed, of the 395 downregulated KTvCT genes, 44 were annotated with the term “RNA processing” (Appendix M). Given the high amount of redundancy of genes contained within these functional categories, the genes annotated as “RNA processing” were selected for further investigation, as it represented a large number of genes (n=44) while still being among the 10 highest fold enriched terms (Figure 12 A). Finally, using network analysis of predicted functional interactions a network of 21 RNA metabolic process genes (Figure 12 B) were identified from 44 the “RNA processing” annotated genes. The networked genes are listed and briefly described in Table 6.

Taken together, these data show that *trx* is required for the induction of some genes after courtship training, and is also required for the maintenance of expression for genes

related to RNA processing in a task dependent manner. Specifically, *trx* seems to be responsible for regulating the expression of RNA processing genes that act in a predicted network for RNA processing.

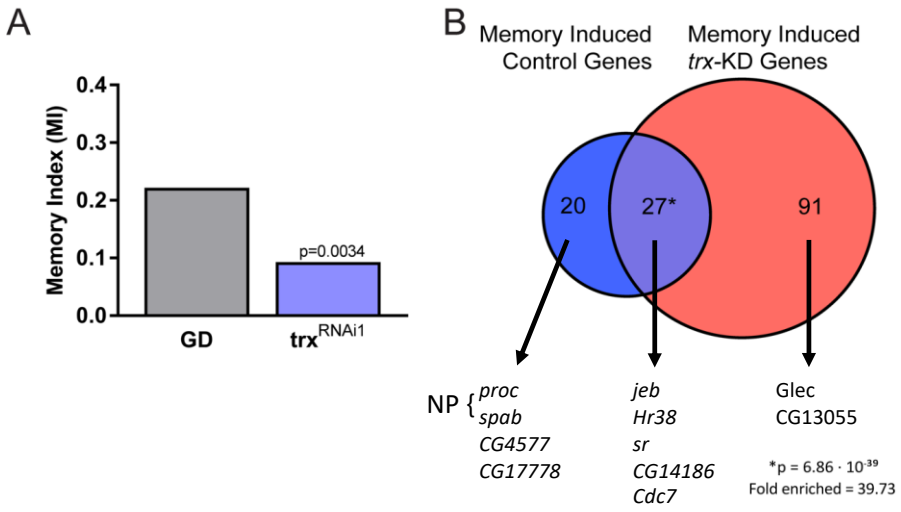

Figure 11: Effects of *trx*-KD on courtship conditioning dependent gene expression.

(A) Comparison between MIs of knockdown trx^{RNAi1} and GD controls for RNA-sequencing shows a significant reduction in memory (randomization test, 10,000 bootstrap replicates). (B) Venn diagram showing the overlap between memory-induced genes of the control and *trx*-KD flies following courtship conditioning. The overlap of 27 genes is larger than expected by random chance, based on a hypergeometric test ($p= 6.86 \bullet 10^{-39}$, 39.73 fold enrichment). Candidate neuronal activity induced genes are indicated below the diagram, along with neuropeptide genes (NP)

A

GO terms for downregulated KTvCT genes	Fold Enrichment	p-value
ribosomal large subunit assembly	11.22	$3.60 \cdot 10^{-2}$
ribosomal large subunit biogenesis	6.19	$4.69 \cdot 10^{-2}$
RNA modification	4.83	$2.84 \cdot 10^{-2}$
rRNA processing	4.76	$1.41 \cdot 10^{-3}$
rRNA metabolic process	4.41	$3.69 \cdot 10^{-3}$
ribosome biogenesis	3.78	$2.09 \cdot 10^{-3}$
ncRNA processing	3.66	$3.11 \cdot 10^{-4}$
ncRNA metabolic process	3.27	$2.76 \cdot 10^{-4}$
ribonucleoprotein complex biogenesis	3.07	$1.04 \cdot 10^{-2}$
RNA processing	3.01	$1.10 \cdot 10^{-6}$

B

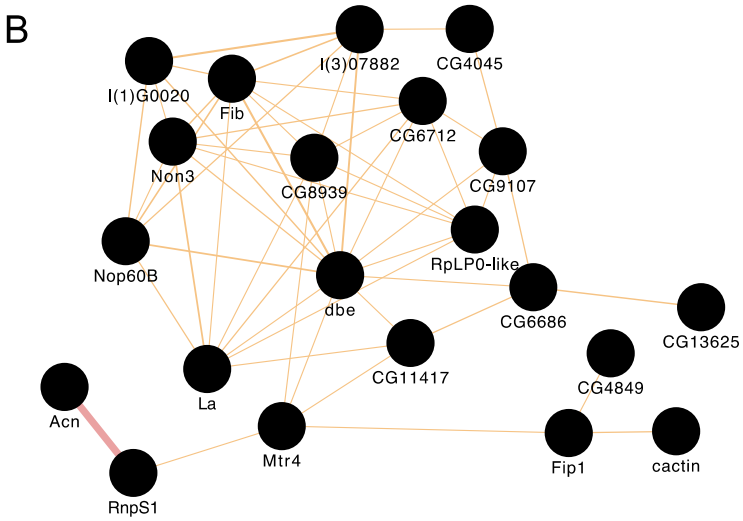

Figure 12: Functional association and interaction of downregulated genes in trained flies following *trx*-KD.

(A) Gene ontology (GO) enrichment analysis was performed on downregulated genes from trained flies during *trx*-KD. p-values and fold enrichment indicated in table (Fisher's Exact test with Bonferroni correction). (B) Of the 44 "RNA processing" genes identified by GO analysis in (A), 21 of them form a single network based on physical and predicted functional interactions by geneMANIA.

Table 6: List of genes found to network in the "RNA processing" GO term from downregulated KTvCT genes.

FlyBase ID	Gene name	Description
FBgn0031764	CG9107	Ribosomal small subunit assembly
FBgn0032388	CG6686	RNA splicing
FBgn0039566	CG4849	RNA splicing
FBgn0037707	RnpS1	RNA splicing
FBgn0011638	La	RNA polymerase III transcription termination
FBgn0263198	Acn	RNA splicing and apoptosis functions
FBgn0031114	cactin	RNA splicing
FBgn0030720	CG8939	rRNA methyltransferase
FBgn0032408	CG6712	Ribosomal large subunit assembly
FBgn0025629	CG4045	tRNA methyltransferase
FBgn0024364	CG11417	Pre-rRNA processing
FBgn0010926	l(3)07882	Ribosomal small subunit assembly
FBgn0038585	Non3	Mitotic spindle assembly
FBgn0003062	Fib	rRNA methyltransferase
FBgn0033485	RpLP0-like	Ribosomal large subunit assembly
FBgn0027330	l(1)G0020	RNA acetyltransferase
FBgn0020305	dbe	Ribosomal small and large subunit assembly
FBgn0037255	Fip1	pre-mRNA cleavage for polyadenylation
FBgn0001986	Mtr4	RNA helicase and RNA splicing
FBgn0039210	CG13625	RNA splicing
FBgn0259937	Nop60B	rRNA pseudouridylate synthase

Chapter 4

4 Discussion

In this study, *Set1*, *trx*, and the *trx* associated *Mnn1* were all shown to be necessary for regulating courtship memory in *Drosophila*. Critically, this study demonstrated a requirement for *trx* and *Mnn1* in LTM in an adult-specific manner, and are dispensable for STM and development in the MB. Through cell specific RNA-sequencing in the MB, the memory centre of the fly brain, specific transcriptional changes in response to *trx*-KD were identified. The results of RNA-sequencing identified two possible routes that *trx* is necessary for memory function, 1) by maintaining expression of MB enriched genes such as *Ldh* to maintain MB identity; 2) by maintaining and promoting the expression of genes in response to courtship conditioning, including genes involved in RNA processing.

4.1 Histone H3K4 methyltransferases play a critical role in *Drosophila* memory

This study demonstrated that MB-specific knockdown of *Set1* caused loss of both short-term and long-term courtship memory (Figure 3). This effect is likely due to the genome wide or "bulk" histone modification it is known to catalyze (Hallson et al., 2012; Mohan et al., 2011; Wu et al., 2008). With such broad targeting across the genome *Set1* target genes could include a variety of developmental and adult-specific genes that contribute to both phenotypes. Conversely, *trx*-KD in the mushroom revealed that *trx* is required for LTM and dispensable for STM (Figure 4). This difference could arise from the increased specificity of *trx* for specific loci only relevant to LTM processes instead of pan-genomic activity (Guenther et al., 2005; Hallson et al., 2012).

Previous studies have identified that mammalian orthologues of *trx* (Figure 2) are required for murine memory (Gupta et al., 2010; Kerimoglu et al., 2013, 2017), yet the requirement in different phases of memory was not clearly defined. This is partly due to the fact that primary memory assays in rodents are limited mostly to longer time frames associated with LTM. However, rodent novel object recognition tests have demonstrated a need for *Kmt2b* in short-term object recognition memory, but this was not recapitulated in *Kmt2a* knockouts. The discrepancy between the rodent paralogues may arise from

differential specificity related to isoform-specific PTM or protein interactions (Kerimoglu et al., 2017). For example, it has been recently shown that protein kinase Msk1 can control KMT2A-dependent gene expression, while not necessarily altering its binding (Wiersma et al., 2016). Additionally, it is well established that KMT2A and KMT2B must both be proteolytically cleaved by Taspase1 forming independent amino- and carboxyl-terminals, before activating the *Hox* gene region (Hsieh et al., 2003). The amino- and carboxyl-terminals have independent binding sites, thereby facilitating different routes to gene regulation (Petruk et al., 2008; Schwartz et al., 2010). Having different active terminals for one protein results in a multilayered path to gene regulation that is difficult to unravel between the different types and phases of memory.

Part of what gives trx its specificity is the co-factor Mnn1 (Hughes et al., 2004; Milne et al., 2005). In this study it appears that *trx* and *Mnn1* converge on LTM phenotypes, with *Mnn1*-KD having a clear effect on LTM function like *trx*. This phenotypic convergence is also consistent through developmental stages, with both *trx* and *Mnn1* being dispensable to MB derived memory function through development yet being required during the adult stage. The post-developmental requirements of *trx* are consistent with what has been modeled in murine conditional knockouts of *Kmt2b*. In these studies, *Kmt2b* was knocked out in 4 month old mice via viral mediated knockout in the dentate gyrus and shown to still be necessary in long-term fear conditioning (Kerimoglu et al., 2013).

For further characterization of *Drosophila* H3K4 histone methyltransferases, future studies should look at the contribution of general COMPASS complex partners in memory, such as WRAD or other complex specific co-factors like Wdr82 or LPT (Mohan et al., 2011). To date, little analysis has been performed on how these complex members are contributing to memory function and it will be an interesting addition to the developing story of epigenetic regulation in memory if the genes encoding these proteins are eventually characterized.

4.2 *trx* may regulate memory through the expression of MB identity genes

In this study, 129 genes that are targets of *trx* independent of the flies experience were identified (Figure 10 A). Identification was based on the overlap between downregulated genes from experimental comparisons KNvCN and KTvCT to isolate the effect of social interaction on *trx* regulation of MB identity genes (Figure 9 C and D).

Within the 129 downregulated genes, 10 MB-enriched genes were identified, and were considered candidate targets of *trx*-regulated MB identity. Among these 10 genes are the metabolic genes *MFS3*, *bond*, and *Ldh*. Ldh is a metabolic enzyme that is responsible for the reversible conversion of lactate into pyruvate with concomitant conversion of NAD+ into NADH. The directionality of this conversion depends on the isozyme conformation of Ldh (Magistretti and Allaman, 2015). Metabolic reprogramming from aerobic glycolysis to oxidative phosphorylation is required to shift the proliferative neuroblast into a post-mitotic neuron. Failure of a neuroblast to reprogram ultimately results in neuronal death (Zheng et al., 2016). This is because adult neurons rely almost exclusively on oxidative phosphorylation to meet energy demands, leading to the prevailing hypothesis that lactate can be a sufficient substitute for glucose, and may even be required to meet the extreme metabolic demands of certain neurons (Duka et al., 2014; Magistretti and Allaman, 2015). Thus, lactate metabolism is especially important for memory related function. Previous studies have shown that astrocyte derived lactate is necessary for LTM formation in rodents (Suzuki et al., 2011), along with increased pyruvate metabolism occurring in *Drosophila* MB neurons after training (Plaçais et al., 2017). Increased pyruvate metabolism is hypothesized to occur in preparation for LTM dependent cellular changes. The role of lactate in LTM formation within neurons may be to help support higher energy demands of memory related protein synthesis, or by sparing glycolytic products to be used as precursors for the biosynthesis required in synaptic creation and remodelling during memory formation (Segarra-Mondejar et al., 2018).

With *Ldh* as the 4th most enriched gene in the MBs (Jones et al., 2018), it is likely critical for MB related functions, particularly for the primary function of MBs which is the formation of memory. The requirement of *Ldh* for memory was assessed via a preliminary

screen for LTM phenotypes. It was observed that the memory of the training was not significantly maintained in *Ldh*-KD flies (Figure 10 C). Further investigation into the role of *Ldh* in memory, including validation of the memory phenotype, will be required to make a strong conclusion as to the role of *Ldh* in memory, but as it stands regulation of *Ldh* expression appears to be a good candidate for *trx* mediated regulation of LTM through key MB processes.

4.3 *trx* may regulate memory by maintaining RNA processing factors after courtship conditioning

It was also of interest for this study to identify how *trx* may regulate gene expression in response to courtship conditioning. To do so, we identified the 47 memory genes that were induced in controls in response to courtship conditioning (Figure 9 A). These conditioning responsive genes include *jeb*, a well characterized Ras/ERK pathway activator required for olfactory memory (Gouzi et al., 2011), along with neuropeptides spab and proc. Moreover, putative markers for neuronal activation such as *Hr38* and *sr* (Chen et al., 2016; Fujita et al., 2013; Lutz and Robinson, 2013) were also identified. *Hr38* and *sr* are thought to be analogous to *c-Fos* in rodents which is induced in response to neuron firing during memory induction (Mayford and Reijmers, 2016). Following *trx*-KD many of these genes were expected to be misregulated. However, the memory genes that were identified in controls significantly overlapped with upregulated genes in *trx*-KD flies (Figure 11 B). Therefore, it was concluded that *trx* had only a limited effect on inducing memory genes after training. Nevertheless, the identified neuropeptides *spab* and *proc*, and neuron activity responsive *CG4577* and *CG17778*, were not upregulated in *trx*-KD, and may be candidate memory induced *trx* target genes.

To determine if *trx* was necessary for regulating expression of any genes dependent on courtship conditioning, 395 differentially downregulated genes from the experimental comparison KTvCT (Figure 9 D) were identified. This comparison was of interest as it shows the relative expression changes after *trx*-KD and courtship conditioning relative to controls. Functional GO term analysis of the 395 downregulated genes showed enrichment for numerous terms revolving around RNA splicing and ribosome biosynthesis (Figure 12

A). Within the term “RNA processing” (n=44) (Figure 12 A, Appendix M), there was a large group of proteins that form a single network (n=21) (Figure 12 B).

Current literature suggests that post transcriptional processing of mRNA is important for normal memory function. For example, selective downregulation of alternatively spliced transcripts reduces stress enhanced memory formation, suggesting that alternative splicing may be an activity dependent response to facilitate memory stability (Nijholt et al., 2004). Further to this point, genetic removal of activity dependent alternative exons in *Apoer2*, a component of the NMDA receptor complex, results in mice with poor memory formation and perturbed long-term potentiation – long-term potentiation being a well evidenced cellular correlate of memory (Beffert et al., 2005). Additionally, the coupling of activity induced transcription to *de novo* protein synthesis required for LTM formation relies on a concomitant induction of rRNA and maintenance of nucleolar integrity in the rodent hippocampus (Allen et al., 2014). Indeed, selective disruption of RNA polymerase 1, and thus rRNA synthesis, results in perturbed long-term potentiation and neuronal plasticity. Therefore, it seems the two processes of alternative splicing and ribosomal biosynthesis are both required to link transcription and translation to memory regulation. In such a way, it is quite serendipitous that *trx* was found to regulate a large number of genes involved in these processes. This study is the first to implicate H3K4 methyltransferases in memory function through the regulation of RNA processing genes.

4.4 Limitations and future directions

To study the function of genes in *Drosophila,* RNAi is a common and effective tool. However, RNAi approaches to genetic study are limited due to their potential for insufficient target gene KD and the off target effects of siRNAs. Given *Set1, trx,* and *Mnn1* are lethal as null mutants, a lethality assay with ubiquitous knockdown was used to estimate KD efficiency (Table 2). However, an observation of lethality does not guarantee that there were no false positives, as lethality could be caused by ubiquitously occurring off-target knockdowns. To better quantify RNAi knockdown of target genes future studies should strive to measure gene product levels via qPCR or Western blotting. In this study, validation of KD specificity was done using a minimum of two RNAi lines that target different regions of the mRNAs, and ideally were sourced from different transgenic

libraries (*trx* and *Mnn1*). In this manner, consistency of phenotypes acts as a control where convergent phenotypes in both lethality and memory would be unlikely via false positive hits on off target genes. Although this consistency raises confidence in the findings presented here, the limitations of this assay should be noted.

A major assumption of this study is that the genetic KD of *trx*, *Set1,* and *Mnn1* results in perturbed H3K4 methylation at certain loci. Without quantifying H3K4 methylation levels, one can only assume the mechanism of action for SET1 family proteins. Indeed, SET1 proteins are important components in COMPASS methyltransferase activity, yet core components of COMPASS, the WRAD, have extra functions beyond methylation, such as cell cycle regulation and endosomal transport (Ali and Tyagi, 2017). It is not yet clear if SET1 proteins are involved in these activities, yet it is possible that reduced levels of SET1 proteins may affect the titration of WRAD and thus its function. To account for this, and to support the conclusion that histone methyltransferase activity results in memory phenotypes, immunohistochemistry on adult MB nuclei can be done to broadly quantify levels of H3K4me1 and H3K4me3 in response to genetic KD. Additionally, direct quantification of histone profiles of H3K4 histone methyltransferases could also be done using ChIP-sequencing with antibodies against H3K4me1 or H3K4me3.

In this study, the role of histone H3K4 methyltransferases in courtship memory was chosen for investigation because it is a practical and easy memory paradigm to assay with ethological relevance. However, in rodent studies of KMT2A and KMT2B, there are notable differences in the necessity of these enzymes across memory subsystems (Kerimoglu et al., 2013, 2017). To further build on the role of *Drosophila* SET1 proteins in memory, it may be necessary to examine the role *Set1* and *trx* in different brain regions and memory tests, like the central complex for visual pattern memory (Pan et al., 2009; Zars et al., 2000b). While targeted knockdown in the central complex may not be possible with current genetic tools, investigating the requirement of *Set1* and *trx* in these brain regions would still be of interest as it can further build upon the role of SET1 proteins in memory. Targeting knockdown to the central complex may also be of interest due to its role in olfactory memory consolidation (Wu et al., 2007). Courtship conditioning is a well-defined and ethological assay for memory that is easily relatable to memory systems in

other animals. As such, courtship conditioning is a good choice for first pass screening of memory phenotypes, yet nevertheless by only studying the MB and courtship memory the breadth of our understanding for H3K4 methylation in memory may be limited. Future studies could aim to ameliorate this by broadening the memory systems they investigate.

A candidate gene list (Table 5 and Table 6) has been drawn up among the different post-sequencing analyses on *trx*-KD nuclei performed in this study. A major next step from these findings would be to explore the necessity of each of these genes in memory, similar to the initial analysis of *Ldh* in this study. Ideally, a short list of candidates would be identified as necessary for LTM and experiments could be done to overexpress those candidates in an attempt to rescue the original *trx*-KD phenotype. In doing so, it can be shown that either the various targets of *trx* are all contributing to memory function by affecting different biological processes simultaneously, or that a single key target of *trx* is the linchpin in *trx*-dependent memory. Finally, it would be interesting to see if candidate targets of *trx* are mutually regulated by *Mnn1*. Since mammalian MNN1 only interacts with the KMT2A-related COMPASS 21% of the time (van Nuland et al., 2013), transient activity of Mnn1 may only contribute to localizing trx to some of the loci identified in this study. Demonstrating the necessity of *Mnn1* for regulation of certain *trx* targets could be done with qPCR on INTACT MB samples to measure the levels of target gene transcripts during *Mnn1*-KD.

4.5 Research implications and conclusions

To summarize, this study presents the first data implicating the *Set1* and *Mnn1* genes in memory function, and identified *trx* and *Mnn1* as required genes for LTM formation that are dispensable in STM. The effects of *trx* and *Mnn1* on memory were also shown to be the result of adult-specific processes. Finally, through sequencing of RNA extracted from fly MBs, it was determined that *trx* may be regulating memory through a number of different mechanisms. Overall, transcriptional investigation identified 129 genes that were downregulated during *trx*-KD independent of courtship experience, along with 299 genes that were downregulated only in naïve flies and another 266 downregulated only in trained flies. Additionally, some memory induced genes were not found to be

induced following *trx*-KD. Among these differentially expressed genes, a number of genes were identified as potential effectors of *trx*-mediated LTM. These include:

- 10 MB enriched genes that may be required for normal MB neuron identity. *Ldh* is one particularly strong candidate that has preliminarily been identified as being necessary for long-term courtship memory.

- 2 neuropeptide genes, *spab* and *proc*, which were induced in controls during memory formation but absent following *trx*-KDs.

- 2 neuronal activity induced genes, *CG4577* and *CG17778*, which were induced in controls during memory formation but absent following *trx*-KD.

- Numerous genes that were associated with RNA processing, including mRNA alternative splicing and ribosome biogenesis. A subset of these genes, defined as "RNA processing" genes, formed a single 21 gene network. Disturbance of this network could be contributing to memory phenotypes during *trx*-KD.

In conclusion, this study established new and varied roles for a number of H3K4 methyltransferases in courtship memory, providing a launch pad for future mechanistic studies relating to *trx* regulated genes in LTM.

5 References

Achim, K., Salminen, M., and Partanen, J. (2014). Mechanisms regulating GABAergic neuron development. Cellular and Molecular Life Sciences *71*, 1395–1415.

Agranoff, B.W., Davis, R.E., and Brink, J.J. (1966). Chemical studies on memory fixation in goldfish. Brain Research *1*, 303–309.

Aken, B.L., Ayling, S., Barrell, D., Clarke, L., Curwen, V., Fairley, S., Fernandez Banet, J., Billis, K., García Girón, C., Hourlier, T., et al. (2016). The Ensembl gene annotation system. Database : The Journal of Biological Databases and Curation *2016*, 942–950.

Ali, A., and Tyagi, S. (2017). Diverse roles of WDR5-RbBP5-ASH2L-DPY30 (WRAD) complex in the functions of the SET1 histone methyltransferase family. Journal of Biosciences *42*, 155–159.

Allen, K.D., Gourov, A. V., Harte, C., Gao, P., Lee, C., Sylvain, D., Splett, J.M., Oxberry, W.C., Van De Nes, P.S., Troy-Regier, M.J., et al. (2014). Nucleolar integrity is required for the maintenance of long-term synaptic plasticity. PLoS ONE *9*, 1–16.

Anders, S., Pyl, P.T., and Huber, W. (2015). HTSeq-A Python framework to work with high-throughput sequencing data. Bioinformatics *31*, 166–169.

Ashburner, M., Ball, C.A., Blake, J.A., Botstein, D., Butler, H., Cherry, J.M., Davis, A.P., Dolinski, K., Dwight, S.S., Eppig, J.T., et al. (2000). Gene ontology: Tool for the unification of biology. Nature Genetics *25*, 25–29.

Aso, Y., Hattori, D., Yu, Y., Johnston, R.M., Iyer, N.A., Ngo, T.T.B., Dionne, H., Abbott, L.F., Axel, R., Tanimoto, H., et al. (2014). The neuronal architecture of the mushroom body provides a logic for associative learning. ELife *3*, e04577.

Avdic, V., Zhang, P., Lanouette, S., Groulx, A., Tremblay, V., Brunzelle, J., and Couture, J.-F. (2011). Structural and Biochemical Insights into MLL1 Core Complex Assembly. Structure *19*, 101–108.

Bannister, A.J., and Kouzarides, T. (2011). Regulation of chromatin by histone modifications. Cell Research *21*, 381–395.

Beffert, U., Weeber, E.J., Durudas, A., Qiu, S., Masiulis, I., Sweatt, J.D., Li, W.P., Adelmann, G., Frotscher, M., Hammer, R.E., et al. (2005). Modulation of synaptic plasticity and memory by Reelin involves differential splicing of the lipoprotein receptor Apoer2. Neuron *47*, 567–579.

Blum, A.L., Li, W., Cressy, M., and Dubnau, J. (2009). Short- and Long-Term Memory in Drosophila Require cAMP Signaling in Distinct Neuron Types. Current Biology *19*, 1341–1350.

Bourtchuladze, R., Frenguelli, B., Blendy, J., Cioffi, D., Schutz, G., and Silva, A.J. (1994). Deficient long-term memory in mice with a targeted mutation of the cAMP-responsive element-binding protein. Cell *79*, 59–68.

Breen, T.R. (1999). Mutant alleles of the Drosophila trithorax gene produce common and unusual homeotic and other developmental phenotypes. Genetics *152*, 319–344.

Brunelli, M., Castellucci, V., and Kandel, E.R. (1976). Synaptic facilitation and

behavioral sensitization in Aplysia: possible role of serotonin and cyclic AMP. Science (New York, NY) *194*, 1178–1181.

Carew, T.J., Walters, E.T., and Kandel, E.R. (1981). Classical conditioning in a simple withdrawal reflex in *Aplysia californica*. The Journal of Neuroscience *1*, 1426–1437.

Castellucci, V., Pinsker, H., Kupfermann, I., and Kandel, E.R. (1970). Neuronal mechanisms of habituation and dishabituation of the gill-withdrawal reflex in Aplysia. Science (New York, NY) *167*, 1745–1748.

Cervantes-Sandoval, I., Martin-Pena, A., Berry, J.A., and Davis, R.L. (2013). System-Like Consolidation of Olfactory Memories in Drosophila. Journal of Neuroscience *33*, 9846–9854.

Chen, X., Rahman, R., Guo, F., and Rosbash, M. (2016). Genome-wide identification of neuronal activity-regulated genes in Drosophila. ELife *5*, 15–19.

Chwang, W.B., O'Riordan, K.J., Levenson, J.M., and Sweatt, J.D. (2006). ERK/MAPK regulates hippocampal histone phosphorylation following contextual fear conditioning. Learning & Memory (Cold Spring Harbor, NY) *13*, 322–328.

Connolly, J.B., Roberts, I.J., Armstrong, J.D., Kaiser, K., Forte, M., Tully, T., and O'Kane, C.J. (1996). Associative learning disrupted by impaired Gs signaling in Drosophila mushroom bodies. Science (New York, NY) *274*, 2104–2107.

Davis, R.L. (2011). Traces of Drosophila Memory. Neuron *70*, 8–19.

Deneris, E.S., and Hobert, O. (2014). Maintenance of postmitotic neuronal cell identity. Nature Neuroscience *17*, 899–907.

Dietzl, G., Chen, D., Schnorrer, F., Su, K.C., Barinova, Y., Fellner, M., Gasser, B., Kinsey, K., Oppel, S., Scheiblauer, S., et al. (2007). A genome-wide transgenic RNAi library for conditional gene inactivation in Drosophila. Nature *448*, 151–156.

Dobin, A., Davis, C.A., Schlesinger, F., Drenkow, J., Zaleski, C., Jha, S., Batut, P., Chaisson, M., and Gingeras, T.R. (2013). STAR: Ultrafast universal RNA-seq aligner. Bioinformatics *29*, 15–21.

Domjan, M. (2005). Pavlovian conditioning: a functional perspective. Annual Review of Psychology *56*, 179–206.

Drain, P., Folkers, E., and Quinn, W.G. (1991). cAMP-dependent protein kinase and the disruption of learning in transgenic flies. Neuron *6*, 71–82.

Drain, P., Dubin, A.E., and Aldrich, R.W. (1994). Regulation of Shaker K+channel inactivation gating by the cAMP-dependent protein kinase. Neuron *12*, 1097–1109.

Dreijerink, K.M.A., Mulder, K.W., Winkler, G.S., Höppener, J.W.M., Lips, C.J.M., and Timmers, H.T.M. (2006). Menin links estrogen receptor activation to histone H3K4 trimethylation. Cancer Research *66*, 4929–4935.

Dudai, Y., Jan, Y.N., Byers, D., Quinn, W.G., and Benzer, S. (1976). dunce, a mutant of Drosophila deficient in learning. Proceedings of the National Academy of Sciences of the United States of America *73*, 1684–1688.

Duka, T., Anderson, S.M., Collins, Z., Raghanti, M.A., Ely, J.J., Hof, P.R., Wildman,

D.E., Goodman, M., Grossman, L.I., and Sherwood, C.C. (2014). Synaptosomal lactate Dehydrogenase Isoenzyme composition is shifted toward aerobic forms in primate brain evolution. Brain, Behavior and Evolution *83*, 216–230.

Dupont, C., Armant, D.R., and Brenner, C.A. (2009). Epigenetics: definition, mechanisms and clinical perspective. Seminars in Reproductive Medicine *27*, 351–357.

Ejima, A., Smith, B.P.C., Lucas, C., van der Goes van Naters, W., Miller, C.J., Carlson, J.R., Levine, J.D., and Griffith, L.C. (2007). Generalization of Courtship Learning in Drosophila Is Mediated by cis-Vaccenyl Acetate. Current Biology *17*, 599–605.

Ernst, P., and Vakoc, C.R. (2012). WRAD: Enabler of the SET1-family of H3K4 methyltransferases. Briefings in Functional Genomics *11*, 217–226.

Fujita, N., Nagata, Y., Nishiuchi, T., Sato, M., Iwami, M., and Kiya, T. (2013). Visualization of neural activity in insect brains using a conserved immediate early gene, Hr38. Current Biology *23*, 2063–2070.

Geisler, S.J., and Paro, R. (2015). Trithorax and Polycomb group-dependent regulation: a tale of opposing activities. Development *142*, 2876–2887.

Goodwin, S.F., Del Vecchio, M., Velinzon, K., Hogel, C., Russell, S.R., Tully, T., and Kaiser, K. (1997). Defective learning in mutants of the Drosophila gene for a regulatory subunit of cAMP-dependent protein kinase. The Journal of Neuroscience : The Official Journal of the Society for Neuroscience *17*, 8817–8827.

Gouzi, J.Y., Moressis, A., Walker, J.A., Apostolopoulou, A.A., Palmer, R.H., Bernards, A., and Skoulakis, E.M.C. (2011). The receptor tyrosine kinase alk controls neurofibromin functions in drosophila growth and learning. PLoS Genetics *7*.

Guarente, L., Yocum, R.R., and Gifford, P. (1982). A GAL10-CYC1 hybrid yeast promoter identifies the GAL4 regulatory region as an upstream site. Proceedings of the National Academy of Sciences of the United States of America *79*, 7410–7414.

Guenther, M.G., Jenner, R.G., Chevalier, B., Nakamura, T., Croce, C.M., Canaani, E., and Young, R. a (2005). Global and Hox-specific roles for the MLL1 methyltransferase. Proceedings of the National Academy of Sciences *102*, 8603–8608.

Gupta, S., Kim, S.Y., Artis, S., Molfese, D.L., Schumacher, A., Sweatt, J.D., Paylor, R.E., and Lubin, F.D. (2010). Histone methylation regulates memory formation. The Journal of Neuroscience : The Official Journal of the Society for Neuroscience *30*, 3589–3599.

Hallson, G., Hollebakken, R.E., Li, T., Syrzycka, M., Kim, I., Cotsworth, S., Fitzpatrick, K.A., Sinclair, D.A.R., and Honda, B.M. (2012). dSet1 is the main H3K4 di- and tri-methyltransferase throughout Drosophila development. Genetics *190*, 91–100.

Han, P.L., Levin, L.R., Reed, R.R., and Davis, R.L. (1992). Preferential expression of the drosophila rutabaga gene in mushroom bodies, neural centers for learning in insects. Neuron *9*, 619–627.

Hawkins, R.D. (1984). A cellular mechanism of classical conditioning in Aplysia. Journal of Experimental Biology *112*, 113–128.

Heintzman, N.D., Hon, G.C., Hawkins, R.D., Kheradpour, P., Stark, A., Harp, L.F., Ye, Z., Lee, L.K., Stuart, R.K., Ching, C.W., et al. (2009). Histone modifications at human enhancers reflect global cell-type-specific gene expression. Nature *459*, 108–112.

Heisenberg, M., Borst, A., Wagner, S., and Byers, D. (1985). drosophila mushroom body mutants are deficient in olfactory learning: Research papers. Journal of Neurogenetics *2*, 1–30.

Henry, G.L., Davis, F.P., Picard, S., and Eddy, S.R. (2012). Cell type-specific genomics of Drosophila neurons. Nucleic Acids Research *40*, 9691–9704.

Hirano, Y., Ihara, K., Masuda, T., Yamamoto, T., Iwata, I., Takahashi, A., Awata, H., Nakamura, N., Takakura, M., Suzuki, Y., et al. (2016). Shifting transcriptional machinery is required for long-term memory maintenance and modification in Drosophila mushroom bodies. Nature Communications *7*, 1–14.

Hobert, O. (2011). Regulation of Terminal Differentiation Programs in the Nervous System. Annual Review of Cell and Developmental Biology *27*, 681–696.

Holtmaat, A., and Caroni, P. (2016). Functional and structural underpinnings of neuronal assembly formation in learning. Nature Neuroscience *19*, 1553–1562.

Hsieh, J.J.D., Cheng, E.H.Y., and Korsmeyer, S.J. (2003). Taspase1: A threonine aspartase required for cleavage of MLL and proper HOX gene expression. Cell *115*, 293–303.

Huang, Y.C., Shih, H.Y., Lin, S.J., Chiu, C.C., Ma, T.L., Yeh, T.H., and Cheng, Y.C. (2015). The epigenetic factor Kmt2a/Mll1 regulates neural progenitor proliferation and neuronal and glial differentiation. Developmental Neurobiology *75*, 452–462.

Hughes, C.M., Rozenblatt-Rosen, O., Milne, T.A., Copeland, T.D., Levine, S.S., Lee, J.C., Hayes, D.N., Shanmugam, K.S., Bhattacharjee, A., Biondi, C.A., et al. (2004). Menin associates with a trithorax family histone methyltransferase complex and with the Hoxc8 locus. Molecular Cell *13*, 587–597.

Hulsen, T., de Vlieg, J., and Alkema, W. (2008). BioVenn - A web application for the comparison and visualization of biological lists using area-proportional Venn diagrams. BMC Genomics *9*, 1–6.

Ingham, P., and Whittle, R. (1980). Trithorax: A new homoeotic mutation of Drosophila melanogaster causing transformations of abdominal and thoracic imaginal segments - I. Putative role during embryogenesis. MGG Molecular & General Genetics *179*, 607–614.

Jenett, A., Rubin, G.M., Ngo, T.T.B., Shepherd, D., Murphy, C., Dionne, H., Pfeiffer, B.D., Cavallaro, A., Hall, D., Jeter, J., et al. (2012). A GAL4-Driver Line Resource for Drosophila Neurobiology. Cell Reports *2*, 991–1001.

Jones, S.G., Nixon, K.C.J., Chubak, M.C., and Kramer, J.M. (2018). Mushroom Body Specific Transcriptome Analysis Reveals Dynamic Regulation of Learning and Memory Genes After Acquisition of Long-Term Courtship Memory in Drosophila. G3 (Bethesda, Md).

Kamyshev, N.G., Iliadi, K.G., and Bragina, J. V (1999). Drosophila conditioned courtship: two ways of testing memory. Learning & Memory (Cold Spring Harbor, NY)

6, 1–20.

Keleman, K., Vrontou, E., Krüttner, S., Yu, J.Y., Kurtovic-Kozaric, A., and Dickson, B.J. (2012). Dopamine neurons modulate pheromone responses in Drosophila courtship learning. Nature *489*, 145–149.

Kerimoglu, C., Agis-Balboa, R.C., Kranz, A., Stilling, R., Bahari-Javan, S., Benito-Garagorri, E., Halder, R., Burkhardt, S., Stewart, A.F., and Fischer, A. (2013). Histone-methyltransferase MLL2 (KMT2B) is required for memory formation in mice. The Journal of Neuroscience : The Official Journal of the Society for Neuroscience *33*, 3452–3464.

Kerimoglu, C., Sakib, M.S., Jain, G., Benito, E., Burkhardt, S., Capece, V., Kaurani, L., Halder, R., Agís-Balboa, R.C., Stilling, R., et al. (2017). KMT2A and KMT2B Mediate Memory Function by Affecting Distinct Genomic Regions. Cell Reports *20*, 538–548.

Koemans, T.S., Kleefstra, T., Chubak, M.C., Stone, M.H., Reijnders, M.R.F., de Munnik, S., Willemsen, M.H., Fenckova, M., Stumpel, C.T.R.M., Bok, L.A., et al. (2017a). Functional convergence of histone methyltransferases EHMT1 and KMT2C involved in intellectual disability and autism spectrum disorder. PLoS Genetics *13*, e1006864.

Koemans, T.S., Oppitz, C., Donders, R.A.T., van Bokhoven, H., Schenck, A., Keleman, K., and Kramer, J.M. (2017b). Drosophila Courtship Conditioning As a Measure of Learning and Memory. Journal of Visualized Experiments : JoVE *124*, 1–11.

Kohyama, J., Kojima, T., Takatsuka, E., Yamashita, T., Namiki, J., Hsieh, J., Gage, F.H., Namihira, M., Okano, H., Sawamoto, K., et al. (2008). Epigenetic regulation of neural cell differentiation plasticity in the adult mammalian brain. Proceedings of the National Academy of Sciences *105*, 18012–18017.

Korzus, E., Rosenfeld, M.G., and Mayford, M. (2004). CBP histone acetyltransferase activity is a critical component of memory consolidation. Neuron *42*, 961–972.

Krashes, M.J., Keene, A.C., Leung, B., Armstrong, J.D., and Waddell, S. (2007). Sequential Use of Mushroom Body Neuron Subsets during Drosophila Odor Memory Processing. Neuron *53*, 103–115.

Lau, H.L., Timbers, T.A., Mahmoud, R., and Rankin, C.H. (2013). Genetic dissection of memory for associative and non-associative learning in Caenorhabditis elegans. Genes, Brain and Behavior *12*, 210–223.

Lee, T., and Luo, L. (1999). Mosaic Analysis with a Repressible Cell Marker for Studies of Gene Function in Neuronal Morphogenesis. Neuron *22*, 451–461.

Lee, S., Lee, D.-K., Dou, Y., Lee, J., Lee, B., Kwak, E., Kong, Y.-Y., Lee, S.-K., Roeder, R.G., and Lee, J.W. (2006). Coactivator as a target gene specificity determinant for histone H3 lysine 4 methyltransferases. Proceedings of the National Academy of Sciences *103*, 15392–15397.

Levenson, J.M., O'Riordan, K.J., Brown, K.D., Trinh, M.A., Molfese, D.L., and Sweatt, J.D. (2004). Regulation of histone acetylation during memory formation in the hippocampus. Journal of Biological Chemistry *279*, 40545–40559.

Levin, L.R., Han, P.L., Hwang, P.M., Feinstein, P.G., Davis, R.L., and Reed, R.R.

(1992). The Drosophila learning and memory gene rutabaga encodes a Ca2+calmodulin-responsive adenylyl cyclase. Cell *68*, 479–489.

Lim, D.A., Huang, Y.C., Swigut, T., Mirick, A.L., Garcia-Verdugo, J.M., Wysocka, J., Ernst, P., and Alvarez-Buylla, A. (2009). Chromatin remodelling factor Mll1 is essential for neurogenesis from postnatal neural stem cells. Nature *458*, 529–533.

Liu, G., Seiler, H., Wen, A., Zars, T., Ito, K., Wolf, R., Heisenberg, M., and Liu, L. (2006). Distinct memory traces for two visual features in the Drosophila brain. Nature *439*, 551–556.

Livingstone, M.S., Sziber, P.P., and Quinn, W.G. (1984). Loss of calcium/calmodulin responsiveness in adenylate cyclase of rutabaga, a Drosophila learning mutant. Cell *37*, 205–215.

Love, M.I., Huber, W., and Anders, S. (2014). Moderated estimation of fold change and dispersion for RNA-seq data with DESeq2. Genome Biology *15*, 1–21.

Lutz, C.C., and Robinson, G.E. (2013). Activity-dependent gene expression in honey bee mushroom bodies in response to orientation flight. Journal of Experimental Biology *216*, 2031–2038.

Magistretti, P.J., and Allaman, I. (2015). A Cellular Perspective on Brain Energy Metabolism and Functional Imaging. Neuron *86*, 883–901.

Mayford, M., and Reijmers, L. (2016). Exploring memory representations with activity-based genetics. Cold Spring Harbor Perspectives in Biology *8*, 1–18.

McBride, S.M.J., Giuliani, G., Choi, C., Krause, P., Correale, D., Watson, K., Baker, G., and Siwicki, K.K. (1999). Mushroom body ablation impairs short-term memory and long-term memory of courtship conditioning in Drosophila melanogaster. Neuron *24*, 967–977.

McGuire, S.E., Le, P.T., and Davis, R.L. (2001). The role of Drosophila mushroom body signaling in olfactory memory. Science *293*, 1330–1333.

Mi, H., Huang, X., Muruganujan, A., Tang, H., Mills, C., Kang, D., and Thomas, P.D. (2017). PANTHER version 11: Expanded annotation data from Gene Ontology and Reactome pathways, and data analysis tool enhancements. Nucleic Acids Research *45*, D183–D189.

Miller, C.A., and Sweatt, J.D. (2007). Covalent Modification of DNA Regulates Memory Formation. Neuron *53*, 857–869.

Milne, T.A., Hughes, C.M., Lloyd, R., Yang, Z., Rozenblatt-Rosen, O., Dou, Y., Schnepp, R.W., Krankel, C., LiVolsi, V.A., Gibbs, D., et al. (2005). Menin and MLL cooperatively regulate expression of cyclin-dependent kinase inhibitors. Proceedings of the National Academy of Sciences *102*, 749–754.

Milner, B., Squire, L.R., and Kandel, E.R. (1998). Cognitive neuroscience and the study of memory. Neuron *20*, 445–468.

Mohan, M., Herz, H.-M., Smith, E.R., Zhang, Y., Jackson, J., Washburn, M.P., Florens, L., Eissenberg, J.C., and Shilatifard, A. (2011). The COMPASS Family of H3K4

Methylases in Drosophila. Molecular and Cellular Biology *31*, 4310–4318.

Montarolo, P., Goelet, P., Castellucci, V., Morgan, J., Kandel, E., and Schacher, S. (1986). A critical period for macromolecular synthesis in long-term heterosynaptic facilitation in Aplysia. Science *234*, 1249–1254.

Montojo, J., Zuberi, K., Rodriguez, H., Kazi, F., Wright, G., Donaldson, S.L., Morris, Q., and Bader, G.D. (2010). GeneMANIA cytoscape plugin: Fast gene function predictions on the desktop. Bioinformatics *26*, 2927–2928.

Morgan, T.H. (1910). Sex limited inheritance in drosophila. Science *32*, 120–122.

Müller, U. (2000). Prolonged activation of cAMP-dependent protein kinase during conditioning induces long-term memory in honeybees. Neuron *27*, 159–168.

Nelson, S.B., Sugino, K., and Hempel, C.M. (2006). The problem of neuronal cell types: a physiological genomics approach. Trends in Neurosciences *29*, 339–345.

Nijholt, I., Farchi, N., Kye, M., Sklan, E.H., Shoham, S., Verbeure, B., Owen, D., Hochner, B., Spiess, J., Soreq, H., et al. (2004). Stress-induced alternative splicing of acetylcholinesterase results in enhanced fear memory and long-term potentiation. Molecular Psychiatry *9*, 174–183.

Ninkovic, J., Pinto, L., Petricca, S., Lepier, A., Sun, J., Rieger, M.A., Schroeder, T., Cvekl, A., Favor, J., and Götz, M. (2010). The transcription factor Pax6 regulates survival of dopaminergic olfactory bulb neurons via crystallin αA. Neuron *68*, 682–694.

van Nuland, R., Smits, A.H., Pallaki, P., Jansen, P.W.T.C., Vermeulen, M., and Timmers, H.T.M. (2013). Quantitative Dissection and Stoichiometry Determination of the Human SET1/MLL Histone Methyltransferase Complexes. Molecular and Cellular Biology *33*, 2067–2077.

Nüsslein-Volhard, C., and Wieschaus, E. (1980). Mutations affecting segment number and polarity in Drosophila. Nature *287*, 795–801.

O'Meara, M.M., Zhang, F., and Hobert, O. (2010). Maintenance of neuronal laterality in Caenorhabditis elegans through MYST histone acetyltransferase complex components LSY-12, LSY-13 and LIN-49. Genetics *186*, 1497–1502.

Odho, Z., Southall, S.M., and Wilson, J.R. (2010). Characterization of a novel WDR5-binding site that recruits RbBP5 through a conserved motif to enhance methylation of histone H3 lysine 4 by mixed lineage leukemia protein-1. The Journal of Biological Chemistry *285*, 32967–32976.

Ottiger, M., Soller, M., Stocker, R.F., and Kubli, E. (2000). Binding sites of drosophila melanogaster sex peptide pheromones. Journal of Neurobiology *44*, 57–71.

Pan, Y., Zhou, Y., Guo, C., Gong, H., Gong, Z., and Liu, L. (2009). Differential roles of the fan-shaped body and the ellipsoid body in Drosophila visual pattern memory. Learning & Memory *16*, 289–295.

Papaconstantinou, M., Wu, Y., Pretorius, H.N., Singh, N., Gianfelice, G., Tanguay, R.M., Campos, A.R., and Bedard, P.A. (2005). Menin is a regulator of the stress response in Drosophila melanogaster. Mol Cell Biol *25*, 9960–9972.

Pascual, A., and Préat, T. (2001). Localization of long-term memory within the Drosophila mushroom body. Science *294*, 1115–1117.

Perkins, L.A., Holderbaum, L., Tao, R., Hu, Y., Sopko, R., McCall, K., Yang-Zhou, D., Flockhart, I., Binari, R., Shim, H.S., et al. (2015). The transgenic RNAi project at Harvard medical school: Resources and validation. Genetics *201*, 843–852.

Petruk, S., Smith, S.T., Sedkov, Y., and Mazo, A. (2008). Association of trxG and PcG proteins with the bxd maintenance element depends on transcriptional activity. Development (Cambridge, England) *135*, 2383–2390.

Plaçais, P.Y., De Tredern, É., Scheunemann, L., Trannoy, S., Goguel, V., Han, K.A., Isabel, G., and Preat, T. (2017). Upregulated energy metabolism in the Drosophila mushroom body is the trigger for long-term memory. Nature Communications *8*.

Quina, A.S., Buschbeck, M., and Di Croce, L. (2006). Chromatin structure and epigenetics. Biochemical Pharmacology *72*, 1563–1569.

Quinn, W.G., Harris, W.A., and Benzer, S. (1974). Conditioned behavior in Drosophila melanogaster. Proceedings of the National Academy of Sciences of the United States of America *71*, 708–712.

Rai, K., Nadauld, L.D., Chidester, S., Manos, E.J., James, S.R., Karpf, A.R., Cairns, B.R., and Jones, D.A. (2006). Zebra Fish Dnmt1 and Suv39h1 Regulate Organ-Specific Terminal Differentiation during Development. Molecular and Cellular Biology *26*, 7077–7085.

Santos-Rosa, H., Schneider, R., Bannister, A.J., Sherriff, J., Bernstein, B.E., Emre, N.C.T., Schreiber, S.L., Mellor, J., and Kouzarides, T. (2002). Active genes are tri-methylated at K4 of histone H3. Nature *419*, 407–411.

Schmieder, R., and Edwards, R. (2011). Quality control and preprocessing of metagenomic datasets. Bioinformatics (Oxford, England) *27*, 863–864.

Schuettengruber, B., Martinez, A.M., Iovino, N., and Cavalli, G. (2011). Trithorax group proteins: Switching genes on and keeping them active. Nature Reviews Molecular Cell Biology *12*, 799–814.

Schuettengruber, B., Bourbon, H.M., Di Croce, L., and Cavalli, G. (2017). Genome Regulation by Polycomb and Trithorax: 70 Years and Counting. Cell *171*, 34–57.

Schwaerzel, M., Monastirioti, M., Scholz, H., Friggi-Grelin, F., Birman, S., and Heisenberg, M. (2003). Dopamine and octopamine differentiate between aversive and appetitive olfactory memories in \emph{Drosophila}. The Journal of Neuroscience *23*, 10495–10502.

Schwartz, Y.B., Kahn, T.G., Stenberg, P., Ohno, K., Bourgon, R., and Pirrotta, V. (2010). Alternative epigenetic chromatin states of polycomb target genes. PLoS Genetics *6*.

Segarra-Mondejar, M., Casellas-Díaz, S., Ramiro-Pareta, M., Müller-Sánchez, C., Martorell-Riera, A., Hermelo, I., Reina, M., Aragonés, J., Martínez-Estrada, O.M., and Soriano, F.X. (2018). Synaptic activity-induced glycolysis facilitates membrane lipid provision and neurite outgrowth. The EMBO Journal e97368.

Shannon, P., Markiel, A., Ozier, O., Baliga, N.S., Wang, J.T., Ramage, D., Amin, N., Schwikowski, B., and Ideker, T. (2003). Cytoscape: a software environment for integrated models of biomolecular interaction networks. Genome Research *13*, 2498–2504.

Shih, M.-F.M., Davis, F.P., Henry, G.L., and Dubnau, J. (2018). Nuclear Transcriptomes of the Seven Neuronal Cell Types That Constitute the Drosophila Mushroom Bodies. G3 (Bethesda, Md) *489*, 145–149.

Siegel, R.W., and Hall, J.C. (1979). Conditioned responses in courtship behavior of normal and mutant Drosophila. Proceedings of the National Academy of Sciences *76*, 3430–3434.

Suzuki, A., Stern, S.A., Bozdagi, O., Huntley, G.W., Walker, R.H., Magistretti, P.J., and Alberini, C.M. (2011). Astrocyte-neuron lactate transport is required for long-term memory formation. Cell *144*, 810–823.

Swank, M.W., and Sweatt, J.D. (2001). Increased histone acetyltransferase and lysine acetyltransferase activity and biphasic activation of the ERK/RSK cascade in insular cortex during novel taste learning. The Journal of Neuroscience *21*, 3383–3391.

Team, R.C. (2016). R: A Language and Environment for Statistical Com- puting. Vienna, Austria: R Foundation for Statistical Computing.

Tsarovina, K., Reiff, T., Stubbusch, J., Kurek, D., Grosveld, F.G., Parlato, R., Schutz, G., and Rohrer, H. (2010). The Gata3 Transcription Factor Is Required for the Survival of Embryonic and Adult Sympathetic Neurons. Journal of Neuroscience *30*, 10833–10843.

Tully, T., and Quinn, W.G. (1985). Classical conditioning and retention in normal and mutant Drosophila melanogaster. Journal of Comparative Physiology A *157*, 263–277.

Tully, T., Preat, T., Boynton, S.C., and Del Vecchio, M. (1994). Genetic dissection of consolidated memory in *Drosophila*. Cell *79*, 35–47.

Waddell, S., and Quinn, W.G. (2001). Flies, genes, and learning. Annual Review of Neuroscience *24*, 1283–1309.

Wang, Z., Zang, C., Cui, K., Schones, D.E., Barski, A., Peng, W., and Zhao, K. (2009). Genome-wide Mapping of HATs and HDACs Reveals Distinct Functions in Active and Inactive Genes. Cell *138*, 1019–1031.

Wiersma, M., Bussiere, M., Halsall, J.A., Turan, N., Slany, R., Turner, B.M., and Nightingale, K.P. (2016). Protein kinase Msk1 physically and functionally interacts with the KMT2A/MLL1 methyltransferase complex and contributes to the regulation of multiple target genes. Epigenetics and Chromatin *9*, 1–12.

Wu, C.L., Xia, S., Fu, T.F., Wang, H., Chen, Y.H., Leong, D., Chiang, A.S., and Tully, T. (2007). Specific requirement of NMDA receptors for long-term memory consolidation in Drosophila ellipsoid body. Nature Neuroscience *10*, 1578–1586.

Wu, M., Wang, P.F., Lee, J.S., Martin-Brown, S., Florens, L., Washburn, M., and Shilatifard, A. (2008). Molecular Regulation of H3K4 Trimethylation by Wdr82, a Component of Human Set1/COMPASS. Molecular and Cellular Biology *28*, 7337–7344.

Yin, J.C.P., and Tully, T. (1996). CREB and the formation of long-term memory. Current Opinion in Neurobiology *6*, 264–268.

Yin, J.C.P., Wallach, J.S., Del Vecchio, M., Wilder, E.L., Zhou, H., Quinn, W.G., and Tully, T. (1994). Induction of a dominant negative CREB transgene specifically blocks long-term memory in Drosophila. Cell *79*, 49–58.

You, L., Yan, K., Zou, J., Zhou, J., Zhao, H., Bertos, N.R., Park, M., Wang, E., and Yang, X.-J. (2015). The lysine acetyltransferase activator Brpf1 governs dentate gyrus development through neural stem cells and progenitors. PLoS Genetics *11*, e1005034.

Zars, T., Fischer, M., Schulz, R., and Heisenberg, M. (2000a). Localization of a short-term memory in Drosophila. Science *288*, 672–675.

Zars, T., Wolf, R., Davis, R., and Heisenberg, M. (2000b). Tissue-specific expression of a type I adenylyl cyclase rescues the rutabaga mutant memory defect: in search of the engram. Learning & Memory (Cold Spring Harbor, NY) *7*, 18–31.

Zhang, Y., Mittal, A., Reid, J., Reich, S., Gamblin, S.J., and Wilson, J.R. (2015). Evolving catalytic properties of the MLL family SET domain. Structure *23*, 1921–1933.

Zhao, X., Lenek, D., Dag, U., Dickson, B.J., and Keleman, K. (2018). Persistent activity in a recurrent circuit underlies courtship memory in Drosophila. ELife *7*, 1–16.

Zheng, X., Boyer, L., Jin, M., Mertens, J., Kim, Y., Ma, L., Ma, L., Hamm, M., Gage, F.H., and Hunter, T. (2016). Metabolic reprogramming during neuronal differentiation from aerobic glycolysis to neuronal oxidative phosphorylation. ELife *5*, 1–25.

6 Appendices

Appendix A: List of fly stocks used in this project.

Controls and genetic tools			
Stock #	**Supplier**	**Genotype**	**Description**
35785	BDSC	*y^1 sc^* v^1; P{$y^{+t7.7}$ $v^{+t1.8}$=VALIUM20-mCherry}attP2*	*$mCherry^{RNAi}$*: short hpRNA UAS-RNAi against *mCherry* (not present in *Drosophila* genome), TRiP library genetic background control for attP2 landing site, sc^* control
36303	BDSC	*y^1 v^1;P{$y^{+t7.7}$=CaryP}attP2*	TRiP library genetic background control for attP2 landing site
60000	VDRC	*w^{1118}*	GD library genetic background control
60100	VDRC	*y^1 w^{1118};P{attP,y^+ $w^{3'}$}*	KK library genetic background control
24650	BDSC	*w^{1118}; P{w^{+mC}=UAS-Dcr-2.D}2*	*UAS-Dicer2*: Expresses Dicer2 under UAS control
24650	BDSC	*w^{1118}; P{w^{+mC}=UAS-Dcr-2.D}10*	*UAS-Dicer2*: Expresses Dicer2 under UAS control
5137	BDSC	*y^1 w^*; P{w w^{+mC}=UAS-mCD8::GFP.L}LL5, P{UAS-mCD8::GFP.L}2*	*UAS-mCD8::GFP*: Expresses mCD8::GFP under UAS control
n/a	Henry, 2012	*y^1 v^1; P{UAS_unc84-2XGFP}attP2*	*UAS-unc84-GFP*: Expresses UNC84-GFP under UAS control
48667	BDSC	*w^{1118} P{$y^{+t7.7}$ w^{+mC}=GMR14H06- GAL4}attP2*	R14H06-GAL4: Expresses GAL4 under the control of a *rut* (FBgn0003301) enhancer
25374	BDSC	*y^1 w^*;P{Act5C-GAL4-w}E1/CyO*	*Act5C-GAL4*: Expresses GAL4 ubiquitously under control of the *Act5C* (FBgn0000042) promoter
7019	BDSC	*w^*; P{w^{+mC},=tubP-GAL80^{ts}}20; TM2/TM6B, Tb^1*	*tubP-GAL80^{ts}*: Expresses GAL80^{ts} ubiquitously under control of the *αTub84B* (FBgn0003884) promoter
RNAi stocks			
Stock #	**Supplier**	**Genotype**	**Description**

33704	BDSC	*y^1 sc^* v^1; P{ $y^{+t7.7}$ $v^{+t1.8}$=TRiP.HMS00581}attP2*	*$Set1^{RNAi1}$*: short hpRNA UAS-RNAi against *Set1* at attP2 site from the TRiP library
38368	BDSC	*y^1 sc^* v^1; P{ $y^{+t7.7}$ $v^{+t1.8}$=TRiP.HMS01837}attP2*	*$Set1^{RNAi2}$*: short hpRNA UAS-RNAi against *Set1* at attP2 site from the TRiP library
40931	BDSC	*y^1 sc^* v^1; P{ $y^{+t7.7}$ $v^{+t1.8}$=TRiP.HMS02179}attP40*	*$Set1^{RNAi3}$*: short hpRNA UAS-RNAi against *Set1* at attP40 site from the TRiP library
37715	VDRC	*w^{1118}; P{GD4502}v37715*	*trx^{RNAi1}*: long hpRNA UAS-RNAi against *trx* from GD library
31092	BDSC	*y^1 v^1; P{ $y^{+t7.7}$ $v^{+t1.8}$=TRiP.JF01557}attP2*	*trx^{RNAi2}*: long hpRNA UAS-RNAi against *trx* at attP2 site from the TRiP library
17701	VDRC	*w^{1118}; P{GD8117}v17701*	*$Mnn1^{RNAi1}$*: long hpRNA UAS-RNAi against *Mnn1* from GD library
110376	VDRC	*P{KK101050}VIE-260B*	*$Mnn1^{RNAi2}$*: long hpRNA UAS-RNAi against *Mnn1* from KK library
31192	VDRC	*w^{1118}; P{GD6887}v31192/TM3*	*Ldh^{RNAi}*: long hpRNA UAS-RNAi against *Ldh* from GD library.

Appendix B: Differentially expressed genes in CTvCN experimental comparisons.

Sorted by descending Log2 fold change.

Gene name	FlyBase ID	log_2 Fold Change	adj. p-value
Ccp84Ab	FBgn0004782	4.38394996	1.19E-07
CG9733	FBgn0039759	1.90492844	2.52E-07
MtnD	FBgn0053192	1.60632872	3.09E-06
Ets21C	FBgn0005660	1.35437521	0.00026002
CG5966	FBgn0029831	1.20458582	0.00106426
CG8665	FBgn0032945	1.11709763	0.00294216
MFS9	FBgn0038799	0.924025	5.72E-05
NHP2	FBgn0029148	0.90025321	0.03456945
Tig	FBgn0011722	0.86632041	2.43E-06
Spt	FBgn0033348	0.85223105	0.01615231
Cpr47Ef	FBgn0033603	0.79623289	0.02996573
atk	FBgn0036995	0.7873557	0.01265919
Nep7	FBgn0039564	0.78572314	0.00167189
Lgr1	FBgn0016650	0.73961977	7.93E-14
Hr38	FBgn0014859	0.68875015	9.16E-08
CG16743	FBgn0032322	0.65668051	0.01048744
CG4577	FBgn0031306	0.64109771	1.59E-13
CG5776	FBgn0032450	0.63214504	0.03799465
nero	FBgn0261479	0.62961077	0.03727453
lncRNA:CR44566	FBgn0265759	0.62332122	0.00299678
Hsp68	FBgn0001230	0.60461268	0.04390644
LanB2	FBgn0267348	0.58565949	0.00023178
CG8303	FBgn0034143	0.57685997	0.01370654
CG14186	FBgn0036935	0.54109444	8.26E-19
CG2875	FBgn0029672	0.53878557	0.04831416
Nmdmc	FBgn0010222	0.53651115	0.03223298
sr	FBgn0003499	0.53484637	3.44E-05
jeb	FBgn0086677	0.53214153	2.47E-11
Sardh	FBgn0034276	0.51247967	0.02963448
CG12428	FBgn0039543	0.51157937	0.00530633
Proc	FBgn0045038	0.5008936	6.08E-07
Nop60B	FBgn0259937	0.4945812	9.83E-05
comm2	FBgn0041160	0.48164013	0.00844476
Cdc7	FBgn0028360	0.47072373	0.00479963

CG17778	FBgn0023534	0.46568124	5.87E-05
Hsp83	FBgn0001233	0.43285189	1.34E-08
otp	FBgn0015524	0.41979629	0.03727453
tey	FBgn0036899	0.4180948	0.04526914
CG16758	FBgn0035348	0.41253626	0.00496603
CrebA	FBgn0004396	0.40594832	0.01247958
Myo31DF	FBgn0086347	0.40365342	0.01311677
Eip71CD	FBgn0000565	0.40332698	0.00534186
Tbh	FBgn0010329	0.3981745	0.00440911
CG44247	FBgn0265182	0.39447952	2.97E-10
lncRNA:CR44922	FBgn0266227	0.39339826	0.01052168
Drice	FBgn0019972	0.38690569	0.03750146
spab	FBgn0033358	0.37862426	0.00081827
CG9812	FBgn0034860	-0.3831621	0.01502674
Gpdh1	FBgn0001128	-0.3879649	7.63E-05
Cat	FBgn0000261	-0.3904332	0.0112219
ATPCL	FBgn0020236	-0.3920456	3.72E-10
mino	FBgn0027579	-0.3969185	0.039103
CG5059	FBgn0037007	-0.3975817	0.00115961
CG34166	FBgn0085195	-0.398008	0.0240378
teq	FBgn0023479	-0.3985114	0.03750146
Mal-A5	FBgn0050359	-0.4000944	0.01352719
RpLP2	FBgn0003274	-0.4014992	0.00685586
apolpp	FBgn0087002	-0.4047703	0.01925695
CG11241	FBgn0037186	-0.4066706	0.01597031
CG6426	FBgn0034162	-0.4095905	0.02996573
CG6770	FBgn0032400	-0.4096556	0.01573551
whd	FBgn0261862	-0.4118239	0.00283183
CG32407	FBgn0052407	-0.4129598	0.03567546
Sirup	FBgn0031971	-0.4149758	0.03716952
CG3999	FBgn0037801	-0.417992	0.0460156
Ugt36Bc	FBgn0040260	-0.4244221	0.01089146
CG9649	FBgn0038211	-0.425237	0.01479646
AOX3	FBgn0038349	-0.4303107	0.01050881
CG8008	FBgn0033387	-0.4333042	0.02212095
GstZ2	FBgn0037697	-0.4336561	0.00014597
CG3301	FBgn0038878	-0.4418916	0.03799465
GstS1	FBgn0010226	-0.4429071	0.00178854
Clk	FBgn0023076	-0.4477224	0.00858734

CG17549	FBgn0032774	-0.4520331	0.00180114
Acbp2	FBgn0010387	-0.4533882	0.02942465
CG8586	FBgn0033320	-0.4542384	0.016808
CG9331	FBgn0032889	-0.4575703	0.00055047
CG9399	FBgn0037715	-0.4590436	0.00446195
CG9953	FBgn0035726	-0.4592024	0.01103707
fusl	FBgn0031702	-0.4597627	0.011977
CG8180	FBgn0034021	-0.4605665	0.00014597
AcCoAS	FBgn0012034	-0.4606434	8.50E-12
CG4572	FBgn0038738	-0.4620865	0.00517823
Mdr65	FBgn0004513	-0.4624864	0.00079671
CG13003	FBgn0030798	-0.4639468	0.01036234
GNBP3	FBgn0040321	-0.4640543	0.01380027
Echs1	FBgn0033879	-0.466014	0.03649516
Tep4	FBgn0041180	-0.466073	0.00048857
CG2233	FBgn0029990	-0.4767327	0.01188412
GstE12	FBgn0027590	-0.4769854	0.03070309
glob1	FBgn0027657	-0.477875	0.0006204
Mdh1	FBgn0262782	-0.4793759	0.00011606
CG7470	FBgn0037146	-0.4798269	0.00147438
CG9631	FBgn0027563	-0.482256	0.03706415
CG15098	FBgn0034398	-0.4843833	0.00062081
CG11951	FBgn0039656	-0.4882911	0.01036234
CG8036	FBgn0037607	-0.4932214	0.00459866
Adgf-D	FBgn0038172	-0.4934966	0.01050881
Gba1b	FBgn0051414	-0.4938314	0.01947555
CG2145	FBgn0030251	-0.4953775	0.01573551
CG17928	FBgn0032603	-0.4956918	0.00283183
GstT4	FBgn0030484	-0.4968442	0.02452102
Tps1	FBgn0027560	-0.5009859	0.01103707
CG11407	FBgn0038733	-0.5033232	0.00725778
CG42846	FBgn0262035	-0.503958	0.04037723
bmm	FBgn0036449	-0.504574	0.04526914
CG16986	FBgn0035356	-0.5065145	0.01696148
CG7724	FBgn0036698	-0.5067473	0.01164336
Cyp305a1	FBgn0036910	-0.5072995	0.01647097
CG5390	FBgn0032213	-0.5079045	0.00033944
CG1213	FBgn0037387	-0.5094806	0.01188412
Cyp28d1	FBgn0031689	-0.5113988	0.00110796

Cpr65Au	FBgn0042119	-0.5125631	0.04960866
CG30046	FBgn0050046	-0.5126582	0.02336112
CG31673	FBgn0051673	-0.5127587	0.00198778
alpha-Est7	FBgn0015575	-0.5135138	2.72E-06
yellow-e	FBgn0041711	-0.5149397	0.021402
pug	FBgn0020385	-0.5150288	0.01040407
scu	FBgn0021765	-0.5162972	0.0125041
Gart	FBgn0000053	-0.5251833	0.0015487
FASN1	FBgn0027571	-0.5260692	7.98E-06
hid	FBgn0003997	-0.5311616	0.00052524
Npc2h	FBgn0039801	-0.5410185	0.00685586
CG7203	FBgn0031942	-0.542561	0.01497483
CG6175	FBgn0036152	-0.5433735	0.00705142
St1	FBgn0034887	-0.5506802	0.00558946
CG10026	FBgn0032785	-0.5509686	0.03782567
CG33493	FBgn0053493	-0.5517388	0.00106426
Pdh	FBgn0011693	-0.552629	0.00075503
CG17572	FBgn0032753	-0.5533368	0.02455172
Tasp1	FBgn0263602	-0.5533657	0.00258922
Desat1	FBgn0086687	-0.5547858	9.16E-08
CG5793	FBgn0038858	-0.555378	0.02786656
CG6409	FBgn0036106	-0.5573734	0.001639
Gbp2	FBgn0034200	-0.5607478	0.00397278
GstE9	FBgn0063491	-0.577171	0.03383803
CG9312	FBgn0038179	-0.5796703	0.00316955
Got1	FBgn0001124	-0.5871942	1.74E-08
Jabba	FBgn0259682	-0.5872681	5.75E-05
CG9629	FBgn0036857	-0.592585	0.01457248
TpnC25D	FBgn0031692	-0.5928716	0.00444212
Hpd	FBgn0036992	-0.5943022	2.87E-06
Glt	FBgn0001114	-0.5950732	4.05E-05
Cyp12a4	FBgn0038681	-0.5957049	0.00092706
CG13833	FBgn0039040	-0.5965369	0.00246021
CG7720	FBgn0038652	-0.5967476	0.00844476
UK114	FBgn0086691	-0.5981392	0.01625151
Root	FBgn0039152	-0.6003271	0.0033629
CG9747	FBgn0039754	-0.6014016	0.00106534
AkhR	FBgn0025595	-0.6037185	0.02996573
UGP	FBgn0035978	-0.6070141	5.87E-05

CG6084	FBgn0086254	-0.6076299	6.82E-05
fbp	FBgn0032820	-0.607844	7.49E-05
Argl	FBgn0032076	-0.6097	0.0066912
CG2736	FBgn0035090	-0.6110839	0.00149058
CG3036	FBgn0031645	-0.6148044	0.00246021
Hn	FBgn0001208	-0.6164652	0.00115961
SPE	FBgn0039102	-0.6221608	4.17E-12
Rpi	FBgn0050410	-0.6229003	0.00764604
klu	FBgn0013469	-0.6265808	0.00027833
Iris	FBgn0031305	-0.6275174	0.01144401
TpnC73F	FBgn0010424	-0.6282557	0.02829468
yellow-f2	FBgn0038105	-0.6370209	0.00449197
Est-6	FBgn0000592	-0.6376158	5.87E-05
CG16965	FBgn0032387	-0.640879	0.01050881
Cyp6a23	FBgn0033978	-0.6422351	3.91E-06
CG18547	FBgn0037973	-0.646539	9.58E-05
CG14259	FBgn0039483	-0.6501858	0.04913926
Got2	FBgn0001125	-0.6516906	1.00E-07
CG32444	FBgn0043783	-0.6539404	0.0001138
foxo	FBgn0038197	-0.656738	1.16E-05
CG31313	FBgn0051313	-0.6580213	7.74E-05
LManI	FBgn0032253	-0.6582119	0.01036234
Obp57c	FBgn0034509	-0.6591006	0.00178966
fat-spondin	FBgn0026721	-0.6627608	9.58E-05
CG7322	FBgn0030968	-0.6745787	0.00086923
hgo	FBgn0040211	-0.6793678	0.03298202
CG31689	FBgn0031449	-0.6804098	5.80E-07
CG7966	FBgn0038115	-0.681519	0.00638562
Taldo	FBgn0023477	-0.6844127	1.12E-05
CG10621	FBgn0032726	-0.6892397	5.41E-05
Cpr76Bc	FBgn0036880	-0.6895438	0.01311677
CG7135	FBgn0030895	-0.6911971	0.00011827
CG12338	FBgn0033543	-0.695068	0.00095997
Cpr72Ec	FBgn0036619	-0.6966835	0.00024131
CG1468	FBgn0030157	-0.6976626	0.00037503
CG4962	FBgn0036597	-0.6986115	0.01022106
GILT2	FBgn0039099	-0.6992124	0.02388736
CG4000	FBgn0038820	-0.7107107	0.00434176
Spat	FBgn0014031	-0.7133918	0.03834567

CG11400	FBgn0034198	-0.7201569	0.00070953
Tsf1	FBgn0022355	-0.7232453	8.56E-05
LManII	FBgn0027611	-0.7275957	3.72E-10
CG11368	FBgn0040923	-0.7281762	0.00081827
CG16926	FBgn0040732	-0.733113	0.00207444
Cyp6a21	FBgn0033981	-0.7507665	0.0010863
Jheh3	FBgn0034406	-0.7541156	0.00024676
CG32645	FBgn0052645	-0.7590134	0.04458381
CG31205	FBgn0051205	-0.7605397	0.00041454
CG15553	FBgn0039817	-0.761704	0.00108284
CG4716	FBgn0033820	-0.7643422	6.04E-05
Gbp1	FBgn0034199	-0.7669144	0.00024461
CG42329	FBgn0259229	-0.7711147	0.00312258
Obp18a	FBgn0030985	-0.7711412	0.02799052
CG31445	FBgn0051445	-0.7766052	1.56E-07
Kr-h1	FBgn0266450	-0.7807195	3.72E-10
Galk	FBgn0263199	-0.781027	9.11E-06
Sodh-2	FBgn0022359	-0.7856263	0.00246021
Nepl10	FBgn0033742	-0.785742	0.00488776
CG6910	FBgn0036262	-0.7893352	0.00066174
sug	FBgn0033782	-0.79707	0.00023178
CG17108	FBgn0032285	-0.8069058	0.0276674
CG7296	FBgn0032283	-0.8089167	0.01679352
Dr	FBgn0000492	-0.816545	0.00505801
Cyt-b5-r	FBgn0000406	-0.8217499	3.87E-08
Idgf5	FBgn0064237	-0.8229718	4.75E-07
Acer	FBgn0016122	-0.8389698	1.09E-15
dsx	FBgn0000504	-0.8484403	3.77E-11
CG31778	FBgn0051778	-0.8540064	0.00697321
Faa	FBgn0016013	-0.8628002	0.00048857
Drsl4	FBgn0052282	-0.8791564	0.00169049
CG18003	FBgn0061356	-0.8820112	8.87E-07
CG17324	FBgn0027074	-0.8960417	0.00178854
CG3699	FBgn0040349	-0.9491104	0.00033384
CG18302	FBgn0032266	-0.9571212	6.70E-08
bgm	FBgn0027348	-0.9647219	2.42E-08
CG6503	FBgn0040606	-0.9742974	6.08E-07
CG15068	FBgn0040733	-0.9759918	0.00347166
CG15096	FBgn0034394	-0.997764	6.12E-19

Sodh-1	FBgn0024289	-1.0047236	2.58E-08
Achl	FBgn0033936	-1.0047245	5.24E-06
lncRNA:CR43417	FBgn0263336	-1.0053923	0.0001138
Cyp6g1	FBgn0025454	-1.0261601	8.57E-09
Amy-p	FBgn0000079	-1.0521577	0.00576875
Nepl12	FBgn0037727	-1.0610321	0.00075503
alpha-Est2	FBgn0015570	-1.0620103	0.00434176
Cyp18a1	FBgn0010383	-1.0730092	1.22E-07
Amy-d	FBgn0000078	-1.0744039	7.26E-09
CG31075	FBgn0051075	-1.1428167	3.43E-07
CG13315	FBgn0040827	-1.1550721	2.36E-06
CG16898	FBgn0034480	-1.1668651	0.00011324
CG34227	FBgn0085256	-1.1680663	0.01636235
CG34165	FBgn0085194	-1.2064003	0.00048857
phu	FBgn0043791	-1.3518708	2.22E-07
Lsp2	FBgn0002565	-1.7867879	6.70E-08
CG34330	FBgn0085359	-1.8176603	0.00010348
lectin-28C	FBgn0040099	-1.9015045	1.42E-24
tobi	FBgn0261575	-2.3863197	1.48E-41
CAH5	FBgn0040629	-2.3993129	0.00138477

Appendix C: Differentially expressed genes in KTvKN experimental comparison.

Sorted by descending Log_2 fold change.

Gene name	FlyBase ID	log_2 Fold Change	adj. p-value
Ccp84Ab	FBgn0004782	5.46931028	2.85E-11
CG43202	FBgn0262838	2.61100074	0.03769567
CG43236	FBgn0262881	2.2230046	0.03509168
CecC	FBgn0000279	2.20672362	0.03566775
CG8665	FBgn0032945	1.76066139	8.57E-08
CG9733	FBgn0039759	1.70102826	3.32E-06
gammaSnap1	FBgn0028552	1.6258413	0.03628684
IM1	FBgn0034329	1.48531978	0.01745932
slmo	FBgn0029161	1.46984245	0.04764576
CG15065	FBgn0040734	1.3172134	0.01518913
RpS9	FBgn0010408	1.29434912	0.03570412
CG30033	FBgn0050033	1.27082278	0.01148341
Ets21C	FBgn0005660	1.25355642	0.00147224
IM14	FBgn0067905	1.23896111	0.034353

Rpt6	FBgn0020369	1.22075191	0.04529964
CG16743	FBgn0032322	1.18193072	3.97E-08
Nep7	FBgn0039564	1.14404904	2.80E-07
CG5909	FBgn0039495	1.03588835	1.79E-06
PGRP-SA	FBgn0030310	1.03221534	0.04056273
IM2	FBgn0025583	1.02387381	0.0289439
fit	FBgn0038914	1.00238809	0.03384228
Cpr47Ef	FBgn0033603	0.96719679	0.01142696
lmd	FBgn0039039	0.95817719	0.03428546
CG12118	FBgn0030101	0.91616527	0.02964881
Tig	FBgn0011722	0.8626192	3.94E-06
CG5966	FBgn0029831	0.85058216	0.04721258
Hr38	FBgn0014859	0.82912793	3.22E-11
MtnD	FBgn0053192	0.82770622	0.03976179
CG6429	FBgn0046999	0.80348605	0.02001327
Nmdmc	FBgn0010222	0.79940969	0.0002526
Sardh	FBgn0034276	0.78306115	9.18E-05
LanB2	FBgn0267348	0.77519322	2.14E-07
sr	FBgn0003499	0.76554046	8.57E-11
CG5958	FBgn0031913	0.76110284	4.48E-05
CG32091	FBgn0052091	0.75063622	0.00127596
Tsp42Ed	FBgn0029507	0.74597767	0.03519822
CG5791	FBgn0040582	0.74252622	0.02586053
lncRNA:CR44566	FBgn0265759	0.73301099	0.00015532
Hsp68	FBgn0001230	0.73066935	0.00960428
CG8785	FBgn0033760	0.73041863	0.01152374
CG15332	FBgn0029986	0.72647178	0.02771642
Lgr1	FBgn0016650	0.72062242	4.66E-14
CG12560	FBgn0031974	0.71052768	0.00140233
CG33494	FBgn0053494	0.6827715	0.01757453
okr	FBgn0002989	0.65177423	0.00992714
GIIIspla2	FBgn0030013	0.63650327	0.00960428
Hml	FBgn0029167	0.63550597	0.00107965
CG4962	FBgn0036597	0.62650858	0.02964881
CrebA	FBgn0004396	0.61890945	1.44E-05
Lst	FBgn0034140	0.61027637	0.02673253
CG5773	FBgn0034290	0.60999322	5.63E-05
CG18081	FBgn0036537	0.5890457	0.02964881
CG9498	FBgn0031801	0.58863241	0.01081917

RpL38	FBgn0040007	0.58763786	0.01975195
CG7339	FBgn0036188	0.57235056	0.01745932
CG16758	FBgn0035348	0.56962356	2.59E-05
CG8369	FBgn0040532	0.56777697	0.00399734
comm2	FBgn0041160	0.56696455	0.00119515
CG17278	FBgn0046763	0.56668958	0.04721258
GstE3	FBgn0063497	0.5652196	0.00127596
Cdc7	FBgn0028360	0.56194541	0.00039934
RpS3A	FBgn0017545	0.54022043	0.03198094
CG8303	FBgn0034143	0.53892869	0.02484563
CG1572	FBgn0030309	0.53867718	0.02064553
COX8	FBgn0263911	0.53660599	0.00716241
SIFaR	FBgn0038880	0.53377549	2.62E-08
CCT3	FBgn0015019	0.53223692	0.00022368
Myo31DF	FBgn0086347	0.52962001	0.00039934
PIG-Q	FBgn0086448	0.52495167	0.03384228
CG44325	FBgn0265413	0.51731977	0.00727789
Sod3	FBgn0033631	0.51559635	0.02106049
ple	FBgn0005626	0.51440247	0.01527644
Cka	FBgn0044323	0.50228023	0.02946254
Taf12	FBgn0011290	0.50165883	0.00127596
jeb	FBgn0086677	0.49789518	7.73E-10
CG7694	FBgn0038627	0.49743216	0.02771642
CG13055	FBgn0036583	0.49519115	0.00063224
smt3	FBgn0264922	0.49269647	0.00909189
CG10516	FBgn0036549	0.48866623	0.02265856
CG32756	FBgn0052756	0.48791569	0.03006535
glec	FBgn0015229	0.48760146	0.00054586
ImpL2	FBgn0001257	0.48415421	0.00198034
Atf3	FBgn0028550	0.47555842	0.0133855
CG3597	FBgn0031417	0.46965406	0.01269623
CG14186	FBgn0036935	0.46325341	1.48E-13
CG17574	FBgn0033777	0.45618085	0.04100919
RpL27A	FBgn0261606	0.44746388	0.03864961
ytr	FBgn0021895	0.44621554	0.03021306
CG13229	FBgn0033579	0.44525589	0.04561862
CG15117	FBgn0034417	0.44395444	0.02940522
ghi	FBgn0266124	0.44019649	0.02904844
CG44247	FBgn0265182	0.42855693	3.80E-12

Dpck	FBgn0037469	0.42744076	0.02592102
RpL10	FBgn0024733	0.4239874	0.03276715
CG32204	FBgn0052204	0.42319578	0.00053586
Rbp1-like	FBgn0030479	0.4213098	0.02958698
Cpr49Ae	FBgn0033728	0.42026453	0.02438979
CG2865	FBgn0023526	0.4202077	3.04E-06
CG32276	FBgn0047135	0.41837993	0.01913948
Sec61beta	FBgn0010638	0.417979	0.02828142
Tom40	FBgn0016041	0.41321871	2.86E-05
PRL-1	FBgn0024734	0.41110353	0.03276715
CG8031	FBgn0038110	0.4063727	0.03347199
Spase22-23	FBgn0039172	0.40218315	0.02586053
CG11267	FBgn0036334	0.4019889	0.00464431
RpS14a	FBgn0004403	0.40005825	0.04918105
Pisd	FBgn0026576	0.39940124	0.00666219
srl	FBgn0037248	0.39820386	0.02752342
CG43324	FBgn0263029	0.39417172	0.04056273
lama	FBgn0016031	0.3902588	0.00309592
Psf3	FBgn0030196	0.38930155	0.02484563
Rab39	FBgn0029959	0.38820035	0.0407749
SsRbeta	FBgn0011016	0.38261839	0.02484563
mbf1	FBgn0262732	0.38169032	0.00341128
a	FBgn0000008	0.38160034	0.0036337
CG11334	FBgn0039849	0.38107872	0.0017936
Ubc6	FBgn0004436	0.3794708	0.02946254
Ptip	FBgn0052133	0.37934945	0.00041833
ds	FBgn0000497	-0.3803872	0.02964881
CG9953	FBgn0035726	-0.3848603	0.04918105
Clk	FBgn0023076	-0.3875601	0.03566775
ft	FBgn0001075	-0.3979688	0.00769167
Sirt7	FBgn0039631	-0.4000895	0.02750991
Vps20	FBgn0034744	-0.4017767	0.01863414
Got1	FBgn0001124	-0.4034465	0.00063144
CG5390	FBgn0032213	-0.4093577	0.00807018
Sec5	FBgn0266670	-0.4139606	0.0326821
CG32444	FBgn0043783	-0.4177095	0.0427046
Cyt-b5-r	FBgn0000406	-0.4182557	0.02964881
CG12512	FBgn0031703	-0.4190938	0.01269623
CG11438	FBgn0037164	-0.427491	0.01484579

GstZ2	FBgn0037697	-0.4291189	0.00016948
Jabba	FBgn0259682	-0.431026	0.01132359
LManII	FBgn0027611	-0.4382899	0.00136204
Msr-110	FBgn0015766	-0.4416172	0.00262084
CG18302	FBgn0032266	-0.4454038	0.04912493
UGP	FBgn0035978	-0.4457703	0.01141965
CG11951	FBgn0039656	-0.4459315	0.02566326
CG13833	FBgn0039040	-0.452418	0.04778699
CG6409	FBgn0036106	-0.4605063	0.02001327
Cpr72Ec	FBgn0036619	-0.4759823	0.03509168
pug	FBgn0020385	-0.4800069	0.02484563
hid	FBgn0003997	-0.4811664	0.00271467
modSP	FBgn0051217	-0.4832195	0.00168078
CG3376	FBgn0034997	-0.4912695	0.02127559
CG31445	FBgn0051445	-0.4948721	0.00473492
CG9664	FBgn0031515	-0.507219	0.02964881
Flacc	FBgn0030974	-0.5093472	0.02484563
CG15547	FBgn0039809	-0.5100542	0.02322975
CG4849	FBgn0039566	-0.5152695	0.02752342
SCOT	FBgn0035298	-0.5169216	0.01387629
CG30046	FBgn0050046	-0.5264751	0.02586053
CG4752	FBgn0034733	-0.5264876	0.00225036
Root	FBgn0039152	-0.5297065	0.02277397
foxo	FBgn0038197	-0.533056	0.00124364
CG31205	FBgn0051205	-0.5429772	0.03198232
CG31689	FBgn0031449	-0.5486744	0.00022693
Acer	FBgn0016122	-0.5582188	1.40E-06
Got2	FBgn0001125	-0.5776284	7.08E-06
CG11594	FBgn0035484	-0.5902599	0.02064553
CG9890	FBgn0034814	-0.5943182	0.03618956
bw	FBgn0000241	-0.5944508	0.01335336
Gip	FBgn0011770	-0.5947034	0.01563064
nudC	FBgn0021768	-0.6010812	0.02964881
Achl	FBgn0033936	-0.6034177	0.02798936
lncRNA:CR32773	FBgn0052773	-0.6040511	0.02186474
Gart	FBgn0000053	-0.6088297	0.0001693
CG15553	FBgn0039817	-0.6147802	0.01728031
CG7255	FBgn0036493	-0.626583	0.03767662
klu	FBgn0013469	-0.6424084	0.00023088

AkhR	FBgn0025595	-0.6586468	0.01759225
Non3	FBgn0038585	-0.664826	0.03392667
CG42329	FBgn0259229	-0.6685185	0.01939181
Ndg	FBgn0026403	-0.6742818	0.02064553
Galk	FBgn0263199	-0.6887484	0.0002526
dsx	FBgn0000504	-0.6918607	3.59E-07
CG6179	FBgn0030915	-0.6962552	0.02964881
Cyp18a1	FBgn0010383	-0.6990885	0.00272225
Kr-h1	FBgn0266450	-0.7496349	2.53E-09
CG15096	FBgn0034394	-0.7625562	1.16E-10
Sodh-1	FBgn0024289	-0.7629792	0.00013638
Amy-d	FBgn0000078	-0.7678721	0.00020025
GluRIIE	FBgn0051201	-0.7714262	0.04721258
Ku80	FBgn0041627	-0.7733892	0.01269623
CG31075	FBgn0051075	-0.7949794	0.00233525
CG7322	FBgn0030968	-0.8103672	3.45E-05
Mthfs	FBgn0085453	-0.8180188	0.0405976
FMRFa	FBgn0000715	-0.8192734	0.00418816
mldr	FBgn0029858	-0.8223768	0.04926682
CG7135	FBgn0030895	-0.8247232	2.96E-06
CG17005	FBgn0032109	-0.836109	0.04356273
Hpd	FBgn0036992	-0.8777985	2.47E-13
CG14892	FBgn0038447	-0.886476	0.01035312
Odc1	FBgn0013307	-0.9263828	0.03991265
bgm	FBgn0027348	-0.9309449	1.60E-07
alpha-Est2	FBgn0015570	-0.9338966	0.02484563
Cyp6g1	FBgn0025454	-0.9407464	4.08E-07
Obp56a	FBgn0034468	-1.0247482	0.02038606
snsl	FBgn0031646	-1.1239997	0.02905446
phu	FBgn0043791	-1.2102404	2.42E-05
lectin-28C	FBgn0040099	-1.3979137	8.64E-13
tobi	FBgn0261575	-2.1890146	1.84E-34
Obp19a	FBgn0031109	-4.5490637	0.00960428
Obp83a	FBgn0011281	-6.2237261	2.92E-05
a10	FBgn0011293	-6.6846135	0.00127596
a5	FBgn0011294	-8.2716259	0.00053884
Obp83b	FBgn0010403	-8.341559	5.61E-05
Os-C	FBgn0010401	-8.5104579	0.00011176

Appendix D: Differentially expressed genes in KNvCN experimental comparison.

Sorted by descending Log_2 fold change

Gene name	FlyBase ID	log_2 Fold Change	adj. p-value
CG32581	FBgn0052581	7.55604154	9.31E-08
CG15614	FBgn0034168	1.01599684	0.03187109
mus301	FBgn0002899	0.99954024	0.00821184
mir-957	FBgn0262182	0.97001389	0.01059933
CG32147	FBgn0047178	0.93438398	0.04406727
Drep4	FBgn0028406	0.91871246	0.02472266
brv3	FBgn0040333	0.91618244	0.02904885
lncRNA:CR44718	FBgn0265929	0.91245787	0.00228183
CG13679	FBgn0035856	0.85522585	0.02260799
CG31371	FBgn0051371	0.82927697	0.00544999
CG31323	FBgn0051323	0.78411071	1.12E-07
PK2-R2	FBgn0038139	0.77290186	0.00164941
Trissin	FBgn0038343	0.77118476	0.00136602
Osi9	FBgn0037416	0.77055032	0.04134903
lncRNA:CR45429	FBgn0266978	0.76710446	0.00933904
TMEM216	FBgn0037614	0.76234225	0.04135711
CG3149	FBgn0027564	0.75879627	0.01639715
CG11449	FBgn0037162	0.75742272	0.00188782
cm	FBgn0000330	0.71867082	0.00268073
pch2	FBgn0051453	0.70946048	0.00523084
CG11983	FBgn0037654	0.70897111	0.02140404
CG15322	FBgn0031088	0.69371131	0.03452806
CCAP-R	FBgn0039396	0.68521422	1.64E-07
CG14937	FBgn0032377	0.67696397	0.04005161
CG12038	FBgn0035179	0.65593126	9.38E-06
Tbp	FBgn0003687	0.65416315	0.0051445
escl	FBgn0032391	0.6389349	0.04512187
lncRNA:CR31451	FBgn0051451	0.63732669	6.47E-05
Smyd4-1	FBgn0033427	0.63726633	9.47E-08
GAPsec	FBgn0035916	0.63576202	0.00235636
Ddc	FBgn0000422	0.6321344	5.07E-11
CG43373	FBgn0263131	0.62997236	6.80E-09
CG12194	FBgn0031636	0.62466281	0.00041732
Nap1	FBgn0015268	0.62465098	0.04839293
CG10375	FBgn0039116	0.61123936	0.04735124

TkR99D	FBgn0004622	0.60996893	6.47E-05
DAT	FBgn0034136	0.60846707	0.0002929
CG33143	FBgn0053143	0.60030432	1.67E-08
Ir68a	FBgn0036150	0.59562373	0.00303445
DIP-delta	FBgn0085420	0.5924033	2.34E-08
tld	FBgn0003719	0.59235597	0.03233676
lncRNA:CR45382	FBgn0266931	0.58827813	0.02000607
fd102C	FBgn0039937	0.58695643	0.00031081
dpr15	FBgn0037993	0.58243293	2.51E-13
CG4660	FBgn0029839	0.57691702	0.00012705
CG10738	FBgn0036368	0.56963236	1.73E-05
asRNA:CR45600	FBgn0267160	0.56792794	1.82E-05
CG13325	FBgn0033792	0.56737972	2.73E-06
CG32457	FBgn0052457	0.56211691	0.04785697
eag	FBgn0000535	0.55574478	2.00E-10
Syt12	FBgn0261085	0.55165641	1.34E-05
NPFR	FBgn0037408	0.5509639	0.01429698
DJ-1alpha	FBgn0033885	0.54468268	0.00599958
CG43329	FBgn0263034	0.54463365	0.04006474
CG43219	FBgn0262855	0.54124696	0.00021473
CG6142	FBgn0039415	0.53599974	0.02845098
rod	FBgn0003268	0.53243776	0.01534134
RYa-R	FBgn0004842	0.53156905	0.0026533
hig	FBgn0010114	0.53094584	1.08E-07
lncRNA:CR44024	FBgn0264794	0.53018835	1.18E-08
CG13408	FBgn0038929	0.52686313	0.02047775
CG13248	FBgn0036984	0.52464071	0.00062474
CG15236	FBgn0033108	0.52411149	2.24E-08
Sytbeta	FBgn0261090	0.52331283	4.79E-09
CG17359	FBgn0036396	0.52108361	0.04391366
ZnT41F	FBgn0025693	0.52025233	0.00229367
CG32017	FBgn0052017	0.51996627	1.39E-12
DIP-theta	FBgn0051646	0.51880802	3.31E-06
CG12594	FBgn0037941	0.51682066	0.00014058
CG32683	FBgn0052683	0.51580973	5.45E-10
CG15082	FBgn0034397	0.51540635	0.02290418
GABPI	FBgn0031495	0.51475616	0.0137362
AstC-R2	FBgn0036789	0.51381063	1.68E-06
Awh	FBgn0013751	0.50953224	0.0109014

RunxA	FBgn0083981	0.5029028	0.00010361
FoxP	FBgn0262477	0.50251063	2.28E-13
PGAP3	FBgn0033088	0.50243405	0.02548361
vg	FBgn0003975	0.50032161	0.03444349
TkR86C	FBgn0004841	0.4973061	0.0014409
CG43331	FBgn0263036	0.49710878	0.04046026
CG3987	FBgn0038292	0.49506667	0.02692176
CG2875	FBgn0029672	0.49473728	0.04084077
Drip	FBgn0015872	0.49461317	0.0314379
lncRNA:CR45758	FBgn0267322	0.49324274	0.01112705
Grip163	FBgn0026432	0.49229956	5.26E-05
CG42346	FBgn0259677	0.49126166	4.74E-13
beat-VII	FBgn0250908	0.4888489	4.74E-13
CG5282	FBgn0036986	0.48823845	5.28E-05
CG8641	FBgn0035733	0.48775901	1.47E-05
CG5038	FBgn0038324	0.4811407	0.01977767
Grip91	FBgn0001612	0.48032339	0.00190388
Dh31	FBgn0032048	0.47968569	3.19E-06
CG31760	FBgn0051760	0.47912928	1.23E-05
Elp3	FBgn0031604	0.47710141	0.04970821
net	FBgn0002931	0.47663429	1.82E-05
CG17698	FBgn0040056	0.47594968	5.45E-07
CG6154	FBgn0039420	0.47548217	2.41E-06
AstC	FBgn0032336	0.4736151	0.03403799
CCHa2-R	FBgn0033058	0.47335563	0.00873224
Ddr	FBgn0053531	0.47320493	7.93E-08
otp	FBgn0015524	0.47228802	0.00778356
beat-VI	FBgn0039584	0.46840007	1.49E-15
CG4577	FBgn0031306	0.46793251	1.39E-06
ldlCp	FBgn0026634	0.4641034	0.00776772
CG3777	FBgn0024989	0.46333197	0.02417702
beat-Ic	FBgn0028644	0.46288591	2.78E-05
dpr18	FBgn0030723	0.46258688	1.26E-06
beat-IV	FBgn0039089	0.46068248	1.95E-08
CG6218	FBgn0038321	0.45682221	0.00310525
CG1275	FBgn0035321	0.45657457	0.00300326
wls	FBgn0036141	0.45463128	0.02612948
Trh	FBgn0035187	0.45433675	0.04025934
Dh44-R2	FBgn0033744	0.45412568	6.78E-06

Rgk2	FBgn0085419	0.45188792	0.00100332
CG3626	FBgn0029706	0.45009573	0.02761717
CG32104	FBgn0052104	0.44998807	0.00786598
CaMKI	FBgn0016126	0.44870455	0.00312503
CG45002	FBgn0266354	0.44792404	5.59E-06
CG12531	FBgn0031064	0.44652553	2.15E-06
kek2	FBgn0015400	0.44652517	1.24E-06
CG13255	FBgn0040636	0.44367613	0.03765438
PIG-G	FBgn0033187	0.44111542	0.00468819
CG6325	FBgn0037814	0.44029086	0.00078106
Fili	FBgn0085397	0.43910193	3.20E-06
Myo28B1	FBgn0040299	0.43861548	0.00293133
CG6006	FBgn0063649	0.43856593	1.69E-05
5-HT2B	FBgn0261929	0.43794958	6.41E-06
CG17270	FBgn0038828	0.43722169	2.24E-05
CG2269	FBgn0033484	0.43680923	9.80E-07
beat-Ia	FBgn0013433	0.43652184	0.00034685
CG31814	FBgn0051814	0.43567928	0.00012294
CG8248	FBgn0033347	0.43563421	0.00165947
miple1	FBgn0027111	0.43557059	1.21E-05
stan	FBgn0024836	0.43473453	1.26E-07
Oct-TyrR	FBgn0004514	0.43312996	1.28E-08
DIP-zeta	FBgn0051708	0.43229578	0.00018093
CG5694	FBgn0032197	0.4316694	0.00020041
CG18870	FBgn0042180	0.43137795	0.01629626
PlexB	FBgn0025740	0.43122525	0.00931504
CG14314	FBgn0038581	0.43112534	0.00209772
CG34393	FBgn0085422	0.4279709	1.89E-05
Cals	FBgn0039928	0.42378496	1.04E-06
lncRNA:CR45473	FBgn0267029	0.42309423	0.00819829
nAChRbeta2	FBgn0004118	0.42161618	0.00014726
Tmc	FBgn0036017	0.42097588	0.00507809
CG9109	FBgn0031765	0.42095467	0.03186231
amon	FBgn0023179	0.42089806	8.43E-05
Itp-r83A	FBgn0010051	0.41906344	2.66E-05
hec	FBgn0030437	0.41892631	0.0304555
CG12034	FBgn0035421	0.41874358	0.01352872
beat-Va	FBgn0038087	0.41838182	3.55E-05
Rbp1	FBgn0260944	0.4181545	0.01334706

klg	FBgn0017590	0.41388217	2.54E-11
TwdlG	FBgn0037225	0.41358669	0.00691443
Nmdar1	FBgn0010399	0.41352166	0.01067317
lncRNA:CR44909	FBgn0266214	0.41306514	1.01E-07
beat-Ib	FBgn0028645	0.41273785	4.32E-06
DIP-epsilon	FBgn0259714	0.41257454	0.00242109
GABA-B-R3	FBgn0031275	0.41174728	3.31E-05
Eip78C	FBgn0004865	0.41149192	5.45E-07
mus308	FBgn0002905	0.41000136	0.01364398
DIP-gamma	FBgn0039617	0.4098611	1.18E-09
CG43689	FBgn0263772	0.4094315	3.73E-05
CG32944	FBgn0052944	0.40942687	1.34E-06
Tsp86D	FBgn0037848	0.40882993	0.01202307
lncRNA:CR44320	FBgn0265379	0.40825	0.00031954
CG4328	FBgn0036274	0.40748145	0.01597435
Octbeta3R	FBgn0250910	0.40488358	2.76E-11
CG8202	FBgn0037622	0.40487678	0.01429698
CG14082	FBgn0036851	0.40447491	3.38E-06
CG7058	FBgn0030961	0.40407881	0.00053735
CG13743	FBgn0033368	0.40328904	9.75E-08
rdo	FBgn0243486	0.40272195	7.52E-06
nAChRalpha7	FBgn0086778	0.4022408	0.00026545
onecut	FBgn0028996	0.40205002	1.20E-06
dpr11	FBgn0053202	0.40125966	1.24E-06
CG33111	FBgn0053111	0.40075495	0.00696647
CG40228	FBgn0063670	0.40046672	0.01929142
bma	FBgn0085385	0.3994297	3.14E-06
CG1309	FBgn0035519	0.39939549	0.02491243
GABA-B-R1	FBgn0260446	0.39922316	1.51E-10
Zyx	FBgn0011642	0.39893775	0.01853292
rk	FBgn0003255	0.39857092	0.00111748
Proc	FBgn0045038	0.39856904	0.00021501
CG13594	FBgn0035041	0.39806595	3.65E-08
Hasp	FBgn0032797	0.39633954	0.00099062
lncRNA:CR43651	FBgn0263660	0.39628592	0.02201064
CG14431	FBgn0029922	0.39622132	1.33E-07
Ac3	FBgn0023416	0.39597959	2.16E-09
Xpd	FBgn0261850	0.39530973	0.04839293
Tbh	FBgn0010329	0.39475531	0.00343654

CG14535	FBgn0031955	0.39389427	3.20E-06
CadN2	FBgn0262018	0.39327468	1.12E-07
Nplp1	FBgn0035092	0.39324517	0.0004259
lncRNA:roX2	FBgn0019660	0.39265585	0.00164694
CG14459	FBgn0037171	0.3912163	6.53E-06
lncRNA:Hsromega	FBgn0001234	0.39046858	0.00020623
CG6574	FBgn0037846	0.3888441	0.01059933
CG14669	FBgn0037326	0.38812959	6.78E-07
lncRNA:CR44922	FBgn0266227	0.38780342	0.00794934
Nepl16	FBgn0039277	0.38695949	0.00043633
rt	FBgn0003292	0.38668799	0.01039901
ssp6	FBgn0035676	0.38645239	0.00294357
tey	FBgn0036899	0.38606084	0.04135711
Patsas	FBgn0029137	0.38594969	0.00852438
Gyc88E	FBgn0038295	0.38594519	0.00028949
kug	FBgn0261574	0.38493802	2.01E-09
pxb	FBgn0053207	0.38444408	5.59E-06
mGluR	FBgn0019985	0.38407449	7.94E-06
CG1909	FBgn0039911	0.38374774	2.23E-06
bru3	FBgn0264001	0.38251385	3.82E-06
lncRNA:CR45347	FBgn0266886	0.38234935	8.99E-07
igl	FBgn0013467	0.38231606	2.81E-07
Pde1c	FBgn0264815	0.38170533	1.04E-09
CG9837	FBgn0037635	0.38090093	0.00178643
Ent3	FBgn0036319	0.37998428	1.66E-06
CG31475	FBgn0051475	0.37992929	0.00041701
CadN	FBgn0015609	0.37920938	1.45E-08
Slip1	FBgn0024728	0.37863753	0.0001324
Cds	FBgn0010350	0.37856965	2.24E-05
eEF1beta	FBgn0028737	-0.3785244	0.00258365
Gs2	FBgn0001145	-0.3792373	0.01186199
kni	FBgn0001320	-0.3800798	0.03187109
Sod1	FBgn0003462	-0.3801007	0.00043883
apolpp	FBgn0087002	-0.3807419	0.02094251
FASN1	FBgn0027571	-0.3810917	0.00282695
CG31522	FBgn0051522	-0.381898	0.02132761
RpS26	FBgn0261597	-0.3821821	0.00034643
wal	FBgn0010516	-0.3822447	0.0014392
Cyp6a20	FBgn0033980	-0.3838552	0.01667431

Lgr3	FBgn0039354	-0.3839052	0.02309116
Gfat1	FBgn0027341	-0.3845172	0.00175589
CG4842	FBgn0036620	-0.3854117	0.02345374
Nca	FBgn0013303	-0.3859073	0.01140457
RpS7	FBgn0039757	-0.3859092	0.00052661
CG11073	FBgn0034693	-0.3863439	0.01968231
Acer	FBgn0016122	-0.3870404	0.00141063
glob1	FBgn0027657	-0.3879241	0.00662575
ORMDL	FBgn0037110	-0.3886784	0.03143038
Cad99C	FBgn0039709	-0.3900081	0.00062969
Cwc25	FBgn0031452	-0.3905602	0.00265521
Catsup	FBgn0002022	-0.3905857	0.00441072
Vdup1	FBgn0035103	-0.3907776	0.01322094
CG12093	FBgn0035372	-0.3909661	0.0063921
MP1	FBgn0027930	-0.3914551	0.01667431
dsx	FBgn0000504	-0.391744	0.00998483
Hsc70-3	FBgn0001218	-0.3924091	4.75E-05
CG44242	FBgn0265177	-0.393311	0.04129579
CG5009	FBgn0027572	-0.3936773	0.00716931
CG3902	FBgn0036824	-0.3940396	0.03601514
Stoml2	FBgn0034936	-0.3941832	0.00563575
fat-spondin	FBgn0026721	-0.3944818	0.03432013
CG9590	FBgn0038360	-0.3951244	0.01641655
RpL23	FBgn0010078	-0.3958587	0.00351361
Rpt2	FBgn0015282	-0.3963007	0.03550366
vsg	FBgn0045823	-0.3968009	6.01E-05
Rpn11	FBgn0028694	-0.3980074	0.00126216
kay	FBgn0001297	-0.3980793	0.03769502
Paics	FBgn0020513	-0.3982102	0.03455961
CG3301	FBgn0038878	-0.3989749	0.04268893
RpL11	FBgn0013325	-0.3999788	5.59E-06
Pfdn5	FBgn0038976	-0.4002589	0.03822616
CG10576	FBgn0035630	-0.4003663	0.00447292
CG13625	FBgn0039210	-0.401478	0.01509495
CG10889	FBgn0038769	-0.4015731	0.03379797
alphaSnap	FBgn0250791	-0.4020377	0.04406727
CG5862	FBgn0038868	-0.4022737	0.00337327
CG8008	FBgn0033387	-0.4022987	0.02150531
epsilonCOP	FBgn0027496	-0.4026114	0.04197807

Galphai	FBgn0001104	-0.4027275	0.04546682
mRpL28	FBgn0031660	-0.4029702	0.00305938
CG4572	FBgn0038738	-0.4069996	0.01186199
emp	FBgn0010435	-0.407384	0.01024958
CG14984	FBgn0035480	-0.4083907	0.03149145
CG9399	FBgn0037715	-0.4085671	0.01006328
RpS27A	FBgn0003942	-0.4101834	6.51E-06
GstD1	FBgn0001149	-0.4113738	0.00016752
CG7630	FBgn0040793	-0.4113806	0.00372711
RpL28	FBgn0035422	-0.4129614	6.56E-05
Fkbp14	FBgn0010470	-0.4136523	0.02904885
CG13833	FBgn0039040	-0.4138317	0.03943679
CG8036	FBgn0037607	-0.4138783	0.01735907
Prosalpha2	FBgn0086134	-0.4142225	0.01619241
UQCR-11	FBgn0260008	-0.4143806	0.045074
Prat2	FBgn0041194	-0.4157693	0.02383651
alpha-Est3	FBgn0015571	-0.4160016	0.03931415
CG31673	FBgn0051673	-0.4172773	0.01061181
SelG	FBgn0030350	-0.4174213	0.03601035
ND-24	FBgn0030853	-0.4184788	0.00083111
Jafrac1	FBgn0040309	-0.4187475	3.14E-05
Hn	FBgn0001208	-0.419052	0.03703988
CG10680	FBgn0032836	-0.4208519	0.04907715
AOX1	FBgn0267408	-0.4217295	0.01324099
CG4096	FBgn0029791	-0.4222606	0.01445032
CG1789	FBgn0030063	-0.4224678	0.03139499
sosie	FBgn0039232	-0.4225061	0.04985136
CG12746	FBgn0037341	-0.4226636	8.90E-06
CG6180	FBgn0032453	-0.4227549	0.01024958
bcn92	FBgn0013432	-0.423486	0.0018427
Fkbp39	FBgn0013269	-0.4244781	0.01438069
CAH2	FBgn0027843	-0.4258178	0.0008462
CG12007	FBgn0037293	-0.4266364	0.03191012
CG13887	FBgn0035165	-0.4278219	5.12E-06
Tsp	FBgn0031850	-0.4289806	0.02680988
Gp150	FBgn0013272	-0.4292474	0.01024958
RpS3	FBgn0002622	-0.4297472	1.19E-07
ValRS	FBgn0027079	-0.4303052	0.02321038
Ance-4	FBgn0033366	-0.4306949	0.02927287

Galk	FBgn0263199	-0.4307577	0.03150155
daw	FBgn0031461	-0.4325174	0.0029784
Ance-5	FBgn0035076	-0.4325646	0.03765438
CG13003	FBgn0030798	-0.4327931	0.01196207
awd	FBgn0000150	-0.4334636	0.00157508
Sox14	FBgn0005612	-0.4358225	0.00211545
ND-B17	FBgn0001989	-0.4360479	0.01195714
Ahcy	FBgn0014455	-0.4370185	0.00062969
Cyp4e2	FBgn0014469	-0.43781	0.01820146
CG10550	FBgn0039321	-0.4389071	0.01417104
RpS4	FBgn0011284	-0.4390936	0.04785697
CG11417	FBgn0024364	-0.4409257	0.02263824
RanGAP	FBgn0003346	-0.4416962	0.01188512
CG8654	FBgn0034479	-0.4420593	0.03649643
RpS30	FBgn0038834	-0.4420726	0.00193429
LanB2	FBgn0267348	-0.4421207	0.00925518
Snap29	FBgn0034913	-0.4424938	0.00097115
h	FBgn0001168	-0.4433381	0.00819829
Sodh-1	FBgn0024289	-0.4435329	0.04024121
CG15096	FBgn0034394	-0.4440189	0.00069019
CRIF	FBgn0037102	-0.4443297	0.00109246
CG12301	FBgn0036514	-0.4444284	0.02330775
CG1572	FBgn0030309	-0.4458298	0.04324164
CG1703	FBgn0030321	-0.4460669	0.00101501
CG9921	FBgn0030743	-0.4470124	0.04633597
Cat	FBgn0000261	-0.4513362	0.00152966
Hr51	FBgn0034012	-0.4516183	0.00087939
CG3609	FBgn0031418	-0.452497	0.04735124
ADPS	FBgn0033983	-0.4529691	9.15E-06
spirit	FBgn0030051	-0.4531476	0.02097102
CG18003	FBgn0061356	-0.4542234	0.02569884
CG8086	FBgn0032010	-0.4545162	0.02111912
CG6426	FBgn0034162	-0.4556474	0.0070134
St1	FBgn0034887	-0.455946	0.01977767
CG17896	FBgn0023537	-0.4568767	3.01E-05
Cyp6w1	FBgn0033065	-0.4572667	0.01202307
CPT2	FBgn0035383	-0.4578287	0.00757363
CG30431	FBgn0050431	-0.4586212	0.02150531
mRpL12	FBgn0011787	-0.4591887	0.01541314

CG12338	FBgn0033543	-0.4601355	0.03765438
sas	FBgn0002306	-0.4625387	0.0042549
SdhB	FBgn0014028	-0.4627122	0.00059823
Spg7	FBgn0024992	-0.4646481	4.95E-05
SkpA	FBgn0025637	-0.4650352	0.00404528
CG32537	FBgn0052537	-0.4652343	0.02153179
GILT1	FBgn0038149	-0.466737	0.00710034
fon	FBgn0032773	-0.4683072	0.02090877
Prosbeta3	FBgn0026380	-0.4688936	0.01466162
CG16758	FBgn0035348	-0.469265	0.00074087
Obp19d	FBgn0011280	-0.4704837	0.00174231
COX6B	FBgn0031066	-0.4716956	0.00343654
Sec61beta	FBgn0010638	-0.4729333	0.00507103
CG42240	FBgn0250869	-0.473167	0.0026533
CG5114	FBgn0036460	-0.4733866	0.03197989
CG3999	FBgn0037801	-0.4744608	0.00956657
CG6115	FBgn0040985	-0.4749069	4.79E-05
hui	FBgn0033968	-0.4751013	0.00147019
Idh	FBgn0001248	-0.4752447	0.00169205
fus	FBgn0023441	-0.4766873	0.00070783
eEF1delta	FBgn0032198	-0.4780707	1.15E-05
Pdh	FBgn0011693	-0.4794722	0.00385621
Ance	FBgn0012037	-0.4798312	0.0026533
CG13024	FBgn0036665	-0.4804877	0.00026586
vir-1	FBgn0043841	-0.4818904	0.0021499
CG6067	FBgn0029828	-0.4824532	0.0073716
CG6225	FBgn0038072	-0.4825104	0.04044874
CG9312	FBgn0038179	-0.4830931	0.01356688
CG8586	FBgn0033320	-0.4834306	0.00602027
alpha-Est7	FBgn0015575	-0.483975	2.13E-05
CG13751	FBgn0033340	-0.4843451	0.0226885
CG9631	FBgn0027563	-0.4846542	0.01890139
CG7834	FBgn0039697	-0.4847008	0.00326141
CG11368	FBgn0040923	-0.4858872	0.03628753
Ccs	FBgn0010531	-0.4877739	0.02514181
CG7720	FBgn0038652	-0.4879319	0.03056107
CG5921	FBgn0029835	-0.489174	0.00629051
CG5958	FBgn0031913	-0.48999	0.01506744
QIL1	FBgn0036726	-0.4919513	0.00797647

Jheh2	FBgn0034405	-0.4932781	0.00987681
CG32694	FBgn0052694	-0.4938382	0.0382039
Sp7	FBgn0037515	-0.4955333	0.01156491
Aatf	FBgn0031851	-0.4970911	0.02854086
Ssrp	FBgn0010278	-0.4973587	0.00284647
CG33970	FBgn0053970	-0.4982422	0.005393
pst	FBgn0035770	-0.4984234	0.00081054
ND-B18	FBgn0030605	-0.4989182	1.01E-06
maf-S	FBgn0034534	-0.4999404	0.01093425
Gadd45	FBgn0033153	-0.5024358	0.0002929
Desat1	FBgn0086687	-0.5028473	5.17E-06
RpL38	FBgn0040007	-0.5051247	0.03321277
CG4733	FBgn0038744	-0.5073835	0.00690104
CG4408	FBgn0039073	-0.5083574	0.03821718
GNBP3	FBgn0040321	-0.5087944	0.00339594
CG1673	FBgn0030482	-0.5092233	0.01272379
CG10527	FBgn0034583	-0.5098206	0.02017441
CG15739	FBgn0030347	-0.5100699	0.04727389
CG32091	FBgn0052091	-0.5114508	0.03639793
GstE1	FBgn0034335	-0.5115323	0.01968231
Fdx1	FBgn0011769	-0.5117321	0.03825465
Glt	FBgn0001114	-0.5124631	0.00064025
serp	FBgn0260653	-0.5124989	0.02233189
CG15098	FBgn0034398	-0.5127245	0.00021057
Pisd	FBgn0026576	-0.5130841	9.69E-05
Gbp2	FBgn0034200	-0.5146746	0.00696647
CG10516	FBgn0036549	-0.5146987	0.00770954
Hml	FBgn0029167	-0.516818	0.00815745
Taldo	FBgn0023477	-0.5182819	0.00178205
Fmo-2	FBgn0033079	-0.519717	0.00817051
CG11200	FBgn0034500	-0.5204086	0.0013462
JhI-21	FBgn0028425	-0.5206903	0.00191031
srp	FBgn0003507	-0.5211996	0.00036344
Sodh-2	FBgn0022359	-0.5213601	0.04491486
Gbp3	FBgn0039031	-0.5224117	0.00019425
aru	FBgn0029095	-0.523344	3.55E-05
CG18547	FBgn0037973	-0.5259071	0.00193812
RpL23A	FBgn0026372	-0.5267801	0.03233676
Arc1	FBgn0033926	-0.5280543	4.74E-06

Idgf2	FBgn0020415	-0.5281894	0.02224696
pen-2	FBgn0053198	-0.5283791	0.04606849
RpLP0-like	FBgn0033485	-0.5290354	0.00326908
vig2	FBgn0046214	-0.5303083	0.0015854
CG11835	FBgn0031264	-0.5320128	0.01353195
P5cr	FBgn0015781	-0.5322293	0.01130647
Xrp1	FBgn0261113	-0.5340718	1.09E-13
CG30285	FBgn0050285	-0.5354614	0.04064086
La	FBgn0011638	-0.5354676	0.00188206
CG31205	FBgn0051205	-0.5356922	0.01888771
psh	FBgn0030926	-0.5360131	0.02473905
Root	FBgn0039152	-0.5360741	0.00674326
CG6178	FBgn0039156	-0.5389106	0.00038164
Nmdmc	FBgn0010222	-0.539005	0.02061519
CG9336	FBgn0032897	-0.5396197	0.03758492
CG10560	FBgn0039325	-0.5398736	0.0273106
CG42319	FBgn0259219	-0.5403952	0.03434591
CG6870	FBgn0032652	-0.5413746	0.02612948
Iris	FBgn0031305	-0.5431357	0.02381809
CG6770	FBgn0032400	-0.5461286	0.0003372
ox	FBgn0011227	-0.5472189	0.01691495
CG31313	FBgn0051313	-0.5478399	0.0015742
CG17333	FBgn0030239	-0.548399	0.03405513
teq	FBgn0023479	-0.5491089	0.00089531
Ppn	FBgn0003137	-0.5503791	0.00086187
CG11791	FBgn0039266	-0.5513511	0.02809865
Obp99c	FBgn0039682	-0.5524951	0.01195714
SerRS	FBgn0031497	-0.5529156	0.00018093
CG5913	FBgn0039385	-0.5544046	0.03083443
CG13707	FBgn0035578	-0.5553863	0.01698922
UGP	FBgn0035978	-0.5555704	0.00031954
yellow-f2	FBgn0038105	-0.5561559	0.0107829
CG4847	FBgn0034229	-0.5565253	0.02153179
SdhC	FBgn0037873	-0.5566395	8.42E-06
ATPsynG	FBgn0010612	-0.5574001	0.02634777
Ldsdh1	FBgn0029994	-0.5594696	0.00057254
CG11400	FBgn0034198	-0.5595546	0.01011976
Adgf-D	FBgn0038172	-0.5624331	0.00150829
Cpr72Ec	FBgn0036619	-0.5660453	0.00405316

CG14407	FBgn0030584	-0.5669232	9.80E-07
CCHa2	FBgn0038147	-0.5678478	0.00024105
Txl	FBgn0035631	-0.5687091	0.00164694
CG8785	FBgn0033760	-0.5687591	0.04473406
CG11961	FBgn0034436	-0.5710331	6.23E-05
CG11550	FBgn0039864	-0.5717554	0.00310525
knrl	FBgn0001323	-0.5747419	0.00244103
Cyp4d21	FBgn0031925	-0.5775001	0.00222715
CG16743	FBgn0032322	-0.5785604	0.02260799
Cyp6g1	FBgn0025454	-0.5810266	0.00394321
CG18259	FBgn0030956	-0.5816941	0.01156491
CG11777	FBgn0033527	-0.582255	0.04815885
Shmt	FBgn0029823	-0.5822985	0.00182758
ppl	FBgn0027945	-0.5826484	0.00387367
CG16926	FBgn0040732	-0.5830328	0.01568672
dmrt99B	FBgn0039683	-0.5847692	0.03452806
Jheh1	FBgn0010053	-0.5872826	0.00063346
CG12177	FBgn0030510	-0.5873035	0.00064127
Npc2h	FBgn0039801	-0.5886691	0.00184974
Jabba	FBgn0259682	-0.5890178	6.04E-05
CG13807	FBgn0035323	-0.589402	0.02503482
CG9498	FBgn0031801	-0.5920409	0.0054035
ppk29	FBgn0034965	-0.5930644	0.04584972
b	FBgn0000153	-0.5931119	0.04722089
Idgf5	FBgn0064237	-0.5938283	0.00048976
D2hgdh	FBgn0023507	-0.5942613	0.00141233
GstE3	FBgn0063497	-0.5949884	0.00038581
Est-6	FBgn0000592	-0.5956629	0.00023083
Cad96Cb	FBgn0039294	-0.5962965	0.01771239
CG1441	FBgn0033464	-0.5968197	0.00146201
Vps20	FBgn0034744	-0.5976928	1.15E-05
Bet1	FBgn0260857	-0.5992017	0.01334706
RpS21	FBgn0015521	-0.6061895	5.26E-08
CG6345	FBgn0037816	-0.6062223	0.01457513
CG5773	FBgn0034290	-0.6063794	5.61E-05
CG5986	FBgn0043455	-0.6128715	4.65E-06
CG10863	FBgn0027552	-0.6144302	8.42E-06
MED10	FBgn0036581	-0.6148372	0.00069019
CG4306	FBgn0036787	-0.6184203	0.00601437

thw	FBgn0037487	-0.6186967	0.01834002
Nplp2	FBgn0040813	-0.6190463	0.00983066
GstO3	FBgn0035904	-0.6192155	0.01161004
CG8460	FBgn0031996	-0.6192204	0.02111529
Alr	FBgn0031068	-0.6208678	0.00537535
GstE6	FBgn0063494	-0.6216858	0.00300326
NimB2	FBgn0028543	-0.6234145	0.0009678
CG5909	FBgn0039495	-0.6236353	0.01140457
Caf1-180	FBgn0030054	-0.6244281	0.00345416
Prosbeta4	FBgn0032596	-0.6249547	1.98E-05
CG17776	FBgn0040899	-0.6258353	0.00186559
Lsd-1	FBgn0039114	-0.6263811	0.00128218
CG14341	FBgn0031315	-0.6275899	0.02214139
CG9572	FBgn0031089	-0.6290277	0.02334171
LanA	FBgn0002526	-0.6298872	3.59E-11
ems	FBgn0000576	-0.6335353	0.03181506
CG5326	FBgn0038983	-0.6344576	0.00133568
Rpb10	FBgn0039218	-0.6346077	0.00832183
CG34166	FBgn0085195	-0.6388636	2.62E-05
CG5945	FBgn0032494	-0.6433209	0.00534909
sug	FBgn0033782	-0.6468396	0.00343654
CG6503	FBgn0040606	-0.6502502	0.0026972
Cpr49Ae	FBgn0033728	-0.6523742	3.16E-05
Nplp3	FBgn0042201	-0.6568931	0.03379797
CG15021	FBgn0035544	-0.6604298	0.0013733
CG14207	FBgn0031037	-0.6613312	8.42E-06
cactin	FBgn0031114	-0.6630876	3.80E-07
Cyt-b5-r	FBgn0000406	-0.6641657	3.77E-05
CG13631	FBgn0040600	-0.6653693	0.00027853
Ugt35a	FBgn0026315	-0.6676442	0.02472266
CG8306	FBgn0034142	-0.6748501	5.12E-06
CG4716	FBgn0033820	-0.675357	0.00059715
CG10031	FBgn0031563	-0.6756436	0.00312273
CG31075	FBgn0051075	-0.6758646	0.00729115
Pmm2	FBgn0036300	-0.6767033	0.00847395
Vps37B	FBgn0037299	-0.682649	0.00481217
CG7079	FBgn0038849	-0.6829523	0.02321337
Npc2g	FBgn0039800	-0.6853328	0.00153612
CG32695	FBgn0052695	-0.6854644	0.02564311

CG3246	FBgn0031538	-0.6862408	6.91E-05
CG2145	FBgn0030251	-0.6871079	0.00017744
CG6084	FBgn0086254	-0.6927296	5.07E-06
Dgp-1	FBgn0027836	-0.6966253	4.54E-05
Vha36-3	FBgn0040377	-0.6981945	0.01745147
CG15068	FBgn0040733	-0.6983742	0.04349071
Asph	FBgn0034075	-0.7039914	0.04655905
CG9928	FBgn0032472	-0.7096265	0.00753085
GstE12	FBgn0027590	-0.7106702	0.0001781
CG12259	FBgn0039557	-0.7113302	0.00126178
CG12171	FBgn0037354	-0.7266108	0.01270544
GstD3	FBgn0010039	-0.7274367	0.01808221
CG11752	FBgn0030292	-0.7296626	0.00071711
Fib	FBgn0003062	-0.7323107	0.00193429
CG17919	FBgn0037433	-0.7339416	0.00065132
Loxl2	FBgn0034660	-0.7363422	0.0020164
CG10799	FBgn0033821	-0.7431291	0.00715139
CG17572	FBgn0032753	-0.7445656	0.00053339
Agpat4	FBgn0036622	-0.7465861	0.02009297
Gsc	FBgn0010323	-0.7487665	0.0096706
CG33493	FBgn0053493	-0.748957	2.48E-06
RpLP2	FBgn0003274	-0.7530734	1.18E-08
Cyp6a23	FBgn0033978	-0.7561472	5.66E-08
Mthfs	FBgn0085453	-0.7593256	0.03237801
CG6409	FBgn0036106	-0.7619296	4.65E-06
SmydA-9	FBgn0030102	-0.7621723	0.04129579
CG11858	FBgn0039305	-0.7651574	0.01543115
Cyp312a1	FBgn0036778	-0.7658078	0.03608416
Ude	FBgn0039226	-0.7764996	0.00061433
CG42445	FBgn0259916	-0.7775809	0.01506744
CG14618	FBgn0031189	-0.7822027	0.00013066
CG10621	FBgn0032726	-0.7881737	3.31E-06
CG4962	FBgn0036597	-0.791832	0.00154387
CG30151	FBgn0050151	-0.8173696	2.63E-05
CG15067	FBgn0034331	-0.8174102	0.02047775
CG16772	FBgn0032835	-0.8194297	0.00056016
Sirt6	FBgn0037802	-0.8220824	0.00326963
CG12811	FBgn0037779	-0.8338669	1.61E-06
Gbp1	FBgn0034199	-0.834147	4.16E-05

CG15784	FBgn0029766	-0.8355142	3.40E-13
CG5778	FBgn0038930	-0.8366301	0.00043633
CG2233	FBgn0029990	-0.8443479	3.85E-07
eIF2beta	FBgn0004926	-0.845367	7.77E-08
IM33	FBgn0031561	-0.8499796	0.01638987
CG4000	FBgn0038820	-0.8507133	0.00026545
CG13722	FBgn0035553	-0.8609777	0.00075608
ScpX	FBgn0015808	-0.8657212	8.43E-05
Oseg2	FBgn0035317	-0.8660046	0.00196567
IM2	FBgn0025583	-0.8724343	0.04686027
Lip2	FBgn0024740	-0.8785905	0.01196091
Obp18a	FBgn0030985	-0.8810774	0.00483931
CG1468	FBgn0030157	-0.8876278	3.19E-06
CG8519	FBgn0035711	-0.8886897	0.02531135
Ir40a	FBgn0259683	-0.8950181	0.04872369
MFS3	FBgn0031307	-0.8953358	6.47E-05
Cyp6a14	FBgn0033302	-0.8999716	0.01059933
EbpIII	FBgn0011695	-0.901398	2.11E-10
up	FBgn0004169	-0.9033973	0.00898054
Cpr97Eb	FBgn0039481	-0.9076269	0.03270086
Hsp26	FBgn0001225	-0.9096074	5.12E-06
CG34331	FBgn0085360	-0.9179592	1.73E-05
Ir76b	FBgn0036937	-0.92195	0.005393
CG6675	FBgn0032973	-0.9335747	0.01543093
CG9313	FBgn0034566	-0.9364058	0.0034221
Pgd	FBgn0004654	-0.9385794	3.44E-05
CG7130	FBgn0037151	-0.9475732	0.02138742
lncRNA:CR33942	FBgn0062961	-0.9483434	0.01156491
hpRNA:CR18854	FBgn0042174	-0.9517037	0.00828321
IM4	FBgn0040653	-0.9694509	0.0205268
Acbp2	FBgn0010387	-0.9867552	1.18E-08
Act87E	FBgn0000046	-1.0023268	0.03649643
CG8860	FBgn0033691	-1.0076716	0.00852438
Dot	FBgn0015663	-1.0329518	0.00158992
CG7214	FBgn0031940	-1.0362506	0.00742409
CG5867	FBgn0027586	-1.075475	2.01E-12
CG7906	FBgn0036417	-1.093398	0.01156491
CG31777	FBgn0051777	-1.1041153	2.89E-05
CG40198	FBgn0058198	-1.1056489	0.00026545

CG14246	FBgn0040608	-1.1084564	0.01453146
Ldh	FBgn0001258	-1.1178143	5.31E-07
CG34227	FBgn0085256	-1.1222957	0.01552081
CG13315	FBgn0040827	-1.1407619	7.07E-06
mRpS24	FBgn0039159	-1.1462337	0.00033598
CG43071	FBgn0262481	-1.1668127	0.00567288
Cpr100A	FBgn0039805	-1.1786274	0.00246009
PGRP-SB1	FBgn0043578	-1.2056591	0.00917499
dysf	FBgn0039411	-1.2153654	5.31E-08
Fatp2	FBgn0265187	-1.2244442	3.06E-10
Poxm	FBgn0003129	-1.2286512	0.0238347
Obp56a	FBgn0034468	-1.2369889	0.00055341
CheA75a	FBgn0036783	-1.2860157	0.03390771
CG18107	FBgn0034330	-1.2903361	4.88E-05
CG13618	FBgn0039203	-1.3126404	4.72E-08
bond	FBgn0260942	-1.360354	5.31E-08
fit	FBgn0038914	-1.3643184	0.00056391
CG13676	FBgn0035844	-1.3723034	1.47E-07
CG17108	FBgn0032285	-1.3847156	8.33E-06
Act88F	FBgn0000047	-1.3870856	3.38E-06
Cpr47Ef	FBgn0033603	-1.4011707	1.81E-05
Cyp4aa1	FBgn0034053	-1.4485217	2.51E-13
Act79B	FBgn0000045	-1.4563858	0.03187109
CG15213	FBgn0040843	-1.4665282	7.59E-09
lncRNA:CR45717	FBgn0267281	-1.588759	6.47E-05
TotA	FBgn0028396	-1.8779428	0.00215078
snoRNA:U3:9B	FBgn0065046	-2.0682428	0.00175614

Appendix E: Differentially expressed genes in KTvCT experimental comparison.

Sorted by descending Log2 fold change.

Gene name	FlyBase ID	log_2 Fold Change	adj. p-value
Rpt6	FBgn0020369	2.10899594	2.53E-06
slmo	FBgn0029161	1.65644598	0.00282619
RpS9	FBgn0010408	1.46627345	0.00137582
CG15282	FBgn0028855	1.38648767	0.00070566
gammaSnap1	FBgn0028552	1.36382851	0.02398604

Lsp2	FBgn0002565	1.18797975	0.00013615
lncRNA:CR45417	FBgn0266966	1.18512534	0.00020093
RpL39	FBgn0023170	1.15284413	0.01403371
cer	FBgn0034443	1.11689404	8.13E-05
CG34025	FBgn0054025	1.0624851	0.03872244
Nplp4	FBgn0040717	1.02568691	0.0013701
NAAT1	FBgn0029762	0.87326327	0.00027897
FucTB	FBgn0032117	0.85633783	0.0141515
Ssl1	FBgn0037202	0.84994262	0.04063348
CG34165	FBgn0085194	0.80275104	0.01038607
Drip	FBgn0015872	0.79559592	1.05E-05
CG15332	FBgn0029986	0.79517772	0.00200857
Hr3	FBgn0000448	0.7712874	0.0078301
Itgbn	FBgn0010395	0.76338486	0.00328216
Dpck	FBgn0037469	0.75879949	1.89E-07
CG4660	FBgn0029839	0.75034415	2.23E-09
CG31323	FBgn0051323	0.74523321	4.05E-09
CG12118	FBgn0030101	0.71937618	0.03115999
snoRNA:Psi28S-3342	FBgn0086667	0.7152562	0.04832963
CG3987	FBgn0038292	0.69930028	9.83E-05
Lhr	FBgn0034217	0.69724223	0.01712633
CG14086	FBgn0036860	0.67653989	0.01637814
DJ-1alpha	FBgn0033885	0.66716335	4.07E-05
CG17724	FBgn0033802	0.66674135	0.00118352
Cka	FBgn0044323	0.66552862	9.59E-05
mRpL33	FBgn0040907	0.66207385	0.00111337
CG10465	FBgn0033017	0.66177977	0.00080467
tipE	FBgn0003710	0.65656828	0.01021972
CG34039	FBgn0054039	0.65256411	0.02375591
CG4210	FBgn0038302	0.6524106	0.01914613
PlexB	FBgn0025740	0.65004497	9.55E-07
CG12560	FBgn0031974	0.64352865	0.00070739
CG15322	FBgn0031088	0.63964385	0.02018131
lncRNA:CR45758	FBgn0267322	0.62931538	7.74E-05
CG32756	FBgn0052756	0.62795066	0.00018471
robl	FBgn0024196	0.62551568	0.01616493
PIG-Q	FBgn0086448	0.62394563	0.0010314
Tim9a	FBgn0030480	0.62003682	0.01657161
CG33635	FBgn0053635	0.61942388	0.0419653

RpL5	FBgn0064225	0.6190783	2.02E-07
GstZ1	FBgn0037696	0.61416119	0.00351623
xit	FBgn0029906	0.61258654	0.00155864
CG13229	FBgn0033579	0.60392853	0.00026108
Smyd4-1	FBgn0033427	0.601712	4.52E-09
RpS3A	FBgn0017545	0.60159423	0.00137564
Ag5r	FBgn0015010	0.59908746	0.03471094
Trs20	FBgn0266724	0.59819899	0.00471232
lncRNA:CR43651	FBgn0263660	0.59363194	1.56E-05
CG5639	FBgn0039527	0.59056655	0.01570783
Zyx	FBgn0011642	0.58942354	1.22E-05
Arl4	FBgn0039889	0.58445476	8.57E-05
Blos1	FBgn0050077	0.58368866	0.00659037
CG18343	FBgn0033683	0.57297791	0.04539402
CG15168	FBgn0032732	0.56701312	0.00152303
CG12728	FBgn0029825	0.56566133	0.03789027
CG5104	FBgn0037009	0.5568906	0.0419653
CG10375	FBgn0039116	0.5544026	0.03649602
asRNA:CR43259	FBgn0262904	0.55405905	0.01985284
CG8369	FBgn0040532	0.55270576	0.00051513
CG17167	FBgn0039941	0.55090162	0.02927523
UQCR-6.4	FBgn0034245	0.54991676	0.00346965
Acbp1	FBgn0031992	0.5488269	0.0018182
CG18731	FBgn0042213	0.54720692	0.00570644
pch2	FBgn0051453	0.54542636	0.01251246
CaMKI	FBgn0016126	0.54332335	1.55E-05
hec	FBgn0030437	0.53343776	0.0005942
CG4962	FBgn0036597	0.53328807	0.01882129
CG17760	FBgn0033756	0.52646147	0.04963667
ERR	FBgn0035849	0.522678	0.00249962
CG12194	FBgn0031636	0.51763362	0.00077962
Psf3	FBgn0030196	0.51723758	5.46E-05
CG11367	FBgn0037185	0.51307259	0.00561816
eag	FBgn0000535	0.50975963	8.73E-12
CG5611	FBgn0039531	0.50940403	0.01961207
mRpL52	FBgn0033208	0.50737338	0.00117183
CG8818	FBgn0033751	0.50727876	0.00131368
CR43670	FBgn0263745	0.5056941	0.00011612
CG5694	FBgn0032197	0.50566623	1.83E-07

Rap2l	FBgn0025806	0.50405475	1.51E-05
CG17574	FBgn0033777	0.50381368	0.00277186
lncRNA:CR45759	FBgn0267323	0.50367107	0.02795757
Pten	FBgn0026379	0.50149826	0.00012615
Der-2	FBgn0038438	0.49999602	0.00235927
CG9380	FBgn0035094	0.49839815	4.84E-06
ND-MLRQ	FBgn0052230	0.49738697	0.00395382
CG17048	FBgn0033828	0.49655139	0.03527798
scu	FBgn0021765	0.49607555	0.00278848
CG34134	FBgn0083970	0.49413239	0.00160689
CG6231	FBgn0038720	0.4849314	5.99E-07
Mccc1	FBgn0039877	0.48451544	0.00140227
CG43219	FBgn0262855	0.48377047	0.00013615
CG33199	FBgn0053199	0.48374964	0.04186176
zye	FBgn0036985	0.48162344	0.00716496
Hsp67Ba	FBgn0001227	0.48129834	0.03984401
Cpr49Ag	FBgn0033730	0.4803387	0.01855846
CG6006	FBgn0063649	0.47869872	4.73E-08
CG5110	FBgn0032642	0.4702222	0.04998226
CG3857	FBgn0023520	0.46894792	0.0247941
lncRNA:flam	FBgn0267704	0.4677778	0.0246489
Ir68a	FBgn0036150	0.46322699	0.00864649
Pits	FBgn0030400	0.46283257	0.00070499
RpL30	FBgn0086710	0.46167133	0.00760179
ATPsynCF6	FBgn0016119	0.4593853	0.01105641
MED24	FBgn0035851	0.45845764	9.61E-07
lncRNA:CR44024	FBgn0264794	0.45831354	1.03E-08
Tsp96F	FBgn0027865	0.45761921	0.00101897
CG30419	FBgn0050419	0.45504821	2.16E-06
CG3777	FBgn0024989	0.45355389	0.00788681
Dnz1	FBgn0027453	0.45058875	2.97E-06
VhaAC45	FBgn0262515	0.4499958	8.73E-12
lncRNA:roX2	FBgn0019660	0.44936398	1.56E-05
RabX4	FBgn0051118	0.44898046	2.04E-05
sinu	FBgn0010894	0.44891853	0.00056492
CG10019	FBgn0031568	0.44837573	2.12E-07
Pkc53E	FBgn0003091	0.447121	5.73E-06
fh	FBgn0030092	0.44647489	0.01902372
CG31808	FBgn0062978	0.44485713	2.30E-08

Tina-1	FBgn0035083	0.44239337	0.00100411
cm	FBgn0000330	0.44187711	0.04392127
CG3107	FBgn0033005	0.43737633	0.00119922
lncRNA:CR44566	FBgn0265759	0.43632376	0.01221674
CG6836	FBgn0036834	0.43537274	0.02298698
CG2316	FBgn0039890	0.4352281	0.00045181
RpL27A	FBgn0261606	0.43399082	0.00799422
DAT	FBgn0034136	0.43264772	0.00360695
PIP4K	FBgn0039924	0.43250596	2.24E-07
Rbp1	FBgn0260944	0.43103026	0.00224818
CG9536	FBgn0031818	0.42802525	0.00131279
CG43373	FBgn0263131	0.42765805	8.94E-06
CG7289	FBgn0031379	0.42738391	7.47E-08
igl	FBgn0013467	0.42640809	8.73E-12
CCAP-R	FBgn0039396	0.42610277	0.00027995
CG40228	FBgn0063670	0.42516628	0.00251708
Galphaq	FBgn0004435	0.42465335	0.00133916
CG9231	FBgn0036887	0.42411305	0.04725952
Taf12	FBgn0011290	0.42296782	0.00121246
sr	FBgn0003499	0.42220684	0.00021685
CG14431	FBgn0029922	0.42220318	2.89E-11
Cds	FBgn0010350	0.42188256	2.53E-08
CG30423	FBgn0050423	0.42167819	0.00328216
CG12393	FBgn0031768	0.42043038	0.03070056
CG42747	FBgn0261801	0.41711916	3.52E-05
Rbp1-like	FBgn0030479	0.41641325	0.00462778
Cngl	FBgn0263257	0.41640995	9.56E-11
CG7339	FBgn0036188	0.41639334	0.03184475
Lamp1	FBgn0032949	0.41487591	0.00010572
CG40045	FBgn0058045	0.41456069	3.04E-06
Task7	FBgn0037690	0.41321818	0.00033202
CG12355	FBgn0040805	0.4128904	2.54E-05
CG17486	FBgn0032997	0.41255979	0.00194022
CG33639	FBgn0053639	0.41075903	0.00033674
CG42402	FBgn0259821	0.40945363	3.86E-05
CG5676	FBgn0032200	0.40821145	0.00766135
CG15602	FBgn0030694	0.40819019	0.03801661
CG42346	FBgn0259677	0.40791226	4.19E-12
mRpS11	FBgn0038474	0.40741423	0.00752216

CG5026	FBgn0035945	0.4064929	0.00647945
CG12531	FBgn0031064	0.4061565	5.39E-07
CG15695	FBgn0038832	0.40559122	0.0290703
AP-2sigma	FBgn0043012	0.40547215	0.00675275
Hml	FBgn0029167	0.40506956	0.01715178
Gp210	FBgn0266580	0.40465735	7.24E-08
Dop1R1	FBgn0011582	0.40376124	2.06E-06
CG12038	FBgn0035179	0.40366271	0.0027334
ghi	FBgn0266124	0.40249048	0.01021972
Awh	FBgn0013751	0.40225487	0.02067312
CG32683	FBgn0052683	0.40197224	3.06E-08
Fas1	FBgn0262742	0.40168693	1.10E-07
CG8490	FBgn0033715	0.40067134	0.02639834
tyn	FBgn0029128	0.40043909	1.43E-05
CG11267	FBgn0036334	0.39901977	0.00052509
Vha13	FBgn0026753	0.39572232	0.01653424
bsk	FBgn0000229	0.39556114	4.80E-05
REPTOR-BP	FBgn0032202	0.39549608	0.04175984
CG42540	FBgn0260657	0.395173	1.64E-08
GstT4	FBgn0030484	0.39514559	0.02685685
Rdl	FBgn0004244	0.39472051	0.00011102
CG11406	FBgn0034990	0.39460908	0.02935058
Tob	FBgn0028397	0.39172722	0.00028011
Bap55	FBgn0025716	0.39103416	0.04918173
Srp9	FBgn0035827	0.39098761	0.02416193
CG31760	FBgn0051760	0.39094101	4.56E-05
CG43324	FBgn0263029	0.38978024	0.00766924
CG14535	FBgn0031955	0.38948011	7.48E-08
CG7133	FBgn0037150	0.38941565	0.03139877
CG33143	FBgn0053143	0.38868175	4.43E-05
CG17385	FBgn0033934	0.38568433	0.00513408
CG8641	FBgn0035733	0.38538455	8.94E-05
Cals	FBgn0039928	0.38515934	2.33E-07
TkR99D	FBgn0004622	0.38511594	0.00561669
CG7166	FBgn0037107	0.38497662	1.37E-05
bip2	FBgn0026262	0.38480725	0.00121319
eca	FBgn0069242	0.38214212	0.00586901
CG13255	FBgn0040636	0.38186876	0.03455763
Gfrl	FBgn0262869	0.37989102	3.17E-08

anne	FBgn0052000	0.37955493	0.00060811
CG11122	FBgn0030266	-0.3789526	0.00497129
htk	FBgn0085451	-0.3797944	0.01156282
Golgin84	FBgn0039188	-0.3803474	0.03627856
ebd1	FBgn0035153	-0.380674	0.00031016
CG3246	FBgn0031538	-0.3808714	0.0191324
Jheh1	FBgn0010053	-0.3809148	0.01532457
Nca	FBgn0013303	-0.381938	0.00295947
CG3542	FBgn0031492	-0.382537	0.0115876
CG4119	FBgn0028474	-0.3830475	0.00314543
CG8209	FBgn0035830	-0.3832271	0.0041888
dwg	FBgn0000520	-0.383726	0.02342011
c11.1	FBgn0040236	-0.384469	0.00029641
CG6686	FBgn0032388	-0.3863796	0.0001409
Pfdn4	FBgn0035603	-0.3871347	0.00428136
Acn	FBgn0263198	-0.3873895	0.00121773
CG3386	FBgn0035152	-0.3875368	0.03265726
ImpE1	FBgn0001253	-0.3886879	0.03876327
RpL24-like	FBgn0037899	-0.3889345	0.00071866
CG14894	FBgn0038428	-0.3889946	0.01558953
SrpRbeta	FBgn0011509	-0.3899303	0.02530535
CG7135	FBgn0030895	-0.3904969	0.0250947
Gnf1	FBgn0004913	-0.390815	0.00121319
Vps24	FBgn0037231	-0.3917453	0.00145209
CG30046	FBgn0050046	-0.3920986	0.04349211
CG11906	FBgn0034425	-0.3922664	0.03903837
CG1598	FBgn0033191	-0.3929643	0.00793734
Fic	FBgn0263278	-0.3930815	0.01516698
UGP	FBgn0035978	-0.3943266	0.00489237
CG10274	FBgn0035690	-0.3944675	0.03168977
CG4045	FBgn0025629	-0.3946253	0.02441559
Mitofilin	FBgn0019960	-0.3969414	1.63E-05
mRpS30	FBgn0030692	-0.397053	0.00147731
imd	FBgn0013983	-0.3973887	0.01097731
CG11417	FBgn0024364	-0.3974291	0.01784438
RpL13	FBgn0011272	-0.3990712	0.00082116
mRpL24	FBgn0031651	-0.3993065	0.03160555
CG6512	FBgn0036702	-0.3993111	4.66E-05
CG1620	FBgn0033183	-0.4013772	0.00231617

Nop60B	FBgn0259937	-0.40146	0.00027758
Rab30	FBgn0031882	-0.4037778	0.00222003
Ice1	FBgn0034853	-0.404372	0.00082293
MP1	FBgn0027930	-0.4045319	0.0035883
Sec5	FBgn0266670	-0.4049302	0.00673333
mAcon1	FBgn0010100	-0.406186	0.00040242
prod	FBgn0014269	-0.4066237	0.0175904
CG2233	FBgn0029990	-0.4073755	0.00836862
CG1441	FBgn0033464	-0.4076778	0.01642199
GstD1	FBgn0001149	-0.4077251	1.55E-05
CG7650	FBgn0036519	-0.4081921	0.04164015
RpS30	FBgn0038834	-0.4083033	0.00094354
DNApol-iota	FBgn0037554	-0.4108461	0.00636945
Mtr4	FBgn0001986	-0.4109648	0.01979092
Rab32	FBgn0002567	-0.4110849	0.0081547
B-H1	FBgn0011758	-0.4116729	0.0446274
CG12007	FBgn0037293	-0.4125481	0.0155282
nvy	FBgn0005636	-0.4129694	0.00011102
CG5114	FBgn0036460	-0.415576	0.03120276
Shc	FBgn0015296	-0.4156246	0.01707044
Tctp	FBgn0037874	-0.4156488	1.79E-07
Gdh	FBgn0001098	-0.4183293	0.00063715
CG31036	FBgn0051036	-0.4190901	0.02018131
rswl	FBgn0034351	-0.4191672	0.00638883
Irp-1B	FBgn0024957	-0.4202009	0.02466753
Ttc19	FBgn0032744	-0.420444	0.00018447
CG17919	FBgn0037433	-0.4209423	0.03801661
viaf	FBgn0036237	-0.4220517	0.00082465
Trxr-1	FBgn0020653	-0.4221656	0.00345506
gb	FBgn0039487	-0.4227432	0.01551513
CG8586	FBgn0033320	-0.4236171	0.00647945
CG17068	FBgn0031098	-0.4239576	0.03126583
CG10527	FBgn0034583	-0.4242963	0.02675137
ADPS	FBgn0033983	-0.4248559	3.34E-06
eIF2alpha	FBgn0261609	-0.4261053	0.00062148
CG13994	FBgn0031772	-0.4273012	0.01096199
GstE12	FBgn0027590	-0.4287481	0.01354831
Jabba	FBgn0259682	-0.4327757	0.00111686
MED19	FBgn0036761	-0.4329986	0.00542682

LanA	FBgn0002526	-0.4347167	2.89E-07
CalpC	FBgn0260450	-0.4354635	0.04298446
CG43330	FBgn0263035	-0.4359409	0.02092431
CG11504	FBgn0039733	-0.4372287	0.00665163
bcn92	FBgn0013432	-0.4380658	0.00018704
CG11842	FBgn0039629	-0.4385305	0.0374581
CG8078	FBgn0033375	-0.4389279	0.04675841
CG14984	FBgn0035480	-0.439042	0.00800077
DCTN3-p24	FBgn0010622	-0.4397363	0.00910217
CG2662	FBgn0024993	-0.4399241	0.03785965
CG4849	FBgn0039566	-0.441021	0.01718173
Elp1	FBgn0037926	-0.4417146	2.64E-05
sosie	FBgn0039232	-0.4426803	0.01468337
La	FBgn0011638	-0.4445786	0.00356575
CG3732	FBgn0034750	-0.4446816	0.02464122
CG6693	FBgn0037878	-0.4447182	0.01294249
Fitm	FBgn0035586	-0.4454146	0.00027641
CG11141	FBgn0033177	-0.4456581	0.00431559
Adgf-D	FBgn0038172	-0.4458747	0.00597003
Sec15	FBgn0266674	-0.4465367	0.00740789
Nep2	FBgn0027570	-0.4481509	0.00363854
Cdc37	FBgn0011573	-0.4486098	0.00023063
scf	FBgn0025682	-0.4486444	1.73E-05
JhI-21	FBgn0028425	-0.4487264	0.00227724
CHMP2B	FBgn0035589	-0.4489753	0.00087607
CG8042	FBgn0027554	-0.4504042	1.36E-05
CG2145	FBgn0030251	-0.4513898	0.00657388
fkh	FBgn0000659	-0.4519884	7.61E-09
Hpd	FBgn0036992	-0.4523648	0.00016623
CG11835	FBgn0031264	-0.4523942	0.0149759
CG13625	FBgn0039210	-0.4524156	0.00137582
Shmt	FBgn0029823	-0.4531089	0.00587678
RpL34a	FBgn0039406	-0.4536866	0.01329917
CG13024	FBgn0036665	-0.4539212	6.14E-05
NC2alpha	FBgn0034650	-0.4540416	0.00248597
CCT5	FBgn0010621	-0.4547064	0.00874877
CG5913	FBgn0039385	-0.4547119	0.04492315
cv-2	FBgn0000395	-0.4559881	0.00020936
SdhC	FBgn0037873	-0.4592255	4.87E-05

Xpac	FBgn0004832	-0.4600863	0.03314705
CG3294	FBgn0031628	-0.4628399	0.0251959
U4-U6-60K	FBgn0036733	-0.4629546	0.00476788
CG8281	FBgn0035824	-0.4639815	0.02669263
Ing5	FBgn0032516	-0.4643649	0.00027897
Upf3	FBgn0034923	-0.4644851	0.00603541
Sp1	FBgn0020378	-0.4650863	0.04306795
l(3)07882	FBgn0010926	-0.4654524	0.00855446
Root	FBgn0039152	-0.4654535	0.01279192
Samtor	FBgn0035035	-0.4662687	0.01759535
COX6B	FBgn0031066	-0.4663949	0.00065325
CG10778	FBgn0029980	-0.4664623	0.04442348
CG1529	FBgn0031144	-0.4668944	0.00133681
CG30285	FBgn0050285	-0.4669675	0.04492315
CG5921	FBgn0029835	-0.4677496	0.00356642
Mettl3	FBgn0039139	-0.4694185	0.02439982
Ude	FBgn0039226	-0.471451	0.02425399
Arfip	FBgn0037884	-0.4719002	0.0126455
CG4306	FBgn0036787	-0.4720971	0.02804108
CG8441	FBgn0034086	-0.4732742	0.01055209
CNPYb	FBgn0036847	-0.4733706	0.01200681
Eno	FBgn0000579	-0.4734486	5.57E-06
Sirt7	FBgn0039631	-0.473742	0.00059664
CG13751	FBgn0033340	-0.4753948	0.00921048
dbe	FBgn0020305	-0.4764498	0.04918173
Nup93-2	FBgn0038274	-0.4773414	0.01855846
Hsc70-3	FBgn0001218	-0.4778727	3.19E-09
CG9609	FBgn0030787	-0.4800462	0.00185102
rho-7	FBgn0033672	-0.4805571	0.00671529
Jheh2	FBgn0034405	-0.4830575	0.00297948
dmt	FBgn0016792	-0.4832229	0.00111337
CG1434	FBgn0030554	-0.4847364	0.04011046
Fbxl7	FBgn0038385	-0.486046	0.01383079
Vta1	FBgn0035251	-0.4863357	0.00290015
mRpS22	FBgn0039555	-0.4866204	0.00777233
CG6345	FBgn0037816	-0.4870887	0.03213147
Non2	FBgn0035370	-0.4875732	0.00194022
Prp31	FBgn0036487	-0.4878654	0.02223527
asRNA:CR44027	FBgn0264819	-0.4887293	0.01244911

Fib	FBgn0003062	-0.4897721	0.02142704
CG30010	FBgn0050010	-0.4900784	0.04209137
mip130	FBgn0023509	-0.4903167	0.01038602
AIMP3	FBgn0050185	-0.4921497	0.0251959
Ppa	FBgn0020257	-0.4934371	3.40E-08
mid	FBgn0261963	-0.4935473	0.0002031
CG32537	FBgn0052537	-0.4953073	0.00418344
l(1)G0004	FBgn0027334	-0.495438	0.01373798
Cyp6g1	FBgn0025454	-0.4956129	0.00575016
CG4752	FBgn0034733	-0.4957157	0.00060674
l(1)G0020	FBgn0027330	-0.4969038	0.03265726
CG1703	FBgn0030321	-0.4969362	1.66E-05
CG6227	FBgn0030631	-0.4989522	0.00018897
CG15547	FBgn0039809	-0.4997619	0.00476788
RnpS1	FBgn0037707	-0.5000468	0.0002031
Tsp42Ej	FBgn0033132	-0.5014252	0.00305771
CG8939	FBgn0030720	-0.5018739	0.00048829
Arp5	FBgn0038576	-0.5026039	0.00091994
Fip1	FBgn0037255	-0.5047767	0.01294986
CG11594	FBgn0035484	-0.5065956	0.01147661
CG12177	FBgn0030510	-0.50842	0.00133681
CG42319	FBgn0259219	-0.5094368	0.01738501
CG14207	FBgn0031037	-0.5097997	9.83E-05
HBS1	FBgn0042712	-0.509943	0.00115404
RpS4	FBgn0011284	-0.5109668	0.00462778
CG2811	FBgn0035082	-0.5109985	0.00460335
Brd8	FBgn0039654	-0.5112232	6.39E-05
Pdi	FBgn0014002	-0.5116562	0.00188311
lin	FBgn0002552	-0.5124813	0.00014178
SkpA	FBgn0025637	-0.5130317	0.00015574
eyg	FBgn0000625	-0.5130716	0.02597102
GCS2beta	FBgn0032643	-0.5134462	0.00203931
Prosalpha2	FBgn0086134	-0.5146173	0.00032129
Npc2g	FBgn0039800	-0.5159987	0.00710409
CG16890	FBgn0028932	-0.5187736	0.02955691
Syx16	FBgn0031106	-0.5188517	0.04970749
alpha-Est3	FBgn0015571	-0.5189299	0.00242812
Caf1-180	FBgn0030054	-0.5192966	0.00666467
CG11409	FBgn0024366	-0.5195022	0.02806015

CG6067	FBgn0029828	-0.5199002	0.00079739
Sox15	FBgn0005613	-0.5208656	0.01830932
CG7675	FBgn0038610	-0.5235594	0.00321972
CG5515	FBgn0039163	-0.5236752	0.00013818
eIF2Bepsilon	FBgn0023512	-0.5248134	0.00470391
Calr	FBgn0005585	-0.5266388	3.06E-08
CG13623	FBgn0039205	-0.5276474	0.0397675
CG14341	FBgn0031315	-0.5293839	0.02882112
atk	FBgn0036995	-0.5305353	0.04347323
CG14710	FBgn0037920	-0.5310536	0.00827092
CG17361	FBgn0036395	-0.5310935	0.01651803
pwn	FBgn0003174	-0.531259	0.00280695
ems	FBgn0000576	-0.5313746	0.04175984
CG14223	FBgn0031053	-0.5340536	0.01162088
Plap	FBgn0024314	-0.5350876	0.00018464
Catsup	FBgn0002022	-0.5352923	3.88E-06
CG8086	FBgn0032010	-0.5361547	0.00083473
CG4291	FBgn0031287	-0.5371844	0.0085276
CG11752	FBgn0030292	-0.5378036	0.00576746
CG32187	FBgn0052187	-0.5403196	0.01937259
Xrp1	FBgn0261113	-0.5413156	1.86E-19
ND-18	FBgn0031021	-0.5427135	0.0006872
CG14618	FBgn0031189	-0.5451664	0.00493179
CG16789	FBgn0037712	-0.5479622	0.00476788
CG5543	FBgn0034908	-0.5482234	0.01482155
GstT2	FBgn0050005	-0.5490853	0.0108562
Srr	FBgn0037684	-0.5494563	0.02838354
Txl	FBgn0035631	-0.5504383	0.0004694
SPARC	FBgn0026562	-0.5513988	0.03339857
Vps37B	FBgn0037299	-0.551949	0.01132387
CG6712	FBgn0032408	-0.5542342	0.01633598
Ssrp	FBgn0010278	-0.5546131	9.66E-05
Mis12	FBgn0035725	-0.5561568	0.03153184
Vdup1	FBgn0035103	-0.5576962	2.31E-05
CG32695	FBgn0052695	-0.5584708	0.03801661
CG7255	FBgn0036493	-0.5595712	0.02018131
Gp93	FBgn0039562	-0.5597386	1.28E-07
Vps2	FBgn0039402	-0.5613734	0.00225194
CG10889	FBgn0038769	-0.56363	0.00038372

Syx18	FBgn0039212	-0.5642351	0.00096418
Flacc	FBgn0030974	-0.5654654	0.00090449
Sry-delta	FBgn0003512	-0.5663049	0.00137582
CG9449	FBgn0036875	-0.5684045	0.04126315
Rpt2	FBgn0015282	-0.5726419	0.00015343
NimB2	FBgn0028543	-0.573021	0.00043226
Vps28	FBgn0021814	-0.5733539	0.0011492
CG18675	FBgn0040696	-0.5743872	0.0065368
Spg7	FBgn0024992	-0.5769272	7.29E-09
CG1239	FBgn0037368	-0.5778979	0.03152518
CG1785	FBgn0030061	-0.5780373	0.00035892
CG10863	FBgn0027552	-0.5790859	1.97E-06
CG30054	FBgn0050054	-0.5797586	0.00123403
alphaSnap	FBgn0250791	-0.5807354	0.00023886
Non3	FBgn0038585	-0.5815943	0.02018131
Acbp2	FBgn0010387	-0.5821781	0.0002035
nudC	FBgn0021768	-0.5839894	0.00852028
mip40	FBgn0034430	-0.5851656	0.00595437
Dera	FBgn0033735	-0.5889289	0.04126315
Tcs3	FBgn0036615	-0.5908428	0.0271263
VhaM9.7-a	FBgn0035521	-0.5932206	0.00086832
CG5535	FBgn0036764	-0.5943045	0.00115462
Hmg-2	FBgn0026582	-0.6036084	0.00444403
CG11447	FBgn0038737	-0.6048886	0.01450497
CG15046	FBgn0030927	-0.6107143	0.03430428
Sas10	FBgn0029755	-0.6109628	0.000728
janA	FBgn0001280	-0.6111999	0.01027315
CG9890	FBgn0034814	-0.6117214	0.00636945
RpLP0-like	FBgn0033485	-0.6170004	4.80E-05
POLDIP2	FBgn0037329	-0.6176451	0.00161116
SdhB	FBgn0014028	-0.6230335	3.06E-08
CG1463	FBgn0030406	-0.6249947	0.00012541
Cyp309a1	FBgn0031432	-0.6253544	0.00217112
AnxB10	FBgn0000084	-0.6256047	0.0021032
EbpIII	FBgn0011695	-0.6293942	5.91E-07
CG1840	FBgn0030351	-0.6294073	0.04624654
CG8460	FBgn0031996	-0.630489	0.0081547
Orct2	FBgn0086365	-0.6357671	0.00072263
CG14892	FBgn0038447	-0.6368475	0.02967945

CG7236	FBgn0031730	-0.6401867	0.03052093
SerRS	FBgn0031497	-0.6441112	3.40E-07
CG2064	FBgn0033205	-0.6476346	0.01122433
beg	FBgn0036691	-0.654992	0.02984263
peng	FBgn0015527	-0.6554067	0.00011444
CG10916	FBgn0034312	-0.6577742	0.00018837
eIF2D	FBgn0041588	-0.6594306	0.0027376
kin17	FBgn0024887	-0.6625903	0.00018697
NC2beta	FBgn0028926	-0.6648387	0.01109888
CG6409	FBgn0036106	-0.6650625	4.41E-06
nod	FBgn0002948	-0.6670002	0.00619229
CG14695	FBgn0037850	-0.6681687	0.04918173
Spt3	FBgn0037981	-0.6693317	0.01222168
shv	FBgn0031256	-0.6703786	0.00018889
CG30151	FBgn0050151	-0.670638	0.00013615
CG5377	FBgn0038974	-0.6718905	0.00088037
CG4096	FBgn0029791	-0.6720401	2.06E-06
CG14367	FBgn0038170	-0.6756382	0.00332793
Cyp312a1	FBgn0036778	-0.6789169	0.04374129
hpRNA:CR18854	FBgn0042174	-0.6790005	0.03297035
vig2	FBgn0046214	-0.6801911	1.16E-06
Arc1	FBgn0033926	-0.6862866	1.29E-12
P5cr	FBgn0015781	-0.6892786	9.27E-05
cactin	FBgn0031114	-0.6931903	7.29E-10
ValRS	FBgn0027079	-0.7038875	2.76E-06
Dhod	FBgn0000447	-0.7043823	0.00314543
Vps20	FBgn0034744	-0.7063528	1.45E-08
lint	FBgn0033359	-0.7064877	0.04347323
CG3635	FBgn0032981	-0.7075442	0.0304104
Muc91C	FBgn0038642	-0.7106481	0.04665891
bond	FBgn0260942	-0.7132567	0.0018182
CG10208	FBgn0039118	-0.7194318	0.01351258
CG31777	FBgn0051777	-0.7203354	0.00262076
FMRFa	FBgn0000715	-0.7235836	0.00256989
CG13912	FBgn0035186	-0.7242778	0.03935546
CG14567	FBgn0037126	-0.7287545	0.02139054
Dgp-1	FBgn0027836	-0.7337175	4.99E-07
CG14230	FBgn0031062	-0.7340039	0.00079634
GstE5	FBgn0063495	-0.7362528	0.04367464

rempA	FBgn0260933	-0.7372927	0.00019444
CG10185	FBgn0038397	-0.7390316	0.0052433
CG5380	FBgn0038951	-0.7477041	0.03853009
cl	FBgn0000318	-0.747988	0.00021911
ScpX	FBgn0015808	-0.7497152	0.00011457
Srp14	FBgn0038808	-0.7545773	0.00241016
CG31028	FBgn0051028	-0.7569394	0.01330119
Prx2540-2	FBgn0033518	-0.7589613	0.04126315
dmrt99B	FBgn0039683	-0.760537	0.00106386
CG32448	FBgn0052448	-0.7713052	0.01200681
Act88F	FBgn0000047	-0.774193	0.00488074
Mfap1	FBgn0035294	-0.7763461	2.29E-06
Gadd45	FBgn0033153	-0.7821314	7.33E-12
Bdp1	FBgn0032512	-0.7824069	6.59E-07
CG8223	FBgn0037624	-0.794553	0.00402499
CG9107	FBgn0031764	-0.7951455	0.00015343
CG7900	FBgn0037548	-0.7977332	0.00011361
Pex12	FBgn0031282	-0.7984815	0.00821667
up	FBgn0004169	-0.7991273	0.00670528
Aatf	FBgn0031851	-0.7991311	1.06E-05
eIF2beta	FBgn0004926	-0.7994706	4.05E-09
mldr	FBgn0029858	-0.8011269	0.01408981
CG12279	FBgn0038080	-0.8054455	0.03813472
RpL23A	FBgn0026372	-0.8133079	2.72E-05
Klp54D	FBgn0263076	-0.8134312	0.00881005
CG13251	FBgn0037014	-0.8188397	0.02037074
Sirt6	FBgn0037802	-0.8193243	0.0006872
ss	FBgn0003513	-0.8272455	0.04816775
btv	FBgn0023096	-0.8392111	0.01124907
Wdr92	FBgn0036771	-0.8441862	0.00324409
RPA2	FBgn0032906	-0.8459397	0.0054251
mRpS24	FBgn0039159	-0.8670034	0.00309837
Ku80	FBgn0041627	-0.8730424	0.00029549
GluRIIE	FBgn0051201	-0.8775884	0.00305135
RabX6	FBgn0035155	-0.880949	0.00777233
CG8360	FBgn0032001	-0.8952666	0.00013243
CG8860	FBgn0033691	-0.9004717	0.01039513
CG5867	FBgn0027586	-0.9011335	1.08E-11
Mthfs	FBgn0085453	-0.9012213	0.00266675

Kaz1-ORFB	FBgn0063923	-0.9139524	0.01558953
CG14445	FBgn0029851	-0.9151645	0.00458894
CG14694	FBgn0037845	-0.9154169	0.01060495
CG13618	FBgn0039203	-0.9154639	1.90E-05
Ubx	FBgn0003944	-0.9294299	0.00821667
CG13807	FBgn0035323	-0.9374979	2.44E-05
CG3014	FBgn0037519	-0.9440906	0.00944355
CG17108	FBgn0032285	-0.9465394	0.00065735
Pgd	FBgn0004654	-0.9716576	6.73E-07
CG15784	FBgn0029766	-0.9763945	3.68E-23
CG6179	FBgn0030915	-0.9939785	2.54E-05
CG2065	FBgn0033204	-1.0074278	7.64E-05
Gsc	FBgn0010323	-1.0194066	2.54E-05
CG9444	FBgn0037730	-1.0560152	0.00060403
CG7342	FBgn0038716	-1.0962246	9.48E-05
Oseg2	FBgn0035317	-1.1339917	3.47E-06
lncRNA:CR45717	FBgn0267281	-1.1871603	0.00125242
Fatp2	FBgn0265187	-1.1953967	1.60E-11
CG13676	FBgn0035844	-1.2203281	2.19E-07
Cpr47Ef	FBgn0033603	-1.2302068	5.90E-06
Hsp26	FBgn0001225	-1.2313995	1.56E-12
CG15213	FBgn0040843	-1.2329644	9.75E-08
CheA75a	FBgn0036783	-1.2367291	0.01669072
Cyp4aa1	FBgn0034053	-1.2520345	9.32E-13
CG7130	FBgn0037151	-1.2707022	0.00014596
Act79B	FBgn0000045	-1.2828454	0.02555288
MFS3	FBgn0031307	-1.3164473	1.49E-12
CG9492	FBgn0037726	-1.3372743	0.02920376
Ldh	FBgn0001258	-1.3385605	9.32E-13
dysf	FBgn0039411	-1.3594175	9.32E-13
mtSSB	FBgn0010438	-1.5053436	6.03E-05
CG9497	FBgn0031800	-1.5396855	0.00729969
antdh	FBgn0026268	-1.6012668	0.01890288
CG30271	FBgn0050271	-1.6200346	5.54E-08
CG9313	FBgn0034566	-1.6308218	5.78E-10
Obp56a	FBgn0034468	-1.8957497	1.55E-09
OS9	FBgn0042129	-2.3962507	0.00097044
Jhedup	FBgn0034076	-2.41479	0.01294249
CG11391	FBgn0038732	-4.8244196	0.0003925

Obp19a	FBgn0031109	-5.5572596	4.04E-05
Obp83a	FBgn0011281	-6.6972058	1.38E-07
a10	FBgn0011293	-7.8283163	3.04E-06
Obp83b	FBgn0010403	-9.0595606	4.70E-07
a5	FBgn0011294	-9.7404164	1.23E-06
Os-C	FBgn0010401	-11.274291	1.13E-09

Appendix F: Complete GO biological functions for upregulated genes in CTvCN experimental comparison.

p-values determined by Fisher's Exact test with Bonferroni correction.

GO biological process complete	Reference Drosophila genes	Uploaded genes	Expected Genes	Fold Enrichment	P-value
Unclassified (UNCLASSIFIED)	2539	5	8.31	0.6	0.00E+00

Appendix G: Complete GO biological functions for downregulated genes in CTvCN experimental comparison.

p-values determined by Fisher's Exact test with Bonferroni correction.

GO biological process complete	Reference Drosophila genes	Uploaded genes	Expected Genes	Fold Enrichment	P-value
L-phenylalanine catabolic process (GO:0006559)	6	4	0.09	46.10	2.68E-02
L-phenylalanine metabolic process (GO:0006558)	6	4	0.09	46.09	2.68E-02
erythrose 4-phosphate/phosphoenolpyruvate family amino acid catabolic process (GO:1902222)	6	4	0.09	46.09	2.68E-02
erythrose 4-phosphate/phosphoenolpyruvate family amino acid metabolic process (GO:1902221)	6	4	0.09	46.09	2.68E-02
aromatic amino acid family catabolic process (GO:0009074)	10	5	0.14	34.57	5.09E-03
tyrosine metabolic process (GO:0006570)	11	5	0.16	31.42	7.32E-03
aromatic amino acid family metabolic process (GO:0009072)	21	6	0.3	19.75	6.11E-03
cellular amino acid biosynthetic process (GO:0008652)	48	8	0.69	11.52	3.99E-03
alpha-amino acid biosynthetic process (GO:1901607)	44	7	0.64	11	2.49E-02
alpha-amino acid catabolic process (GO:1901606)	44	7	0.64	11	2.49E-02

cellular amino acid catabolic process (GO:0009063)	48	7	0.69	10.08	4.17E-02
drug catabolic process (GO:0042737)	62	8	0.9	8.92	2.23E-02
alpha-amino acid metabolic process (GO:1901605)	131	14	1.89	7.39	6.55E-05
organic acid catabolic process (GO:0016054)	96	10	1.39	7.2	9.14E-03
carboxylic acid catabolic process (GO:0046395)	96	10	1.39	7.2	9.14E-03
small molecule catabolic process (GO:0044282)	147	15	2.13	7.05	3.56E-05
organic acid biosynthetic process (GO:0016053)	153	14	2.21	6.33	3.92E-04
carboxylic acid biosynthetic process (GO:0046394)	153	14	2.21	6.33	3.92E-04
carbohydrate metabolic process (GO:0005975)	247	22	3.57	6.16	1.28E-07
cellular amino acid metabolic process (GO:0006520)	196	15	2.84	5.29	1.19E-03
monocarboxylic acid metabolic process (GO:0032787)	176	13	2.55	5.11	1.06E-02
small molecule biosynthetic process (GO:0044283)	249	17	3.6	4.72	8.89E-04
oxidation-reduction process (GO:0055114)	574	39	8.3	4.7	6.83E-12
carboxylic acid metabolic process (GO:0019752)	420	27	6.08	4.44	7.32E-07
organic acid metabolic process (GO:0006082)	437	28	6.32	4.43	3.52E-07
oxoacid metabolic process (GO:0043436)	435	27	6.29	4.29	1.52E-06
small molecule metabolic process (GO:0044281)	877	46	12.69	3.63	1.31E-10
lipid metabolic process (GO:0006629)	467	22	6.76	3.26	6.42E-03
metabolic process (GO:0008152)	4659	107	67.39	1.59	5.42E-05
Unclassified (UNCLASSIFIED)	2539	43	36.73	1.17	0.00E+00
cellular component organization (GO:0016043)	2627	15	38	0.39	3.22E-02
cellular component organization or biogenesis (GO:0071840)	2753	15	39.82	0.38	8.02E-03
cellular macromolecule metabolic process (GO:0044260)	2197	8	31.78	0.25	7.46E-04
organelle organization (GO:0006996)	1716	6	24.82	0.24	2.00E-02
cellular protein metabolic process (GO:0044267)	1643	4	23.77	0.17	2.12E-03
macromolecule modification (GO:0043412)	1182	2	17.1	0.12	2.67E-02

Appendix H: Complete GO biological functions for upregulated genes in KTvKN experimental comparison.

p-values determined by Fisher's Exact test with Bonferroni correction.

GO biological process complete	Reference Drosophila genes	Uploaded genes	Expected Genes	Fold Enrichment	P-value
Unclassified (UNCLASSIFIED)	2539	14	20.86	0.67	0.00E+00

Appendix I: Complete GO biological functions for downregulated genes in KTvKN experimental comparison.

p-values determined by Fisher's Exact test with Bonferroni correction.

GO biological process complete	Reference Drosophila genes	Uploaded genes	Expected Genes	Fold Enrichment	P-value
small molecule metabolic process (GO:0044281)	877	20	5.67	3.53	2.58E-03
Unclassified (UNCLASSIFIED)	2539	11	16.43	0.67	0.00E+00

Appendix J: Complete GO biological functions for upregulated genes in KNvCN experimental comparison.

p-values determined by Fisher's Exact test with Bonferroni correction.

GO biological process complete	Reference Drosophila genes	Uploaded genes	Expected Genes	Fold Enrichment	P-value
heterophilic cell-cell adhesion via plasma membrane cell adhesion molecules (GO:0007157)	28	7	0.41	16.94	2.01E-03
neuropeptide signaling pathway (GO:0007218)	56	12	0.83	14.52	7.83E-07

cell-cell adhesion via plasma-membrane adhesion molecules (GO:0098742)	73	13	1.08	12.07	1.03E-06
G protein-coupled receptor signaling pathway (GO:0007186)	208	29	3.07	9.45	2.45E-15
G protein-coupled receptor signaling pathway, coupled to cyclic nucleotide second messenger (GO:0007187)	60	8	0.89	9.04	2.07E-02
cyclic-nucleotide-mediated signaling (GO:0019935)	63	8	0.93	8.61	2.87E-02
cell-cell adhesion (GO:0098609)	104	13	1.53	8.47	4.94E-05
cell adhesion (GO:0007155)	170	15	2.51	5.98	2.76E-04
biological adhesion (GO:0022610)	172	15	2.54	5.91	3.18E-04
signal transduction (GO:0007165)	1017	47	15.01	3.13	1.14E-08
signaling (GO:0023052)	1242	52	18.33	2.84	2.25E-08
cell communication (GO:0007154)	1310	53	19.33	2.74	4.68E-08
cellular response to stimulus (GO:0051716)	1497	52	22.09	2.35	1.86E-05
response to stimulus (GO:0050896)	2632	70	38.84	1.8	1.21E-03
regulation of cellular process (GO:0050794)	3472	88	51.23	1.72	1.15E-04
regulation of biological process (GO:0050789)	3782	92	55.81	1.65	2.82E-04
biological regulation (GO:0065007)	4238	95	62.54	1.52	8.60E-03
Unclassified (UNCLASSIFIED)	2539	29	37.47	0.77	0.00E+00

Appendix K: Complete GO biological functions for downregulated genes in KNvCN experimental comparison.

p-values determined by Fisher's Exact test with Bonferroni correction.

GO biological process complete	Reference Drosophila genes	Uploaded genes	Expected Genes	Fold Enrichment	P-value
cytoplasmic translation (GO:0002181)	117	15	3.58	4.19	2.94E-02
oxidation-reduction process (GO:0055114)	574	55	17.57	3.13	1.57E-09

nucleobase-containing small molecule metabolic process (GO:0055086)	364	31	11.14	2.78	2.85E-03
cellular amide metabolic process (GO:0043603)	481	38	14.72	2.58	1.34E-03
peptide metabolic process (GO:0006518)	401	31	12.27	2.53	2.46E-02
carboxylic acid metabolic process (GO:0019752)	420	32	12.85	2.49	2.05E-02
oxoacid metabolic process (GO:0043436)	435	32	13.31	2.40	3.57E-02
organic acid metabolic process (GO:0006082)	437	32	13.37	2.39	3.86E-02
small molecule metabolic process (GO:0044281)	877	59	26.84	2.20	1.25E-04
metabolic process (GO:0008152)	4659	196	142.58	1.37	4.15E-04
Unclassified (UNCLASSIFIED)	2539	84	77.7	1.08	0.00E+00

Appendix L: Complete GO biological functions for upregulated genes in KTvCT experimental comparison.

p-values determined by Fisher's Exact test with Bonferroni correction.

GO biological process complete	Reference Drosophila genes	Uploaded genes	Expected Genes	Fold Enrichment	P-value
Unclassified (UNCLASSIFIED)	2539	28	34.7	0.81	0.00E+00

Appendix M: Complete GO biological functions for downregulated genes in KTvCT experimental comparison.

p-values determined by Fisher's Exact test with Bonferroni correction.

GO biological process complete	Reference Drosophila genes	Uploaded genes	Expected Genes	Fold Enrichment	P-value
ribosomal large subunit assembly (GO:0000027)	22	7	0.62	11.22	3.60E-02
ribosomal large subunit biogenesis (GO:0042273)	57	10	1.62	6.19	4.69E-02
RNA modification (GO:0009451)	95	13	2.69	4.83	2.84E-02

rRNA processing (GO:0006364)	126	17	3.57	4.76	1.41E-03
rRNA metabolic process (GO:0016072)	136	17	3.86	4.41	3.69E-03
ribosome biogenesis (GO:0042254)	196	21	5.56	3.78	2.09E-03
ncRNA processing (GO:0034470)	241	25	6.83	3.66	3.11E-04
ncRNA metabolic process (GO:0034660)	313	29	8.87	3.27	2.76E-04
ribonucleoprotein complex biogenesis (GO:0022613)	276	24	7.82	3.07	1.04E-02
RNA processing (GO:0006396)	515	44	14.6	3.01	1.10E-06
RNA metabolic process (GO:0016070)	824	59	23.36	2.53	6.36E-07
gene expression (GO:0010467)	1088	75	30.84	2.43	1.13E-08
nucleic acid metabolic process (GO:0090304)	1074	73	30.45	2.40	3.49E-08
nucleobase-containing compound metabolic process (GO:0006139)	1439	85	40.79	2.08	4.78E-07
cellular nitrogen compound metabolic process (GO:0034641)	1859	108	52.7	2.05	1.98E-09
heterocycle metabolic process (GO:0046483)	1517	88	43.01	2.05	6.85E-07
cellular aromatic compound metabolic process (GO:0006725)	1573	91	44.59	2.04	2.71E-07
organic cyclic compound metabolic process (GO:1901360)	1627	92	46.12	1.99	8.63E-07
cellular metabolic process (GO:0044237)	3883	160	110.08	1.45	3.52E-04
nitrogen compound metabolic process (GO:0006807)	3776	150	107.05	1.40	1.36E-02
metabolic process (GO:0008152)	4659	181	132.08	1.37	1.89E-03
primary metabolic process (GO:0044238)	3995	155	113.26	1.37	3.37E-02
organic substance metabolic process (GO:0071704)	4342	167	123.09	1.36	1.50E-02
cellular process (GO:0009987)	6645	236	188.38	1.25	7.09E-03

Unclassified (UNCLASSIFIED)	2539	63	71.98	0.88	0.00E+00

Appendix N: List of FlyBase IDs for >2 fold enriched MB genes used in this study.

All genes were previously identified (Jones et al., 2018).

FBgn0000008	FBgn0024150	FBgn0035245	FBgn0085431
FBgn0000046	FBgn0024232	FBgn0035267	FBgn0086906
FBgn0000273	FBgn0024944	FBgn0035710	FBgn0259209
FBgn0000352	FBgn0027586	FBgn0035719	FBgn0259219
FBgn0001085	FBgn0027654	FBgn0035903	FBgn0259241
FBgn0001218	FBgn0027836	FBgn0035917	FBgn0259243
FBgn0001258	FBgn0029685	FBgn0036556	FBgn0259680
FBgn0002789	FBgn0029843	FBgn0036583	FBgn0259821
FBgn0003149	FBgn0029864	FBgn0036890	FBgn0259824
FBgn0003301	FBgn0030090	FBgn0037754	FBgn0260632
FBgn0003887	FBgn0030358	FBgn0038641	FBgn0260942
FBgn0004028	FBgn0030437	FBgn0038880	FBgn0260960
FBgn0004117	FBgn0031114	FBgn0039354	FBgn0261089
FBgn0005558	FBgn0031245	FBgn0039411	FBgn0261285
FBgn0005666	FBgn0031257	FBgn0039620	FBgn0261548
FBgn0005677	FBgn0031264	FBgn0039647	FBgn0262714
FBgn0011582	FBgn0031307	FBgn0041582	FBgn0262737
FBgn0011589	FBgn0031835	FBgn0043005	FBgn0263006
FBgn0013278	FBgn0031855	FBgn0050021	FBgn0263116
FBgn0013725	FBgn0032130	FBgn0050158	FBgn0264489
FBgn0014859	FBgn0032798	FBgn0051146	FBgn0264753
FBgn0015019	FBgn0032840	FBgn0051191	FBgn0265356
FBgn0015602	FBgn0034012	FBgn0051523	FBgn0265597

FBgn0015799	FBgn0034075	FBgn0051760	FBgn0265935
FBgn0019650	FBgn0034145	FBgn0052204	FBgn0266000
FBgn0019662	FBgn0034611	FBgn0052406	FBgn0266137
FBgn0020269	FBgn0034725	FBgn0053517	FBgn0266756
FBgn0022382	FBgn0034911	FBgn0053519	FBgn0267253
FBgn0023179	FBgn0034970	FBgn0085395	
FBgn0023540	FBgn0035144	FBgn0085426	

7 Curriculum Vitae

Name: Nicholas Raun

Post-secondary Education and Degrees:
Western University
London, Ontario, Canada
2017-2019 M.Sc.

University of Alberta
Edmonton, Alberta, Canada
2010-2016 B.Sc.

Related Work Experience
Graduate Teaching Assistant
Western University
2017-2019

Publications:

Chubak MC, Stone MH, **Raun N**, Rice SL, Sarikahya M, Jones SG, Lyons TA, Jakub TE, Mainland RLM, Knip MJ, Edwards TN, Kramer JM. (Preprint). Systematic functional characterization of the intellectual disability-associated SWI/SNF complex reveals distinct roles for the BAP and PBAP complexes in post-mitotic memory forming neurons of the Drosophila mushroom body. bioRxiv, https://doi.org/10.1101/408500

Raun N, Mailo J, Spinelli E, He X, McAvena S, Brand L, O'Sullivan J, Andersen J, Richer L, Tang-Wai R, Bolduc FV. (2017). Quantitative phenotypic and network analysis of 1q44 microdeletion for microcephaly. *American Journal of Medical Genetics, 173,* 972–977.

Selected Conference Presentations:

Raun N, Kramer JM. (2018, September). Unique requirements for the H3K4 methyltransferases *trx* in *Drosophila* long-term memory. Poster presentation at the 5th Canadian Conference on Epigenetics, Estérel, Québec, Canada.

Raun N, Kramer JM. (2017, November). The subunits *trithorax* and *Menin 1* of the epigenetic regulating TRX complex are necessary for long term memory in *Drosophila melanogaster*. Poster presentation at the 4th Canadian Conference on Epigenetics, Whistler, British Columbia, Canada.

Raun N, Kramer JM. (2017, October). The epigenetic regulator *trithorax* is necessary for long-term memory in *Drosophila.* Oral presentation at the 2017 Biology Graduate Research Forum, London, Ontario, Canada.

Honours and Awards:
Children's Health Research Institute Travel Award
2018 ($750)
Children's Health Research Institute Epigenetics Trainee Award
2017 ($10,000)